Evolution of the shell structure in medium-mass nuclei:

Search for the $2d_{5/2}$ neutron orbital in ^{69}Ni

Mohamad Moukaddam
UDS, IPHC Strabourg, France

DREB 2012
26 - 29 March, Pisa , Italy

Introduction

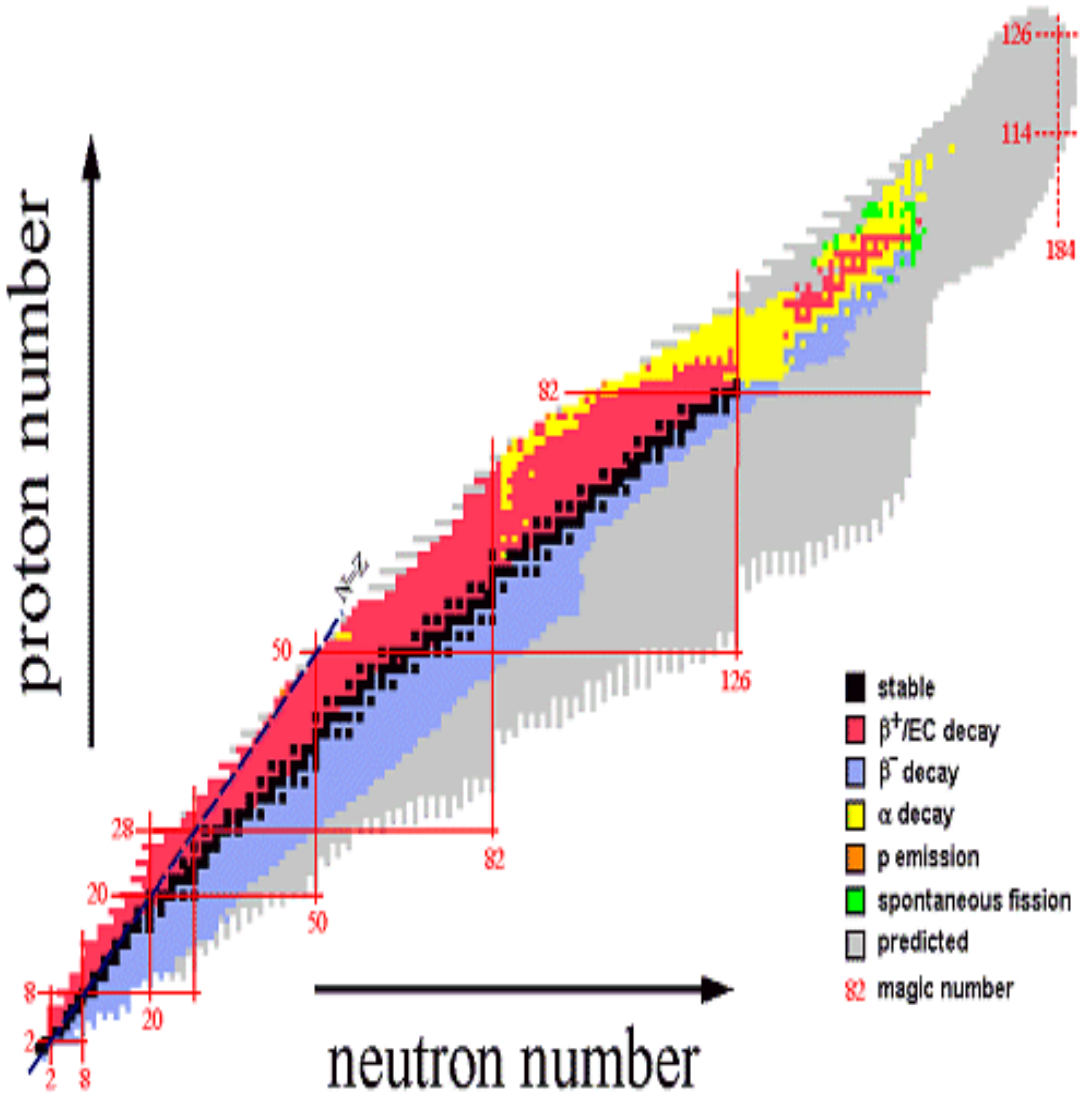

- **Light-mass region :**
  - HO shell closures : 2, 8, 20
- **heavy-mass region :**
  - Spin-orbit shell closures : 50, 82..
- **Structure evolution of neutron-rich nuclei at N=40**

N=40 Region : ^{68}Ni

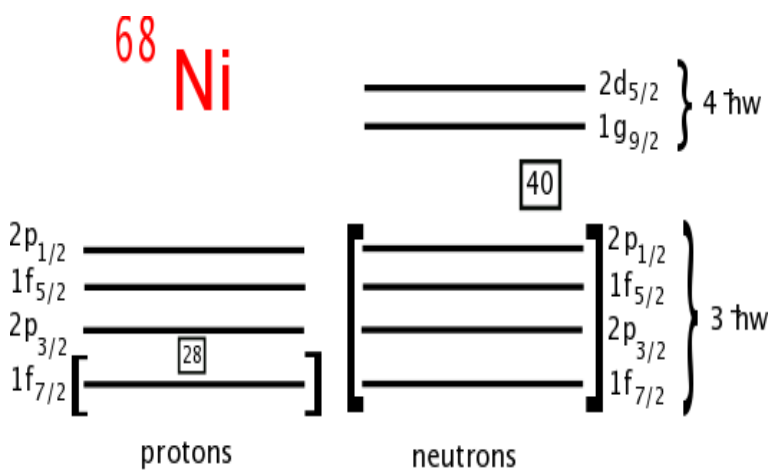

- Semi-magic nucleus (Z=28)
- E(2$^+$) ~ 2 MeV *Broda et al, PRL, 74, 868, 1995*
- B(E2) ~ 3.2 W.u. *Sorlin, PRL, 88, 092501, 2002*
- No trace for magicity according to S_{2n}

Rahaman, EPJ, 32, 87, 2007

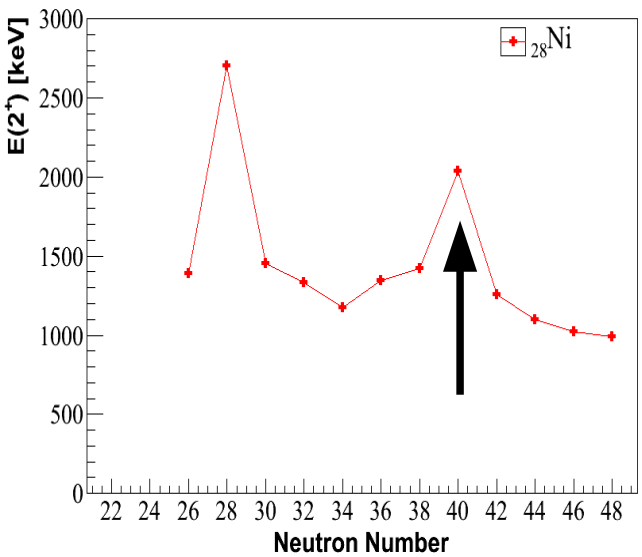

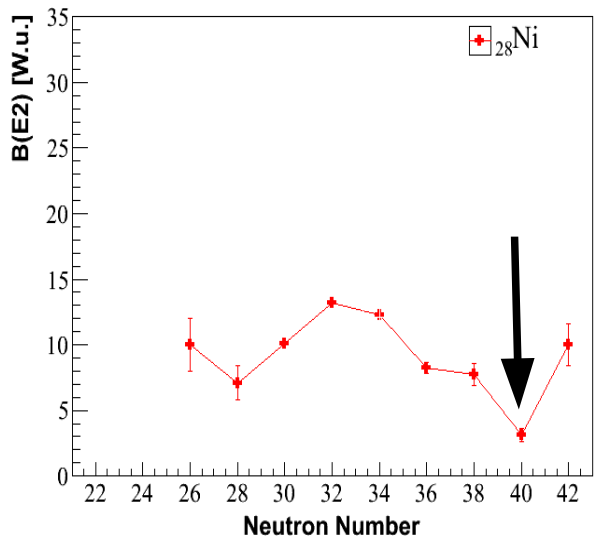

Magic signature

N=40 Region : ^{68}Ni

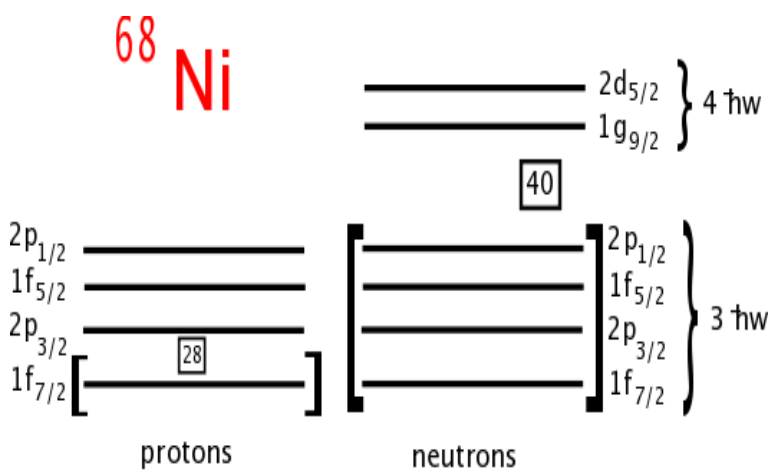

- Semi-magic nucleus (Z=28)
- E(2$^+$) ~ 2 MeV *Broda et al, PRL, 74, 868, 1995*
- B(E2) ~ 3.2 W.u. *Sorlin, PRL, 88, 092501, 2002*
- No trace for magicity according to S_{2n}

Rahaman, EPJ, 32, 87, 2007

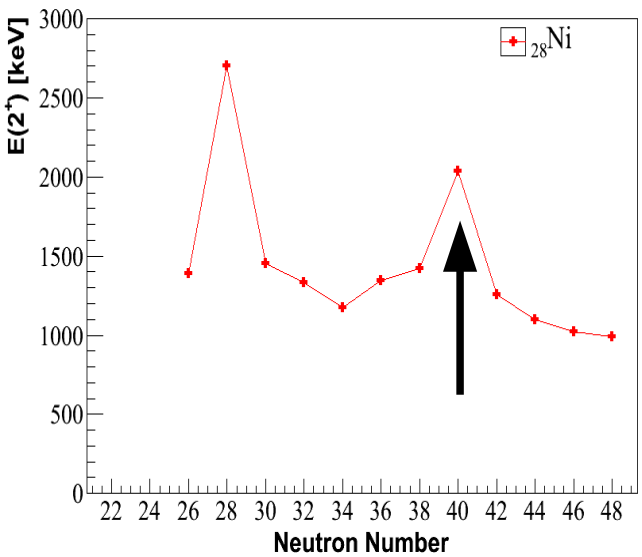

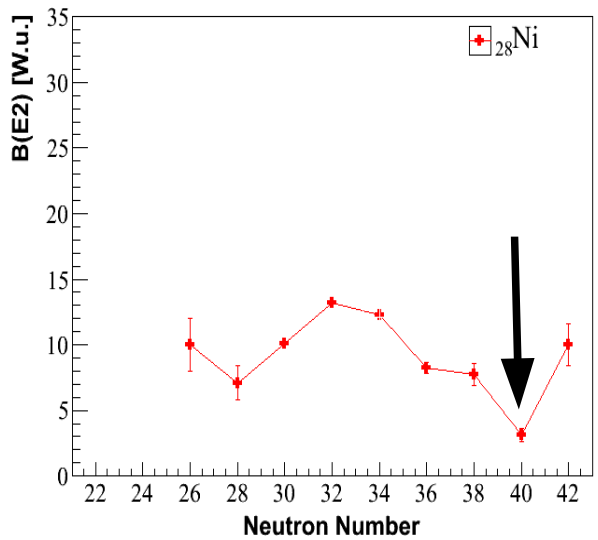

Magic signature

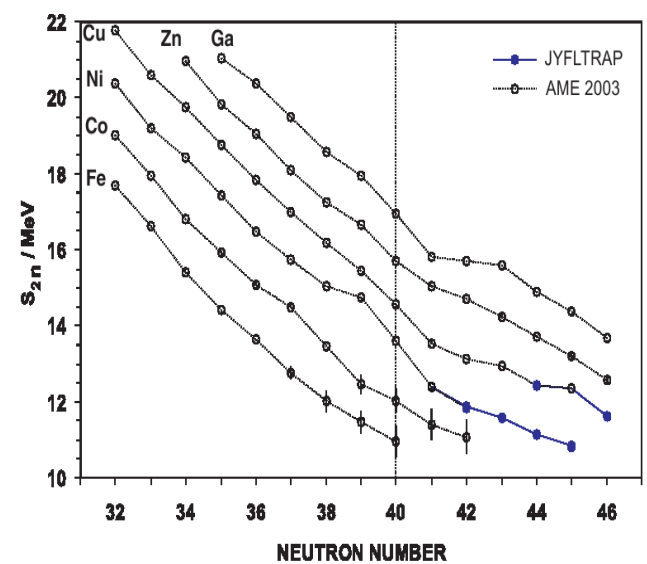

No trace for magicity!

N=40 Region : Deformation in Fe et Cr

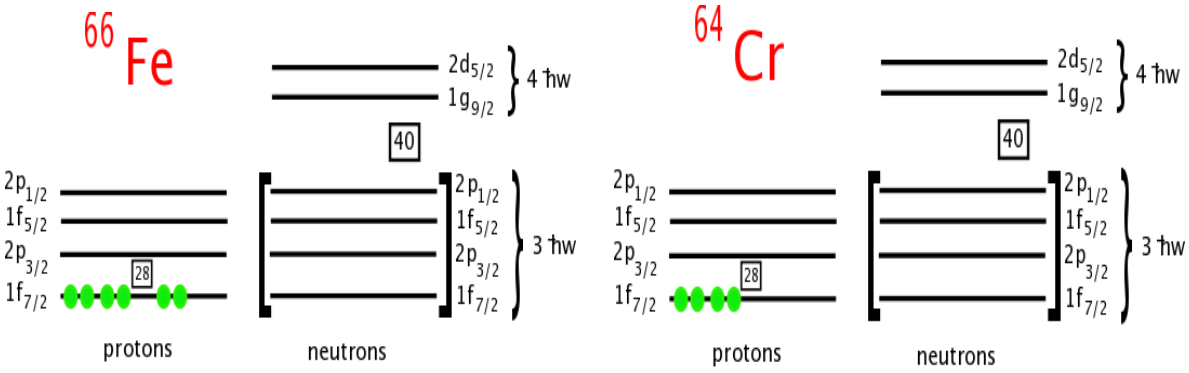

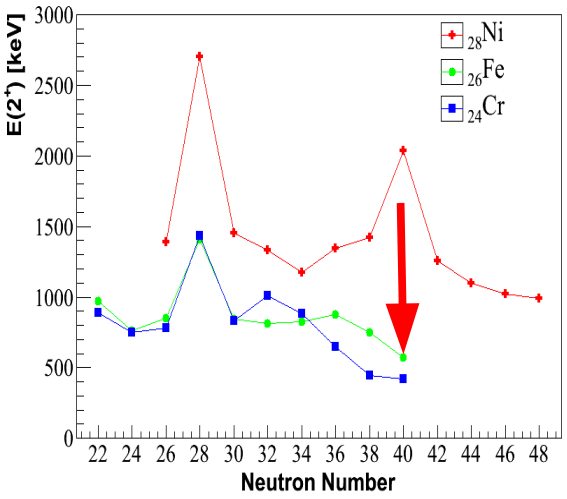

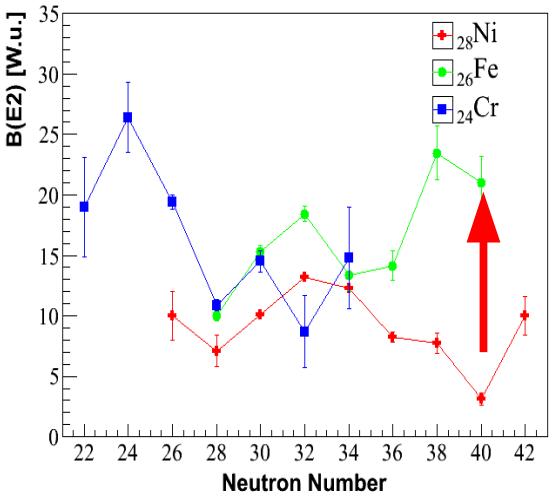

- Fe et Cr : deformation increases when approaching N = 40
- N = 40 HO shell-closure is quickly washed out with removal of proton pairs

N=40 Region : Deformation in Fe et Cr

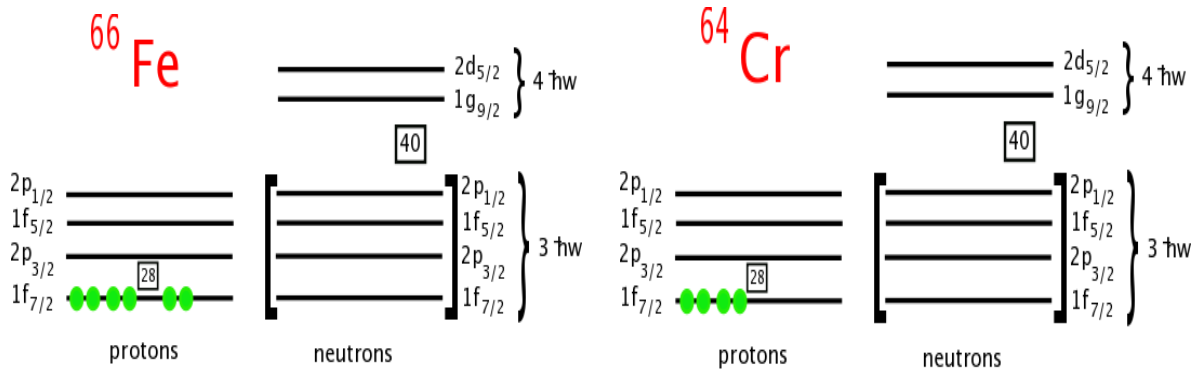

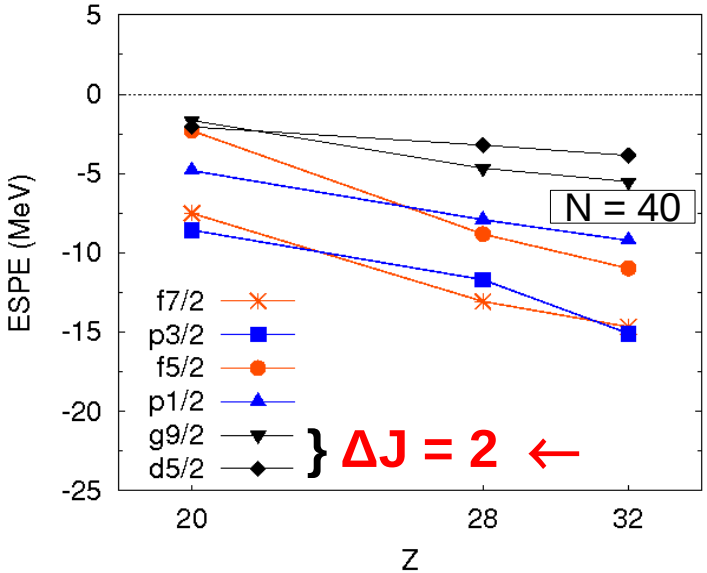

Lenzi et al., PRC, 82, 054301, 2010

$2d_{5/2}$ plays a major role in the deformation mechanism at N = 40 *Caurier et al. EPJ, A, 15, 2002, 145*

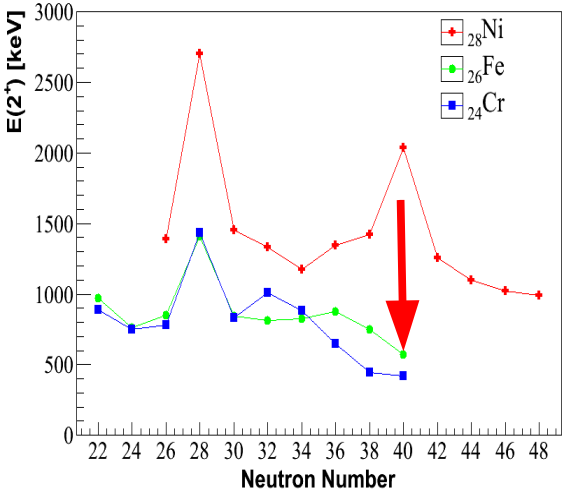

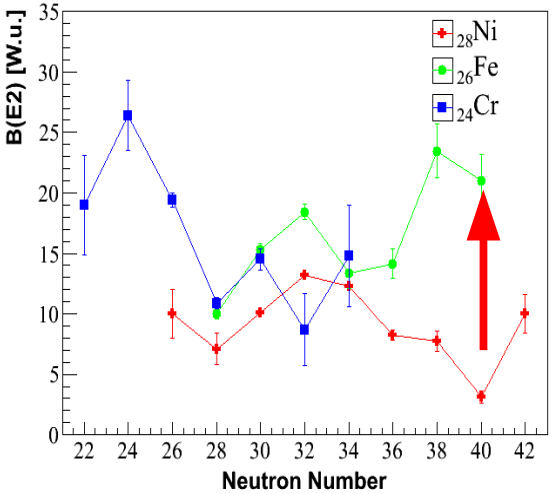

- Fe et Cr : deformation increases when approaching N = 40
- N = 40 HO shell-closure is quickly washed out with removal of proton pairs

Island of inversion and quadrupole deformations

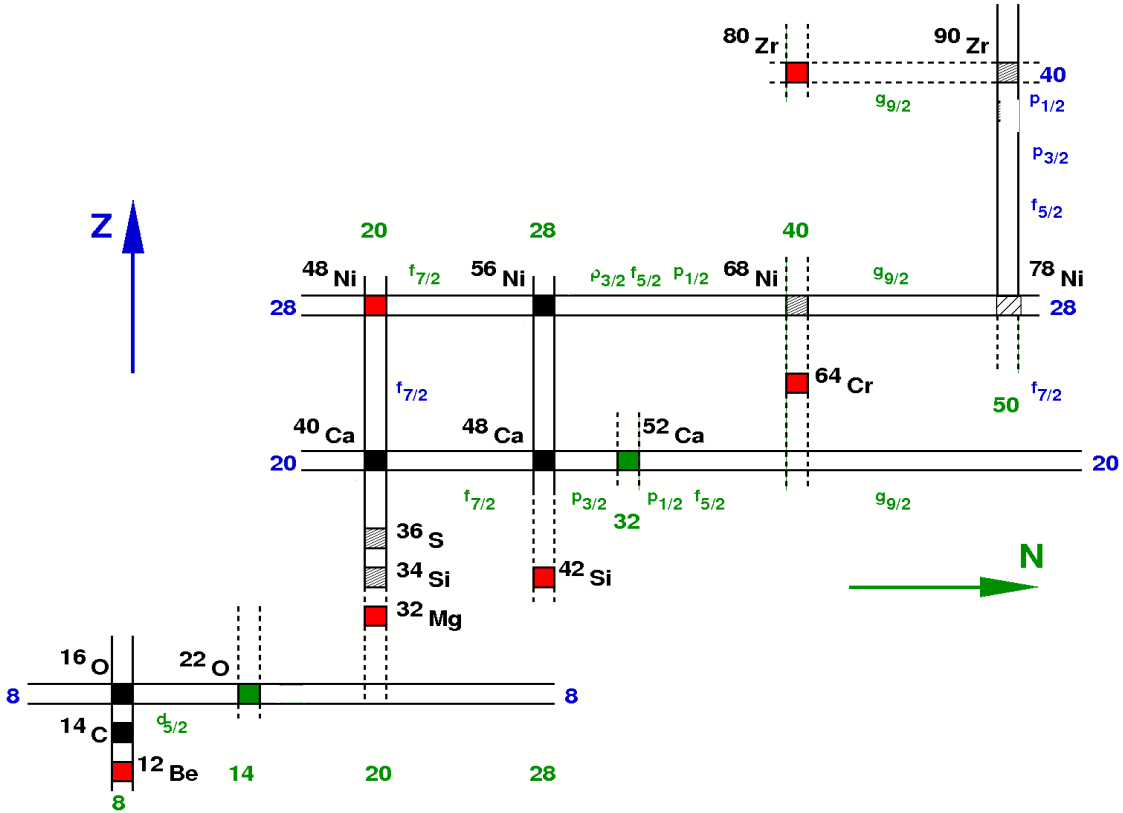

- Presence of quadrupole deformation at HO shell closures (N = 8, 20, 40)
- Island of inversion at N = 40

Caurier et al. EPJ, A, 15, 2002, 145

Island of inversion and quadrupole deformations

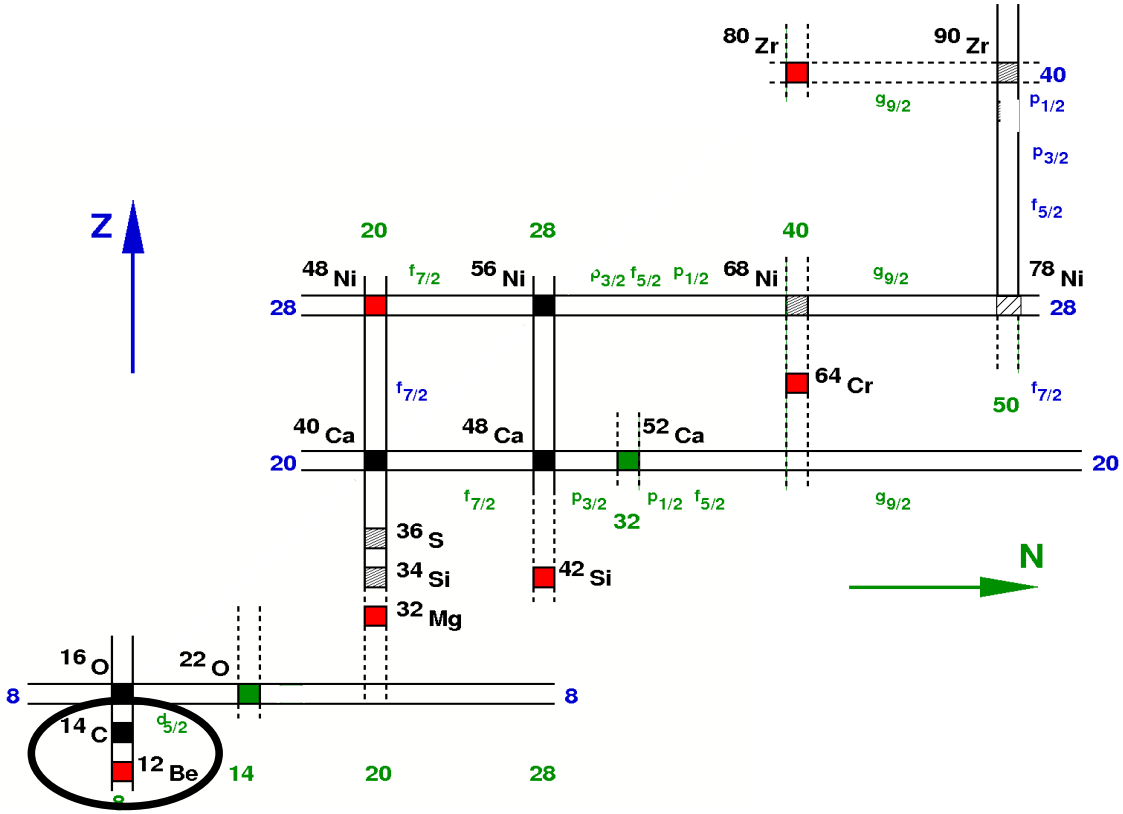

- Presence of quadrupole deformation at HO shell closures (N = 8, 20, 40)
- Island of inversion at N = 40

Caurier et al. EPJ, A, 15, 2002, 145

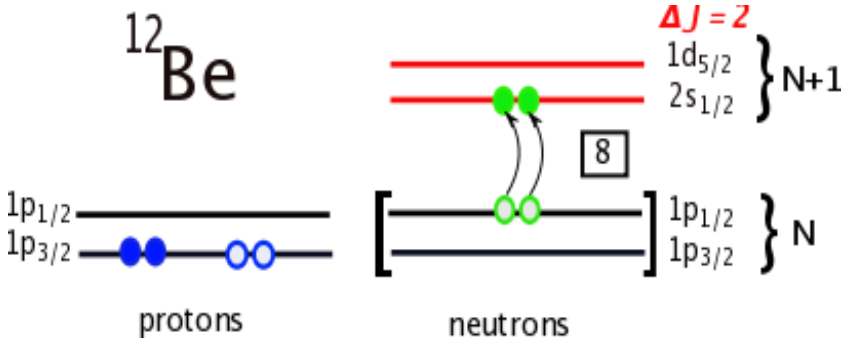

Island of inversion and quadrupole deformations

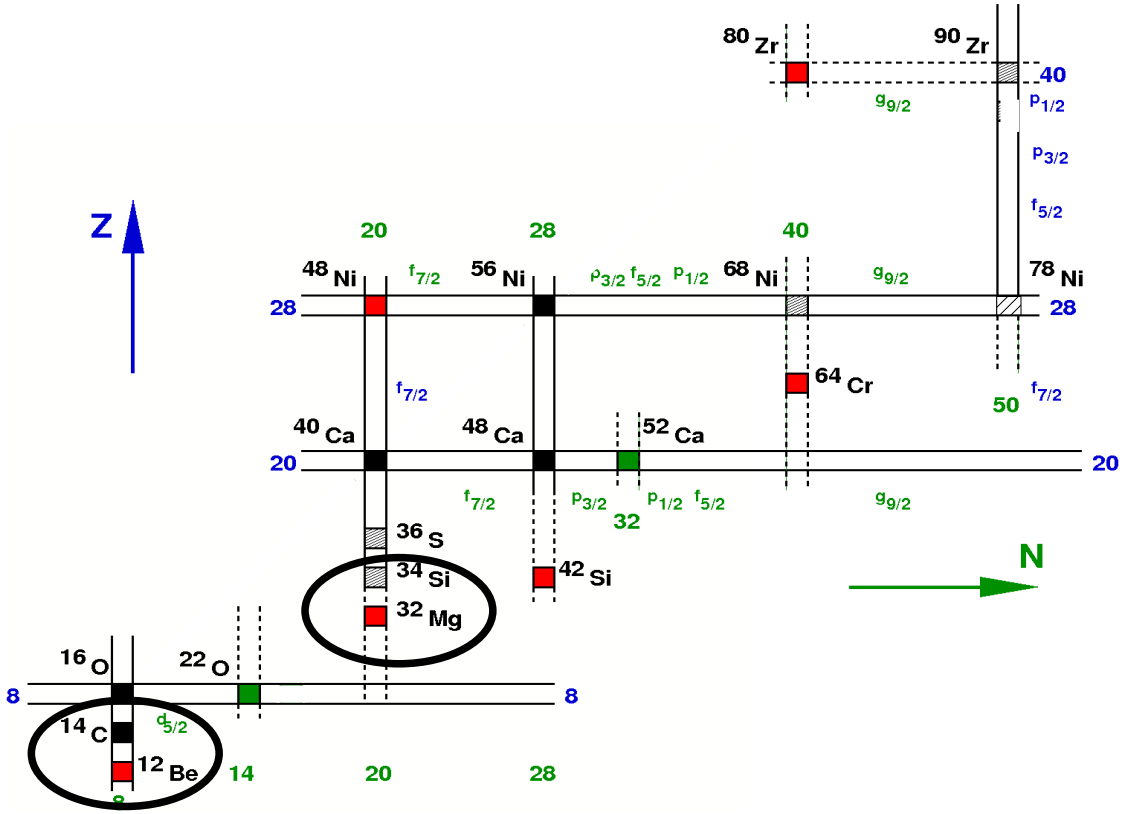

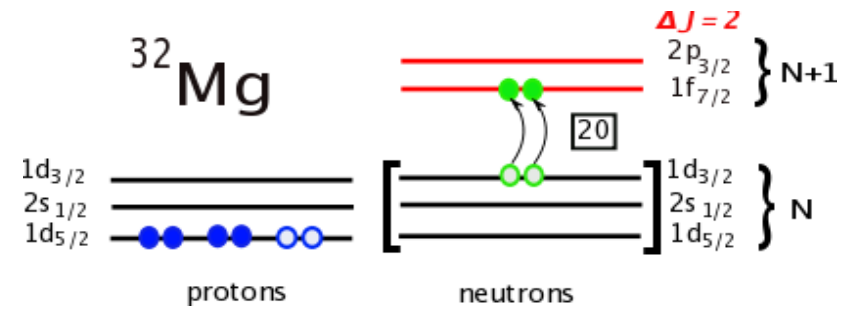

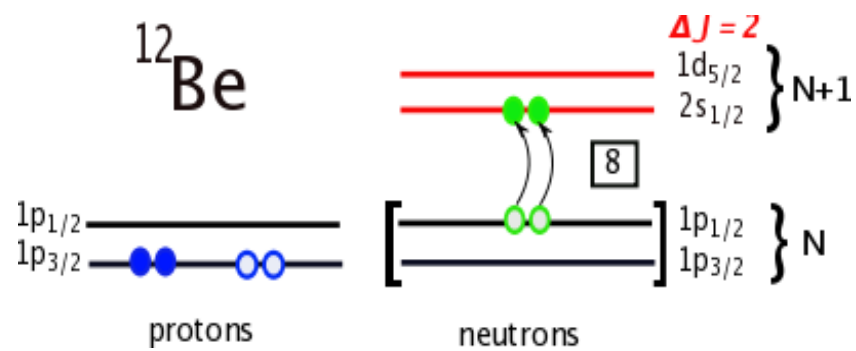

- Presence of quadrupole deformation at HO shell closures (N = 8, 20, 40)
- Island of inversion at N = 40

Caurier et al. EPJ, A, 15, 2002, 145

Island of inversion and quadrupole deformations

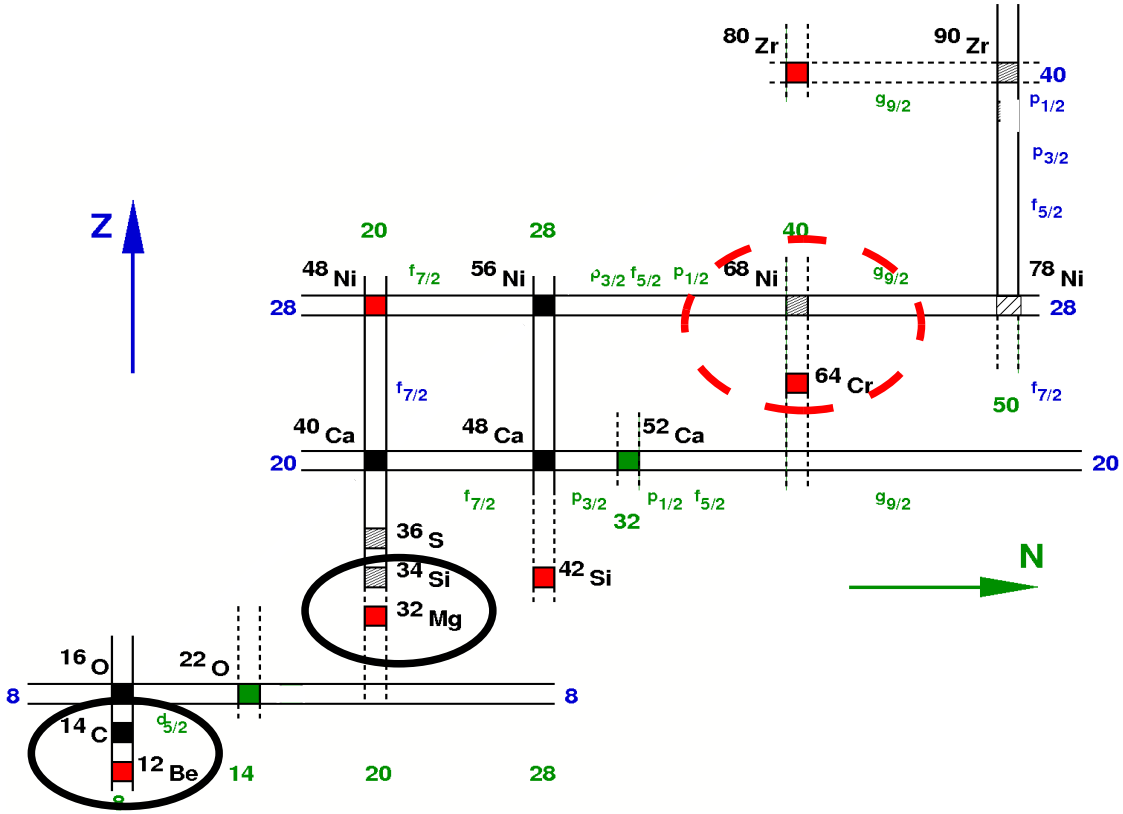

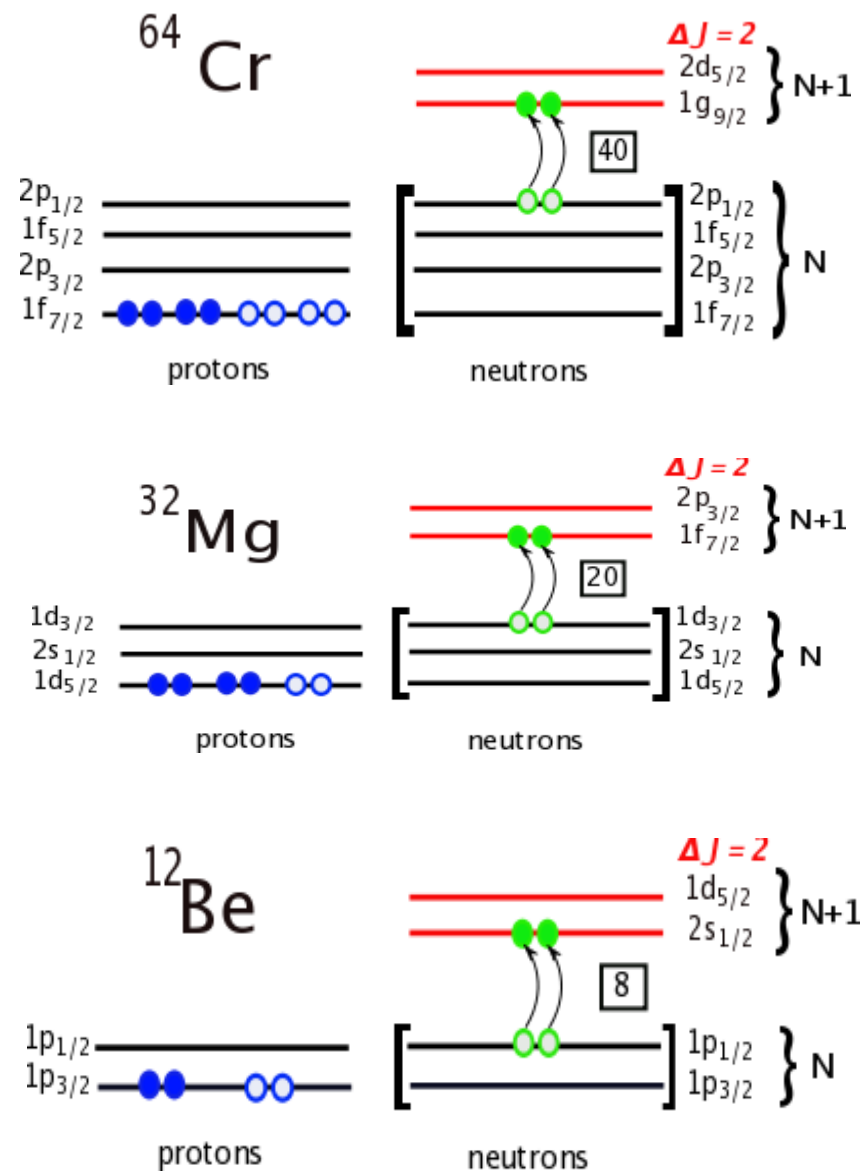

- Presence of quadrupole deformation at HO shell closures (N = 8, 20, 40)
- Island of inversion at N = 40

Caurier et al. EPJ, A, 15, 2002, 145

^{69}Ni : search for the $2d_{5/2}$ neutron orbital

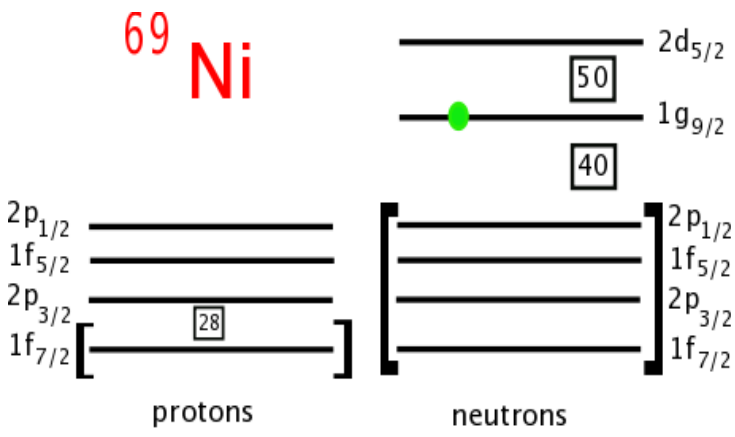

^{69}Ni : search for the $2d_{5/2}$ neutron orbital

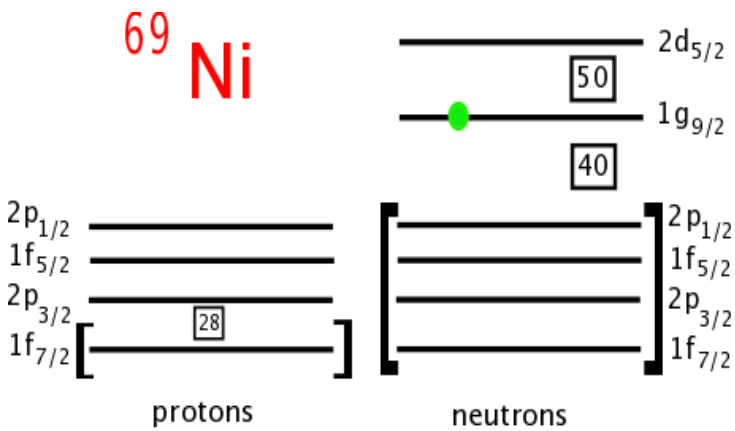

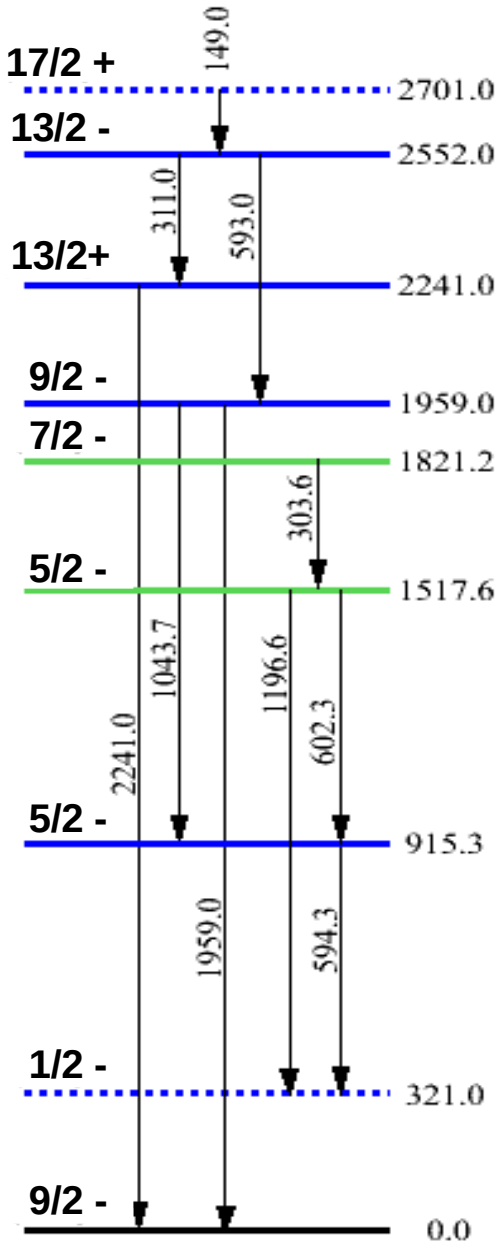

Previous experiments

- Isomer-state decay
  (Grzywacz et al., PRL, 81, 766, 1998)
- β-decay
  (Mueller et al., PRL, 83, 3613, 1999)

$2d_{5/2}$ (5/2+) neutron orbital not observed

^{69}Ni : search for the $2d_{5/2}$ neutron orbital

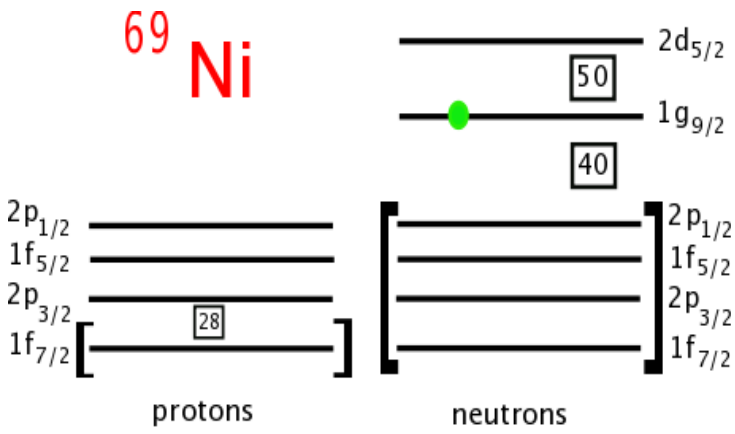

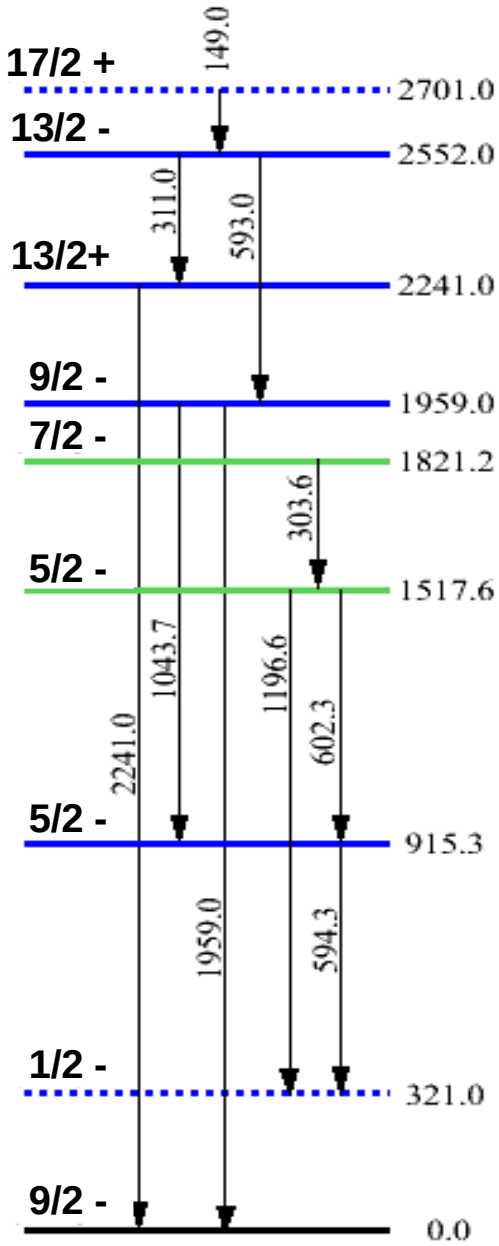

Previous experiments

- Isomer-state decay
  (Grzywacz et al., PRL, 81, 766, 1998)
- β-decay
  (Mueller et al., PRL, 83, 3613, 1999)

$2d_{5/2}$ (5/2+) neutron orbital not observed

Main goal of this work

Search for the neutron $2d_{5/2}$ orbital in ^{69}Ni

$d(^{68}Ni,p)^{69}Ni$

Beam production

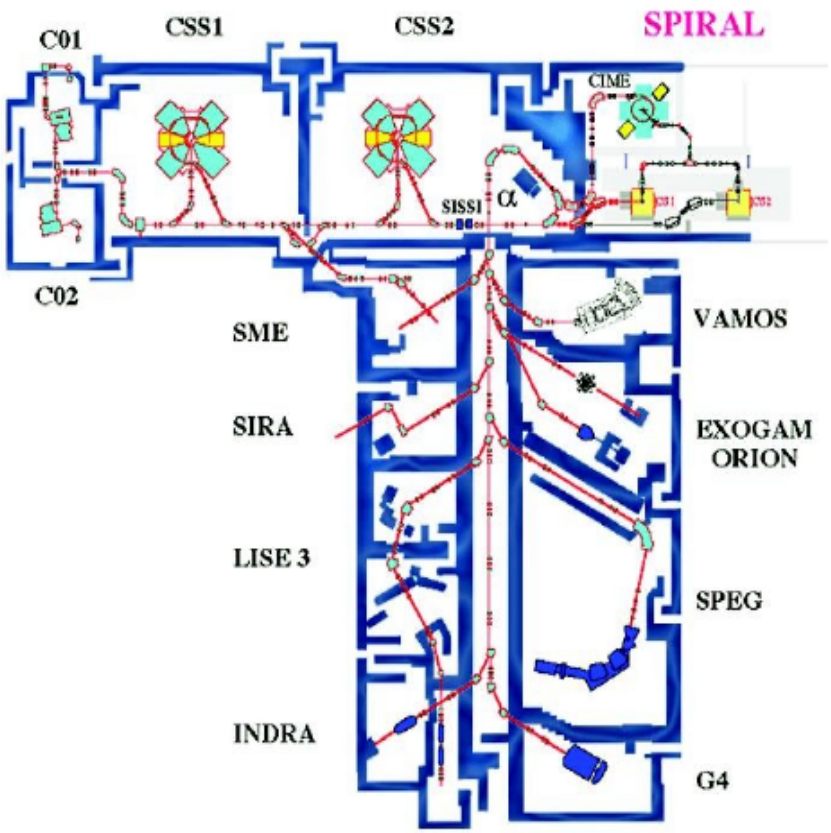

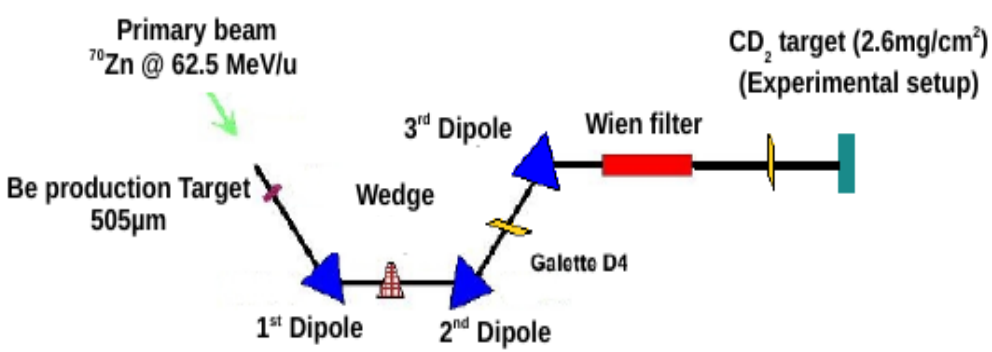

- Primary beam : ^{70}Zn (@62.5 AMeV)
- Primary beam intensity : 1.5 µAe
- Production target : ^{9}Be (505µm, 0°)
- Wedge : ^{9}Be (1099µm)
- Wien filter at 1kV
- Secondary beam intensity ~ 8.10^{4} pps @ 25.14 MeV/u
- **Purity ~ 86%**

Beam production

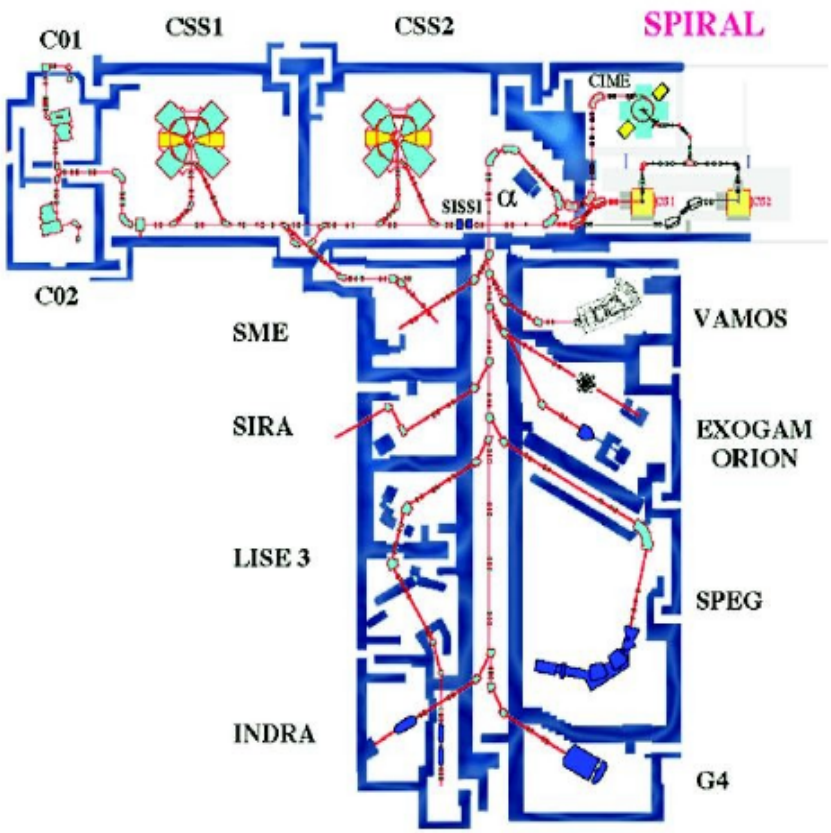

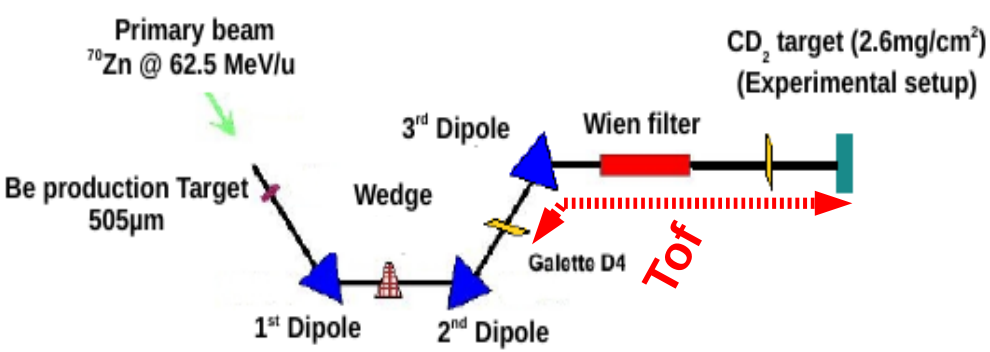

- Primary beam : ^{70}Zn (@62.5 AMeV)
- Primary beam intensity : 1.5 µAe
- Production target : ^{9}Be (505µm, 0°)
- Wedge : ^{9}Be (1099µm)
- Wien filter at 1kV
- Secondary beam intensity ~ 8.10^{4} pps @ 25.14 MeV/u
- **Purity ~ 86%**

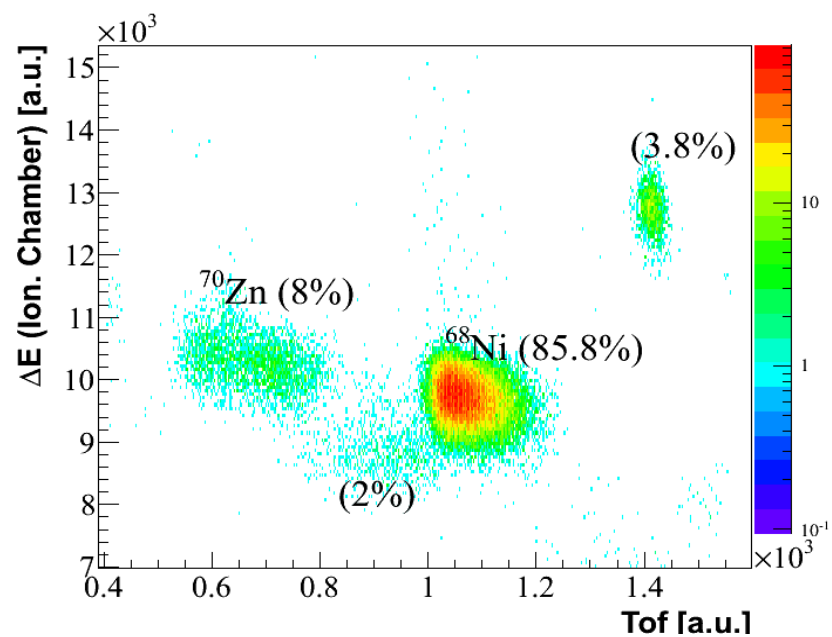

Experimental set-up

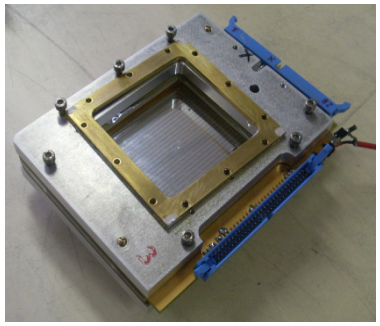

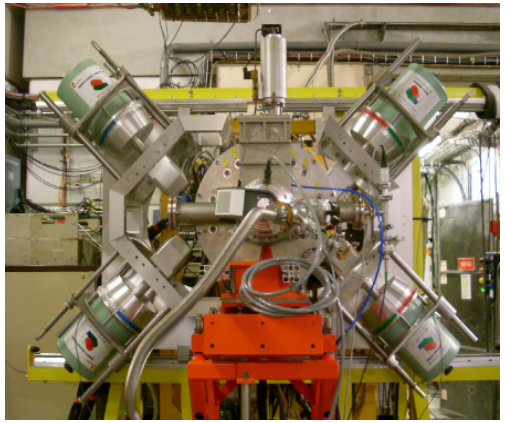

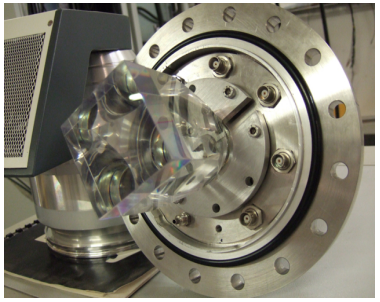

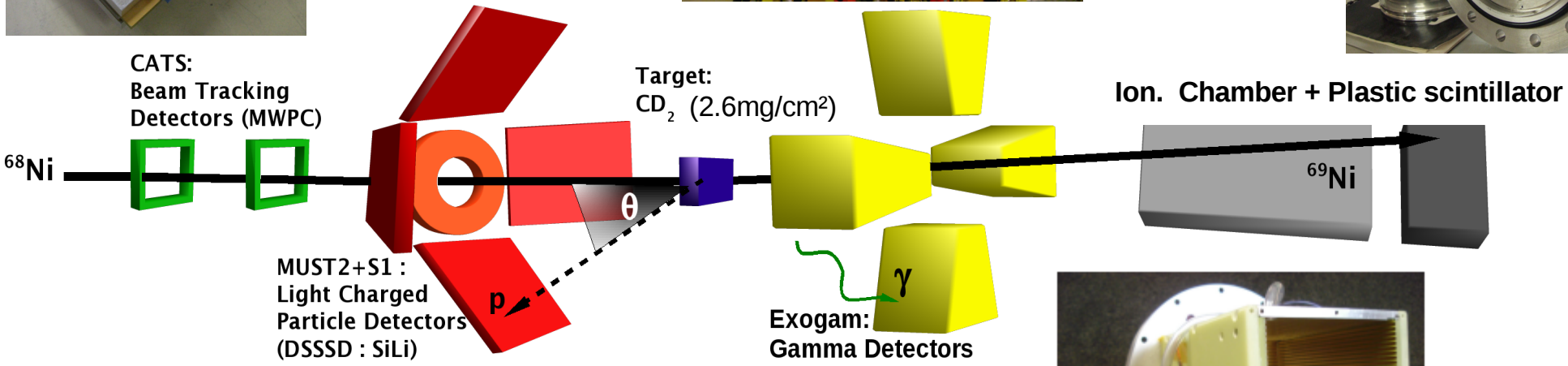

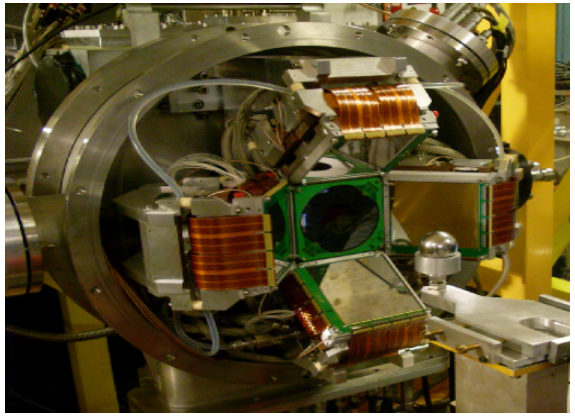

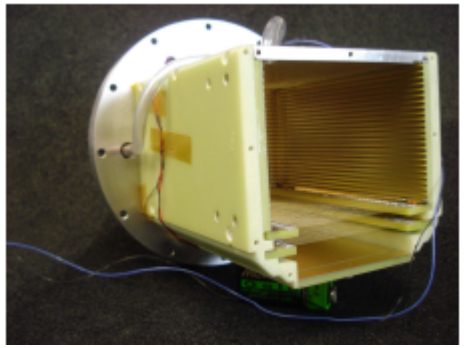

Beam trackers : CATS

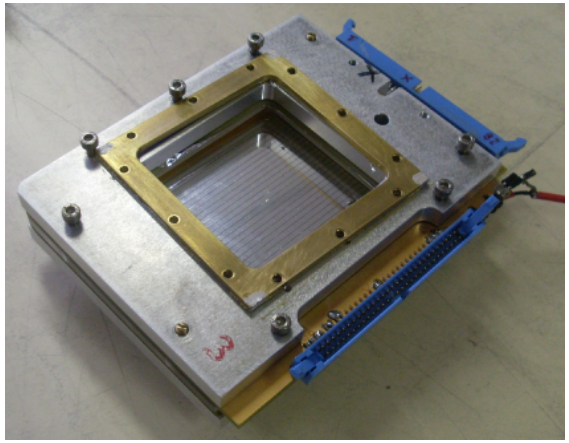

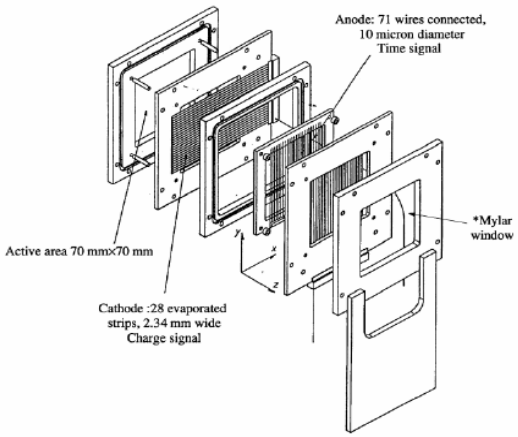

(Ottini-Hustache et al., NIM A, 431, 476, 1999)

- Event by event Reconstruction
- Reconstruction algorithms:
  - Center of gravity
  - **Analytical fit**
- Uncert. ~ 0.65mm (X)
  ~ 0.40 mm (Y)
- Uncert. on incidence angle
  ~ 0.1°
- CATS2 : Time of flight stop signal

$$\overrightarrow{C_1 C_t} = k\,\overrightarrow{C_1 C_2}$$

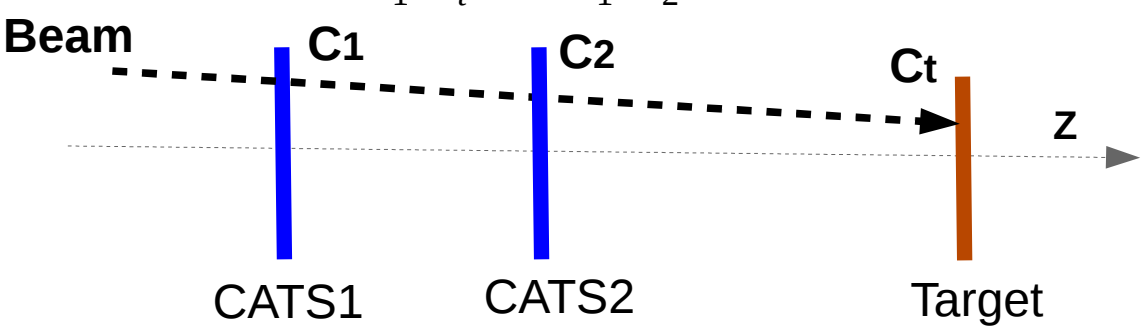

Beam trackers : CATS

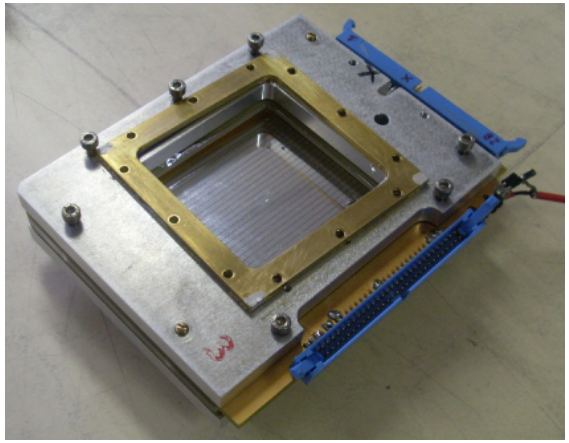

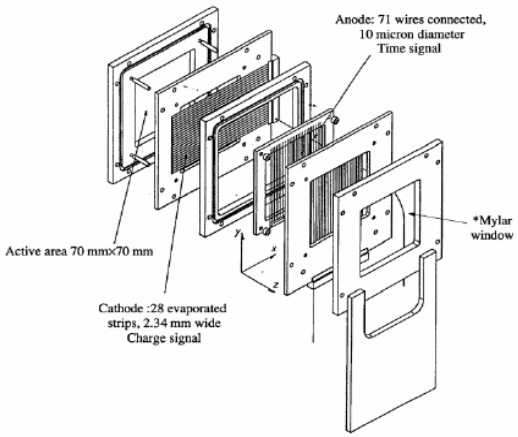

(Ottini-Hustache et al., NIM A, 431, 476, 1999)

- Event by event Reconstruction
- Reconstruction algorithms:
  - Center of gravity
  - **Analytical fit**
- Uncert. ~ 0.65mm (X)
  ~ 0.40 mm (Y)
- Uncert. on incidence angle
  ~ 0.1°
- CATS2 : Time of flight stop signal

$$\overrightarrow{C_1C_t} = k\,\overrightarrow{C_1C_2}$$

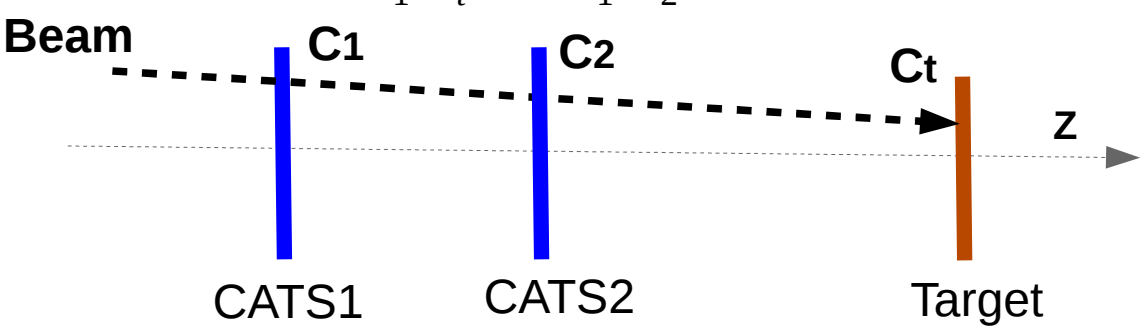

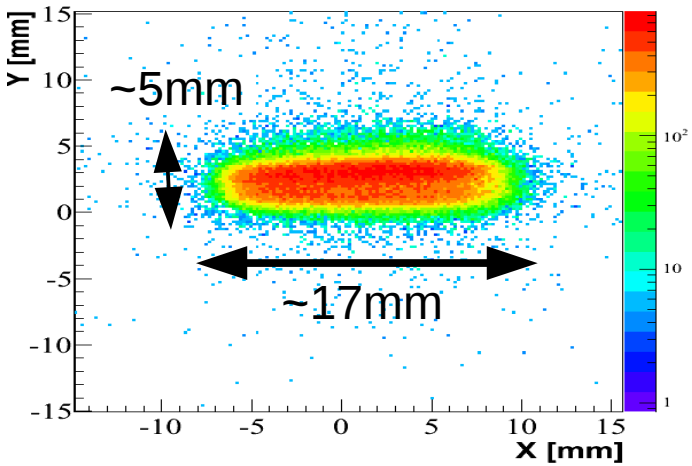

Beam reconstruction
In the target plane

Beam trackers : CATS

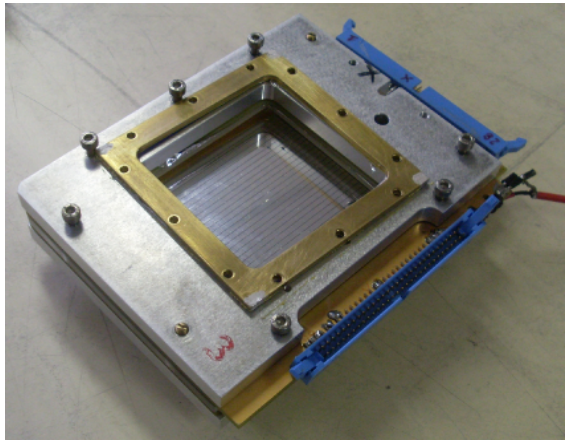

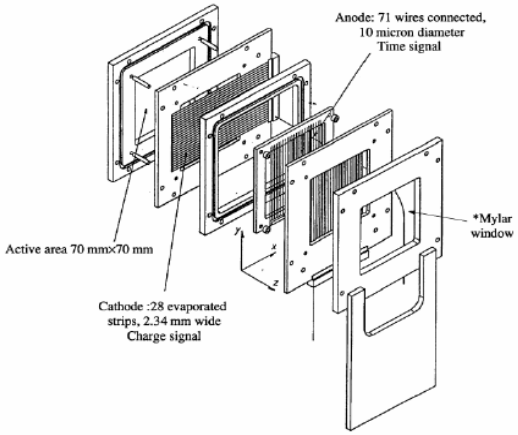

(Ottini-Hustache et al., NIM A, 431, 476, 1999)

- Event by event Reconstruction
- Reconstruction algorithms:
  - Center of gravity
  - **Analytical fit**
- Uncert. ~ 0.65mm (X)
  ~ 0.40 mm (Y)
- Uncert. on incidence angle
  ~ 0.1°
- CATS2 : Time of flight stop signal

$$\overrightarrow{C_1C_t} = k\,\overrightarrow{C_1C_2}$$

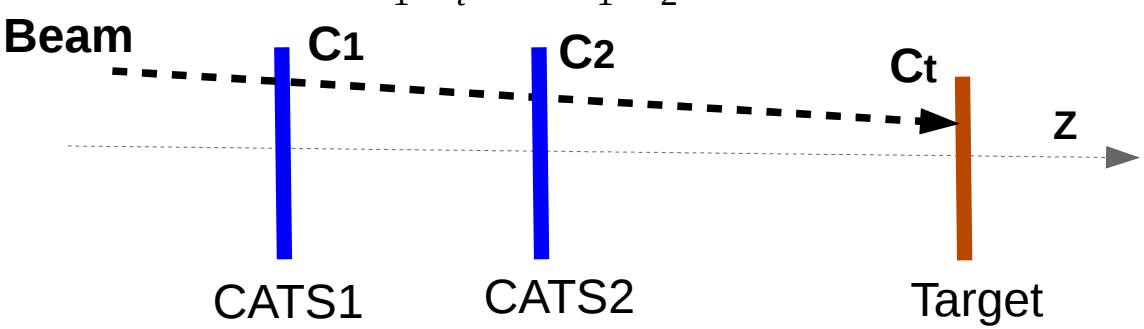

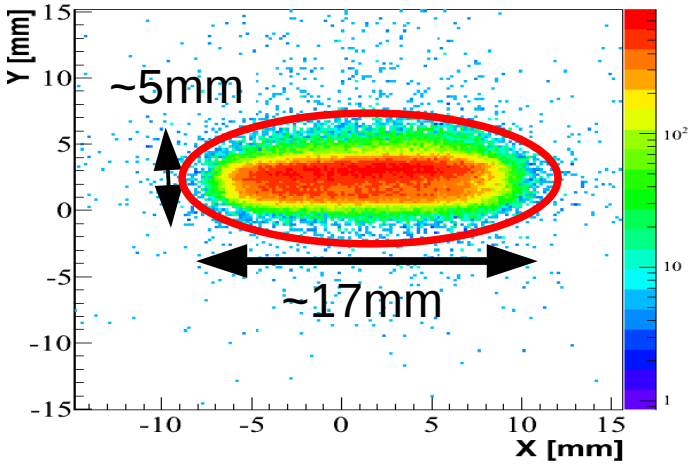

Beam reconstruction
In the target plane

(Ottini-Hustache et al., NIM A, 431, 476, 1999)

Light charged particle detectors : MUST2 and S1

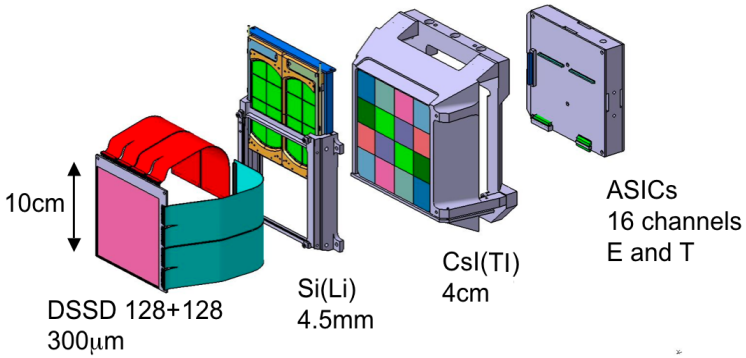

Pollaco et al., NIM A, 25, 287, 2005

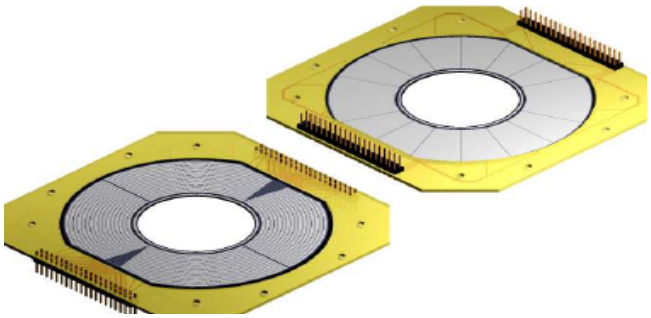

Micron semi-conductors

- DSSD (300 μm)and Si(Li) (4.5 mm)
- Active surface: 100mm*100mm
- 128 strips in X and Y (0.76 mm)

- DSSD (500 μm)
- Active surface : 53mm²
- 64 strip θ, 16 sectors ϕ

MUST2 : DSSD

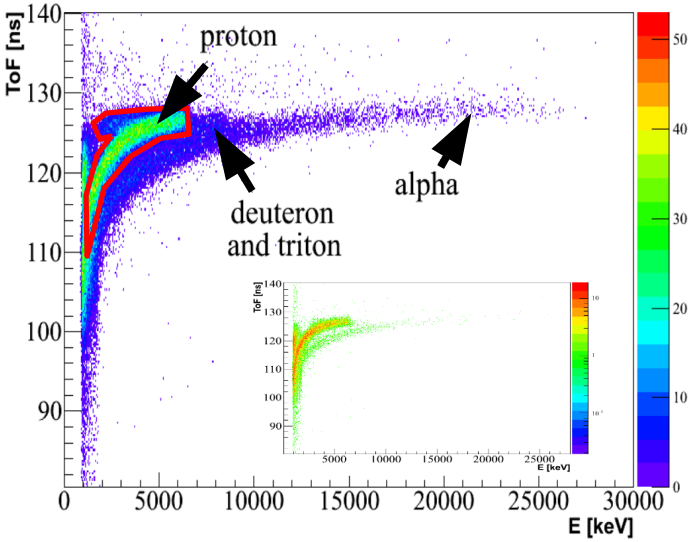

MUST2 : Si(Li)

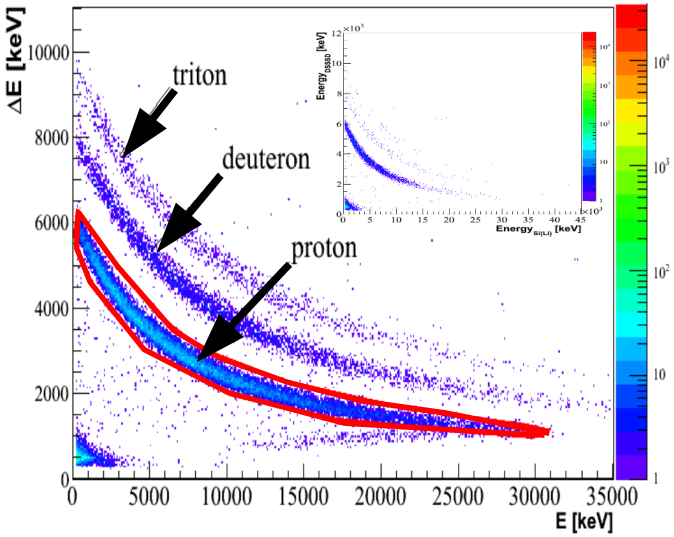

S1: DSSD

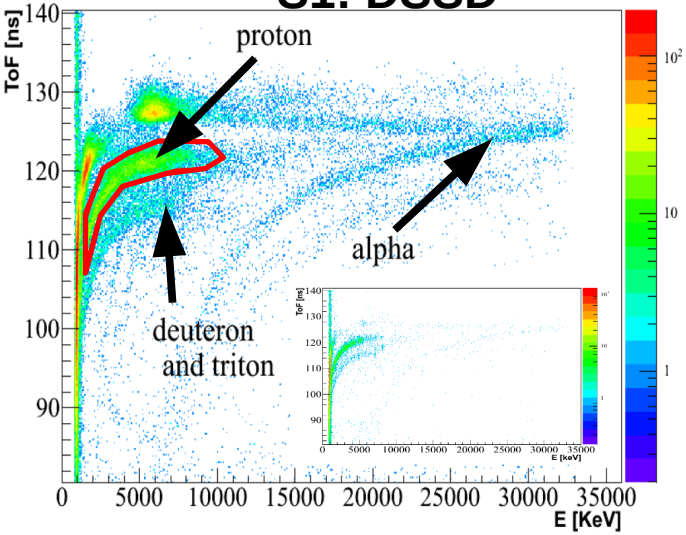

Heavy residue detector

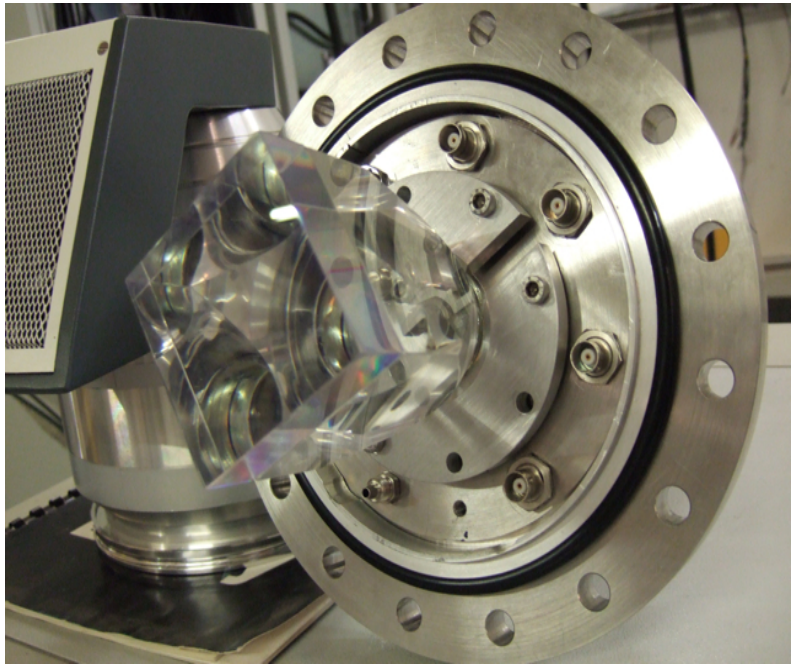

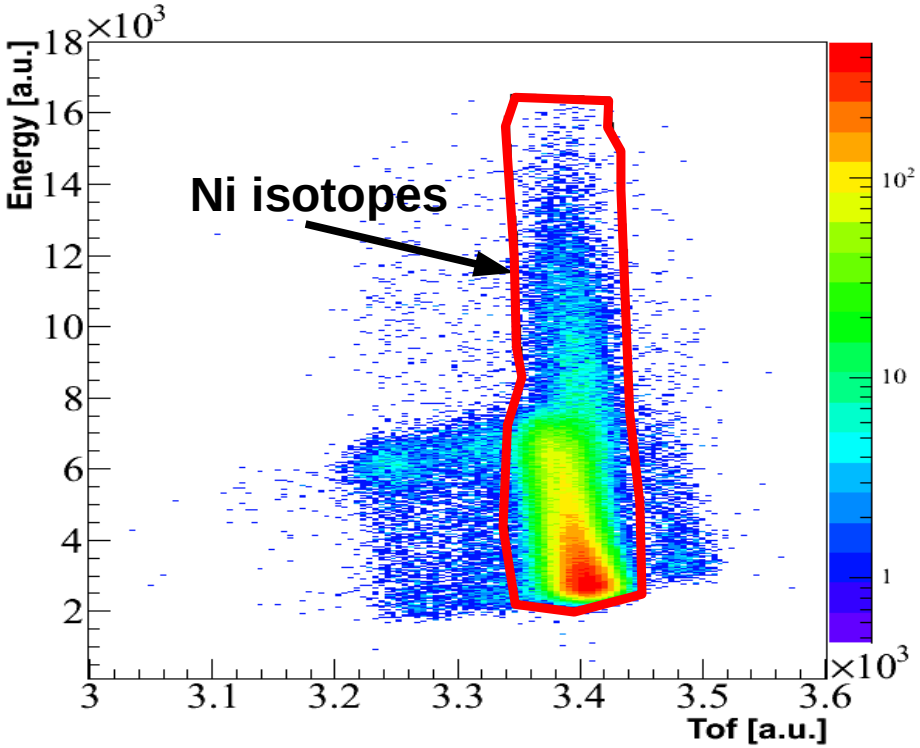

- Plastic scintillator
- Active surface : 60mm*60mm
- Energy and time (ToF)

Excitation energy spectrum

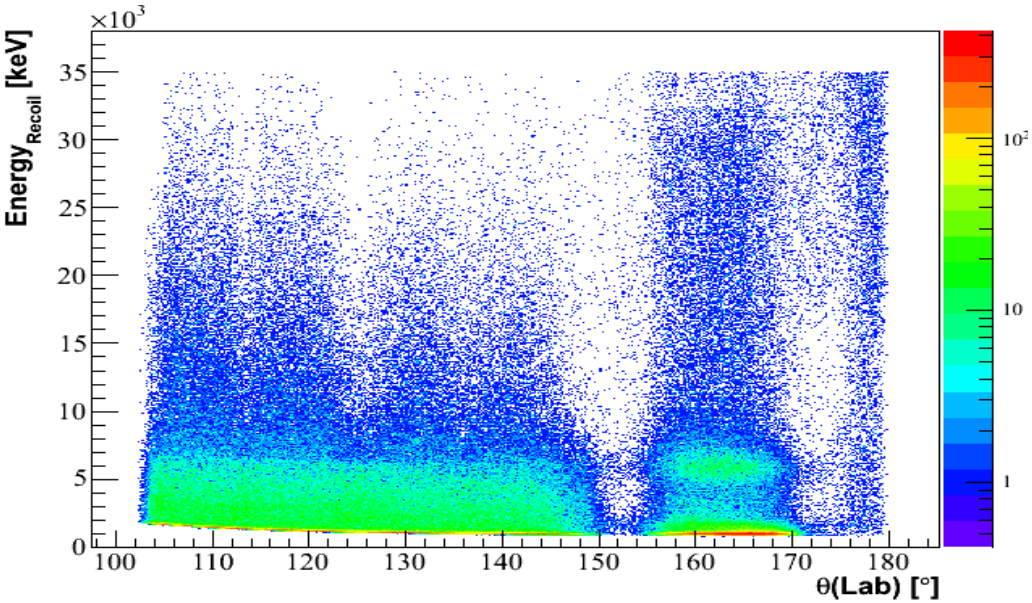

Excitation energy spectrum

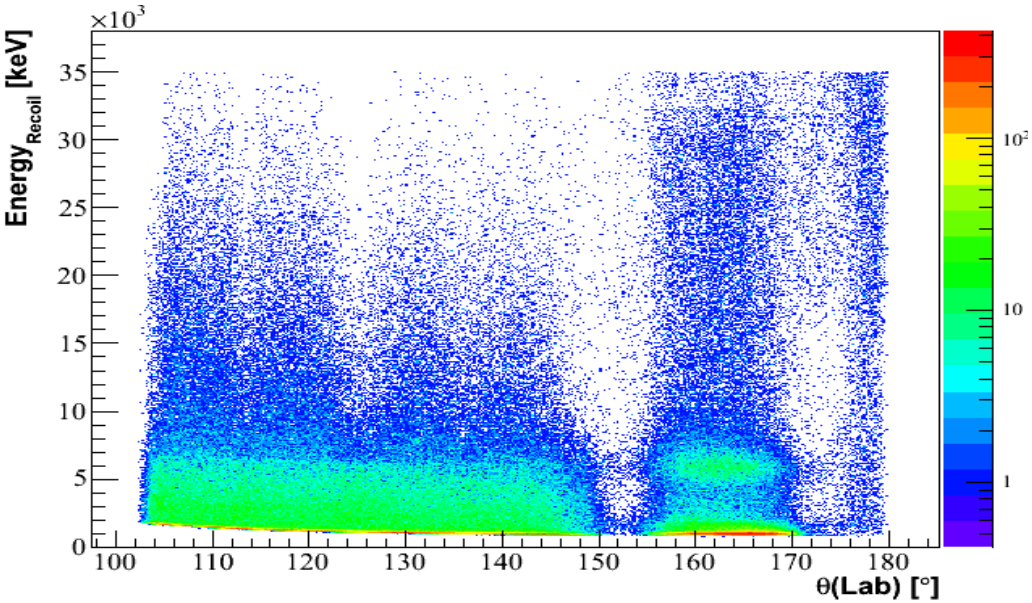

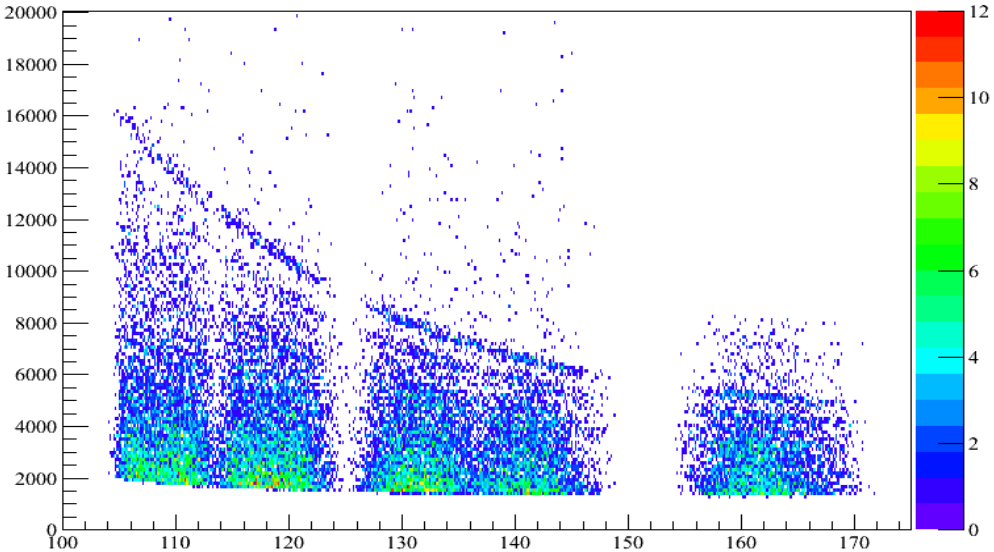

Excitation energy spectrum

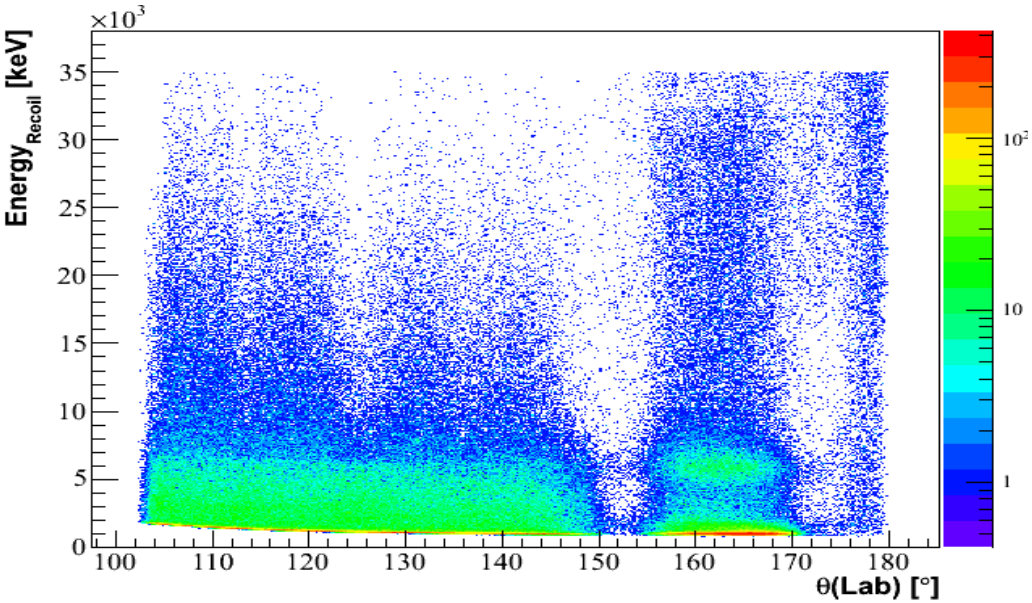

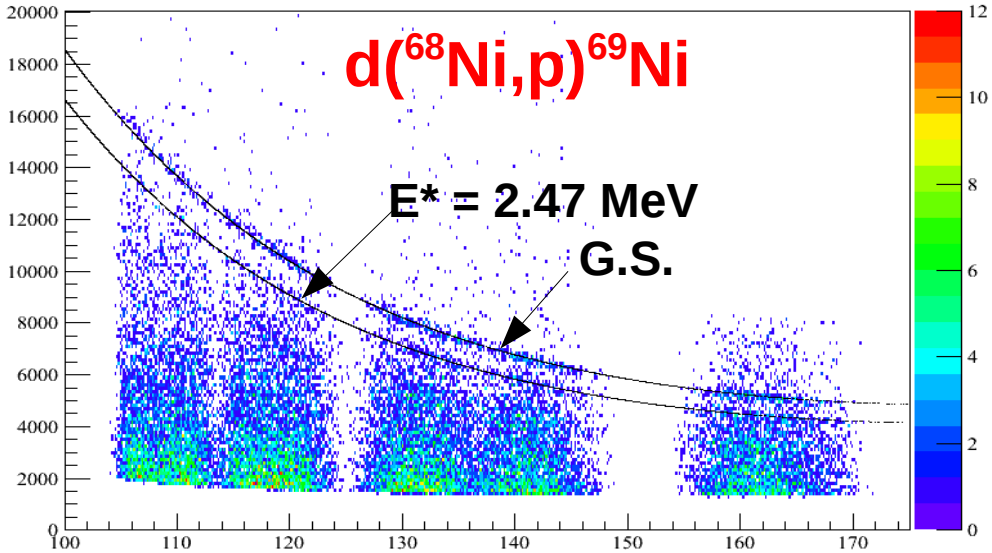

Excitation energy spectrum

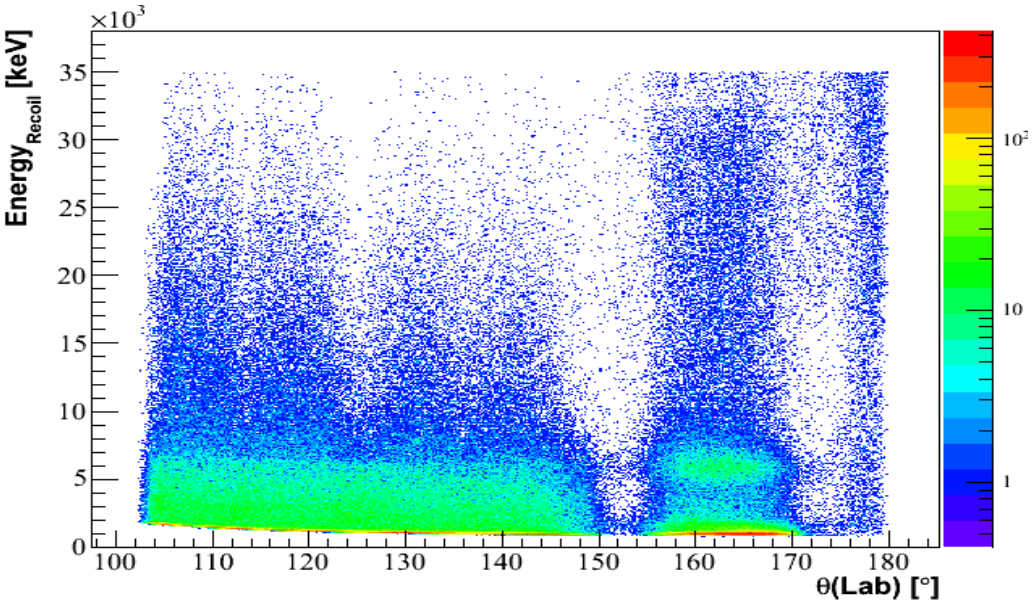

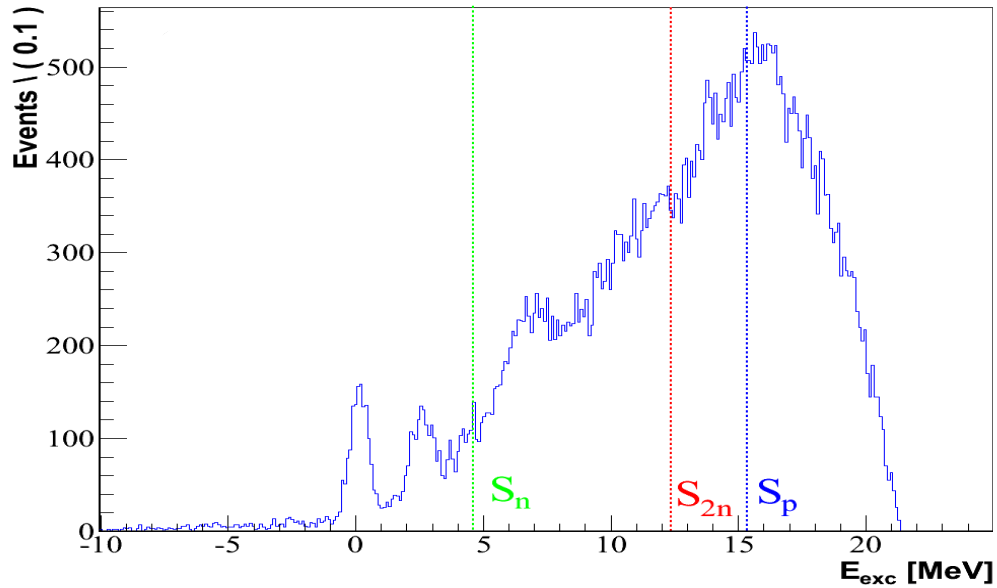

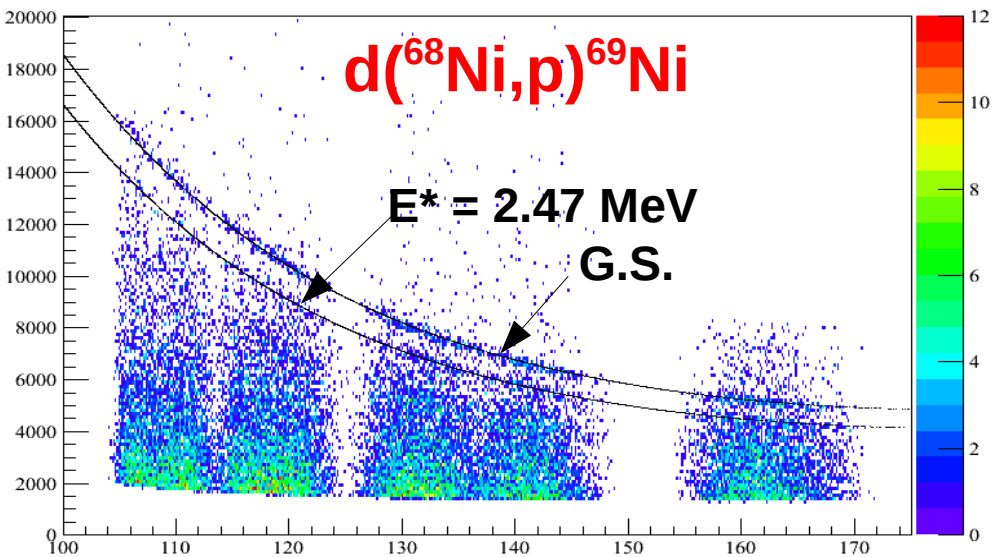

- Pronounced G.S.
- 1st excited state at ~ 2.5 MeV
- Structures ~ 4 MeV and 6−7 MeV (> S_n)

Excitation energy spectrum

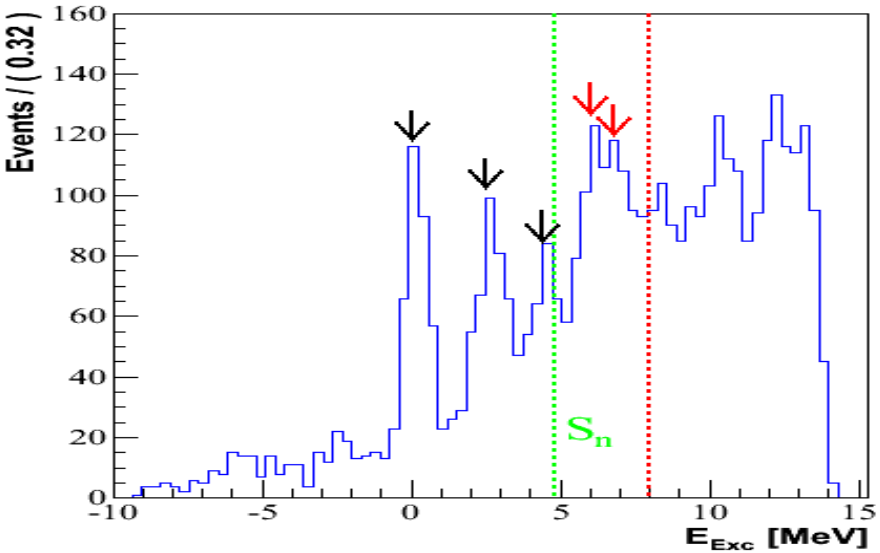

- 3 bound states
- 2 resonances above S_n

Energy reference : S1 [156°-170°]

Excitation energy spectrum

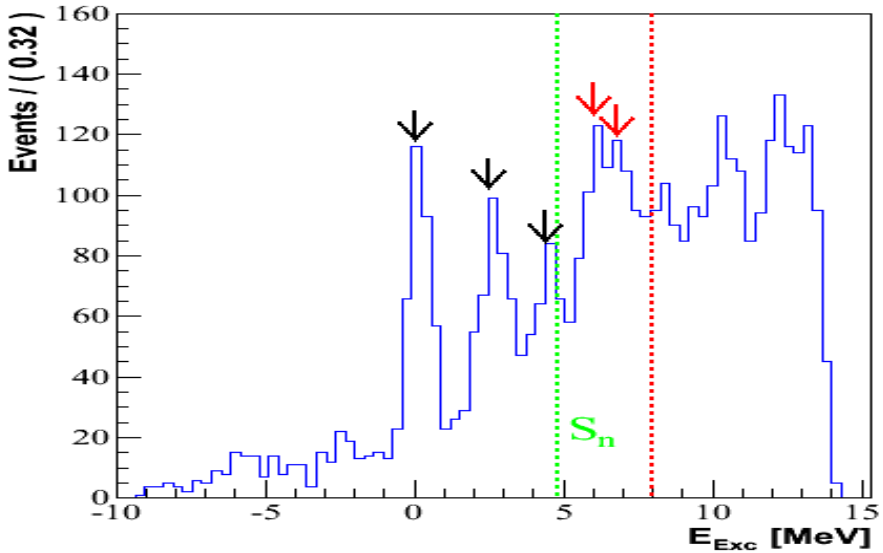

- 3 bound states
- 2 resonances above S_n
- Background reactions

Energy reference : S1 [156°-170°]

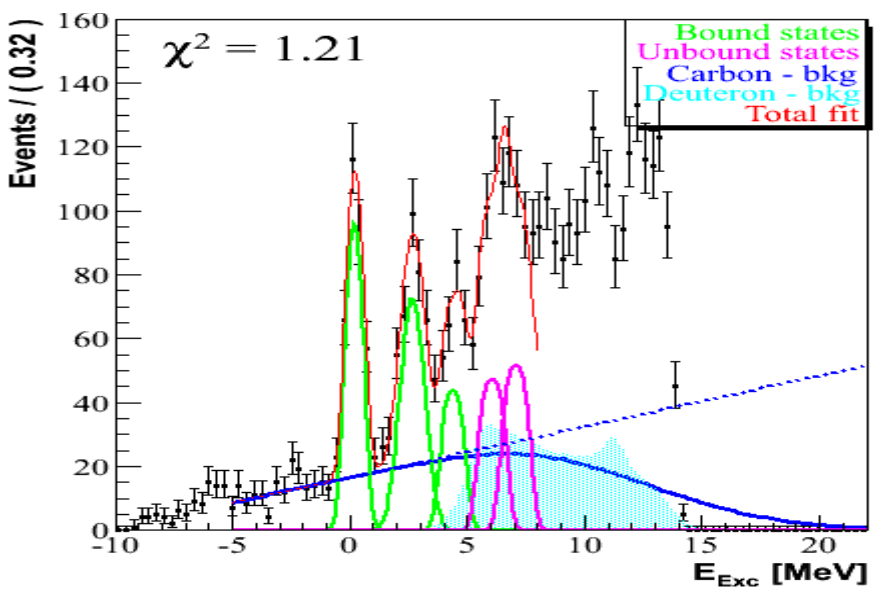

Pic #	Energy [MeV]	FWHM [MeV]
G.S	0.00	1.04
1	2.47	**1.43**
2	4.19	1.27
3	5.88	1.39
4	6.89	1.39

Excitation energy spectrum

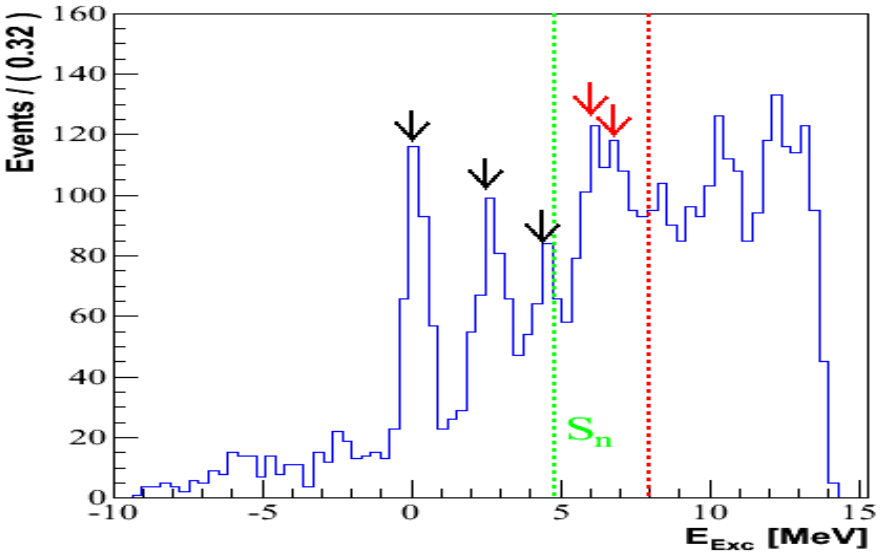

- 3 bound states
- 2 resonances above S_n
- Background reactions

⇒ 6 angular ranges

Energy reference : S1 [156°-170°]

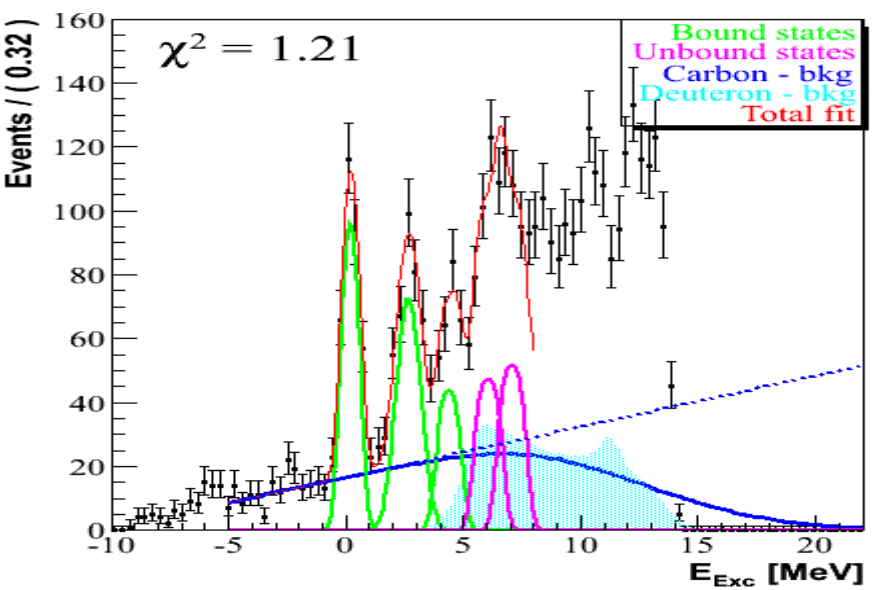

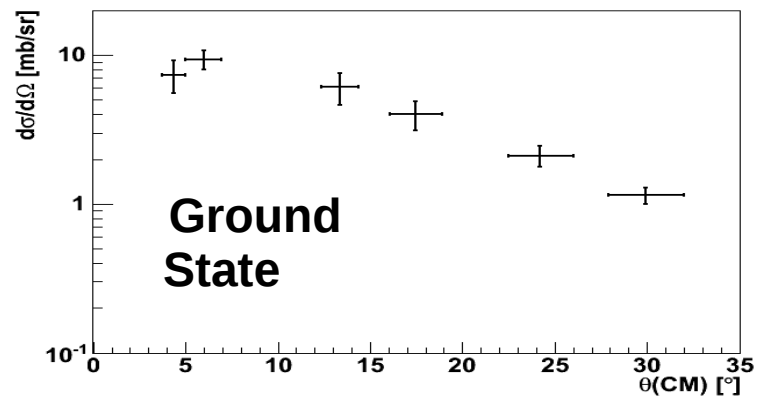

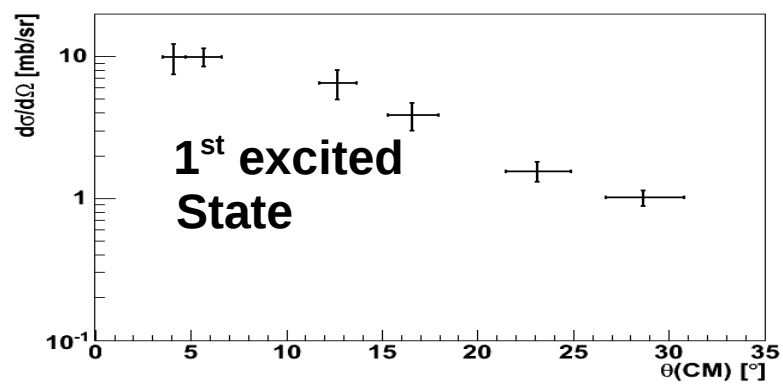

Distorted Waves Born Approximation (DWBA)

- **Code DWUCK4, Zero-Range approximation**
- **Elastic channel ⇒ Global optical potentials**
  - **^{68}Ni + d :**
    - » **E1**: $27 < A < 238$, $12\ \text{MeV} < E_d < 90\ \text{MeV}$

      Daehnick et al. PRC, 21, 2253, 1981
    - » **E2**: Adiabatic Distorted Waves Approximation (ADWA) for the deuteron break-up

      pour $E_d > 20$ MeV : $V = V_p + V_n + V_{pn}$ ($E_n = E_p = E_d/2$)

      Johnson and Soper, PRC, 1, 976, 1970
  - **^{69}Ni + p :**
    - » **S1**: $40 < A < 209$, $16\ \text{MeV} < E_p < 65\ \text{MeV}$

      Varner et al. Phys. Reports, 201, 57, 1991
    - » **S2**: $24 < A < 209$, $1\ \text{keV} < E_p < 200\ \text{MeV}$

      Koning and Delaroche. Nucl. Phys. A, 713, 231, 2003

Analysed differential cross sections : Ground state

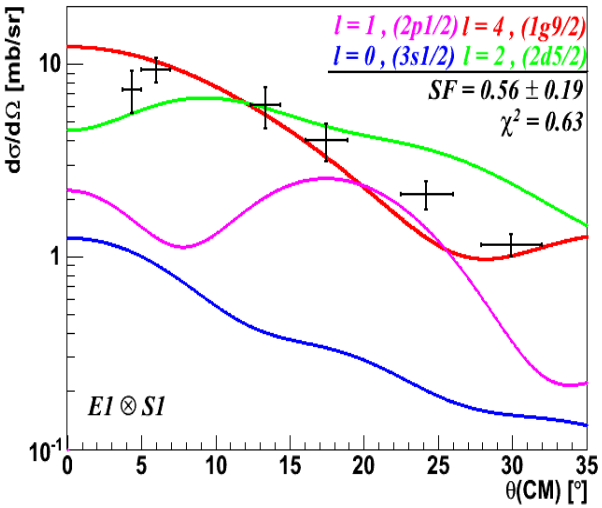

E1 ⊗ S1

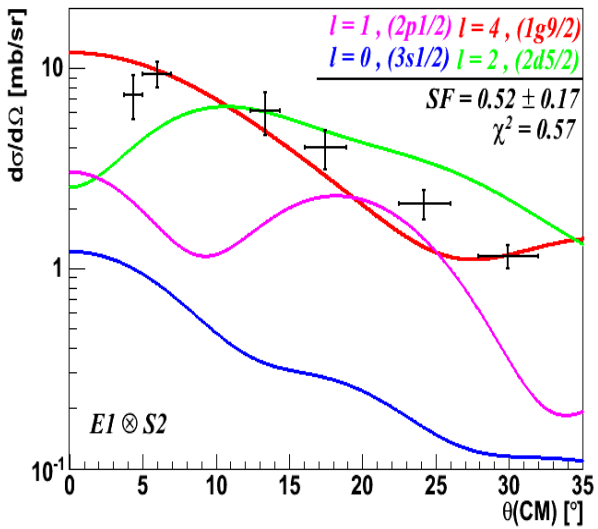

E1 ⊗ S2

- 4 combinations of optical pot.
- G.S. : L = 0, 1, 2 and 4
  - ➔ **L = 4, SF = 0.56±0.19**

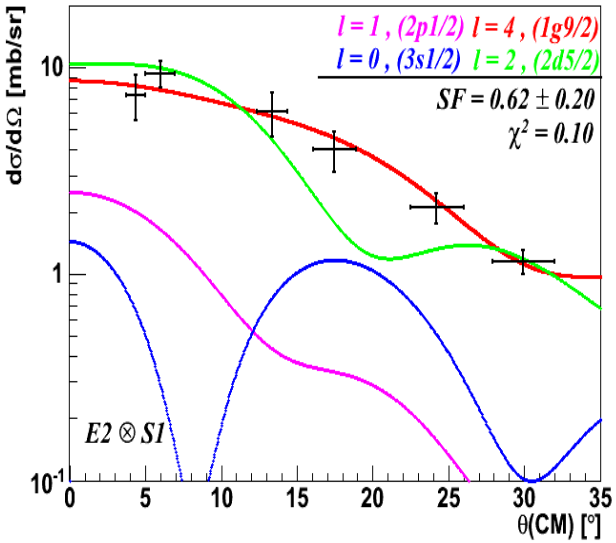

E2 ⊗ S1

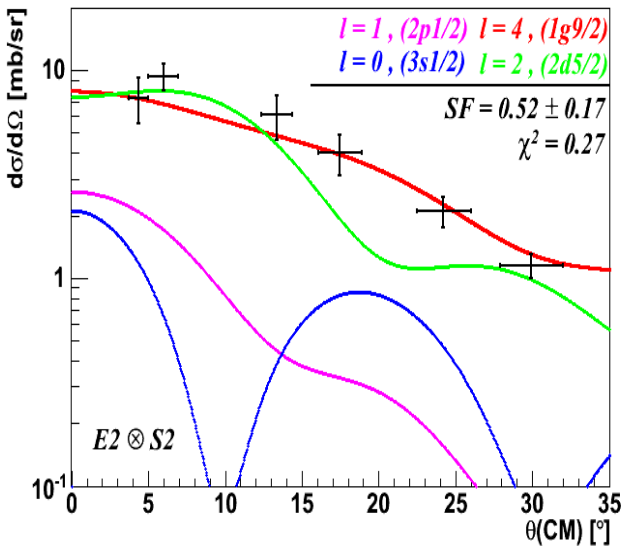

E2 ⊗ S2

Analysed differential cross sections : Ground state

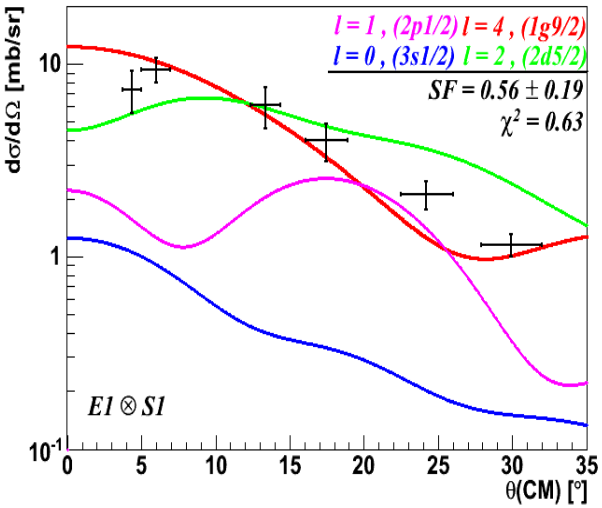

E1 ⊗ S1

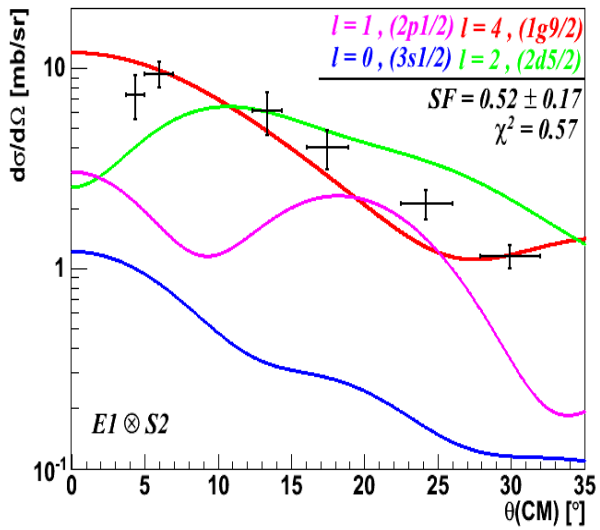

E1 ⊗ S2

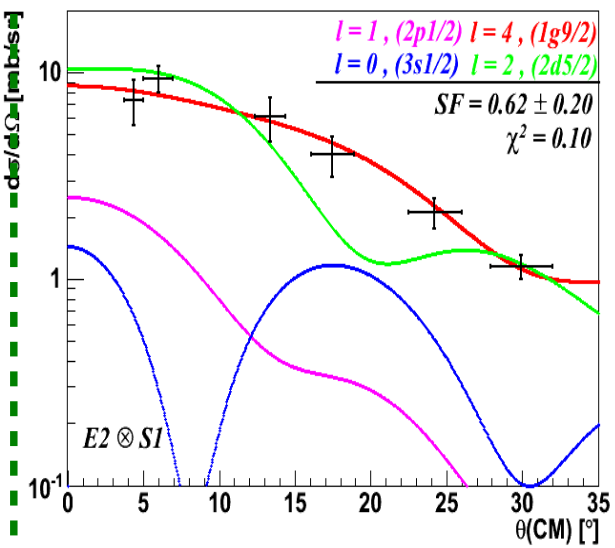

E2 ⊗ S1

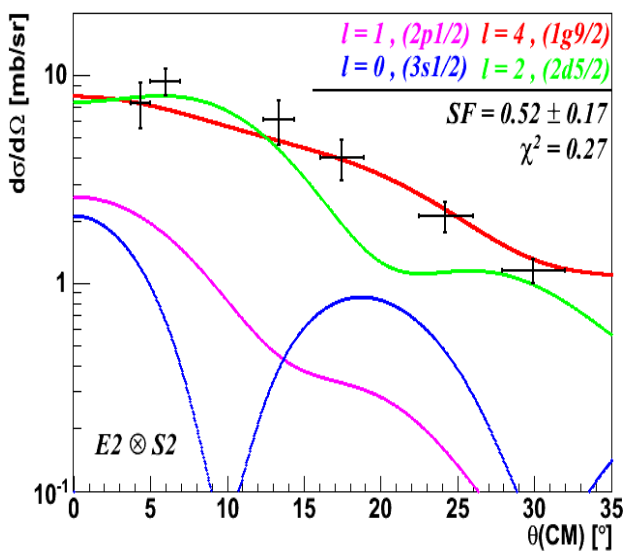

E2 ⊗ S2

- 4 combinations of optical pot.
- G.S. : L = 0, 1, 2 and 4
  - → **L = 4, SF = 0.56±0.19**

- Weak dependency according to the exit pot. parameterization
- Significant dependency according to the entrance pot. parameterization

Analysed differential cross sections : Ground state

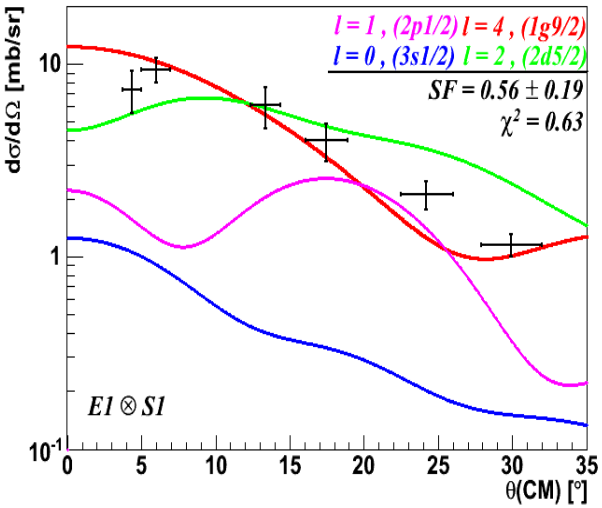

E1 ⊗ S1

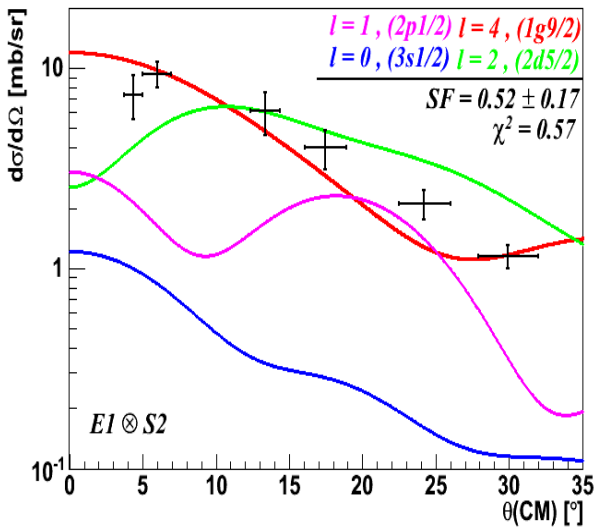

E1 ⊗ S2

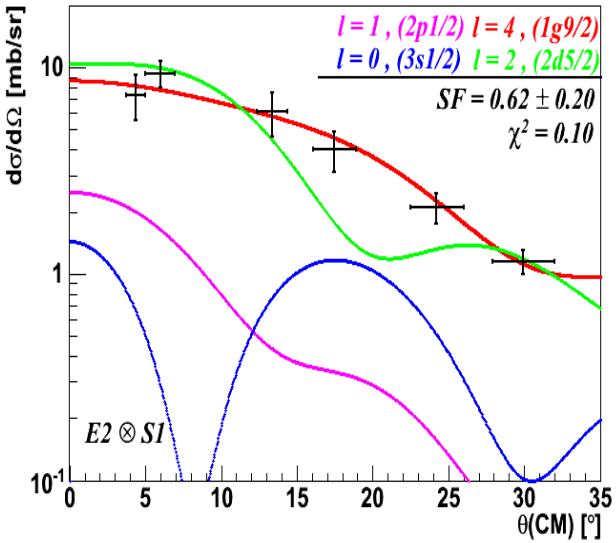

E2 ⊗ S1

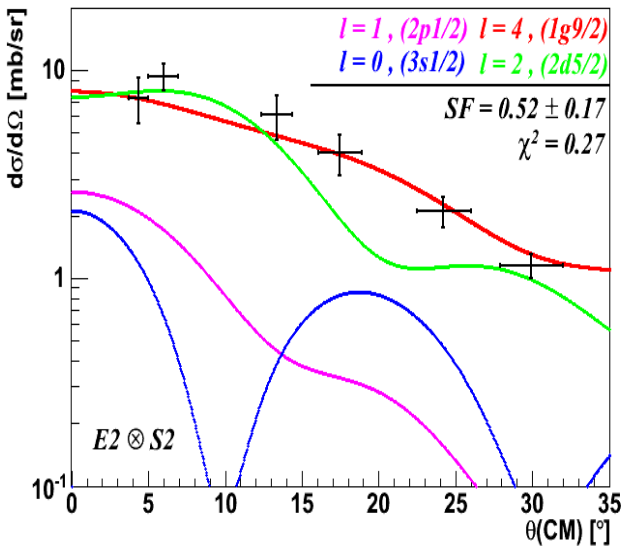

E2 ⊗ S2

- 4 combinations of optical pot.
- G.S. : L = 0, 1, 2 and 4
  - → **L = 4, SF = 0.56±0.19**

- Weak dependency according to the exit pot. parameterization
- Significant dependency according to the entrance pot. parameterization

Analysed differential cross sections : Ground state

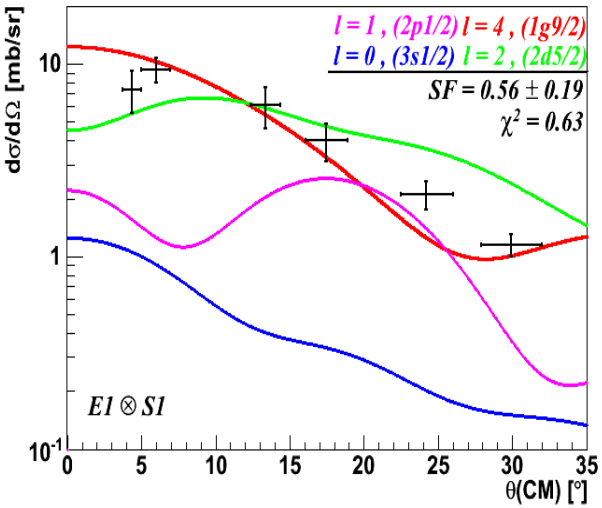

E1 ⊗ S1

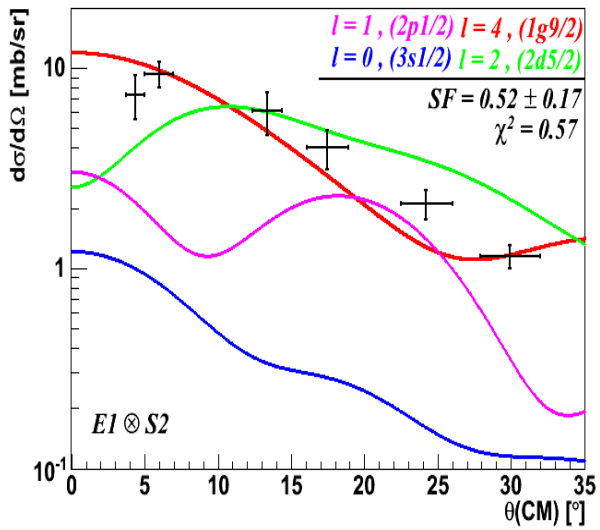

E1 ⊗ S2

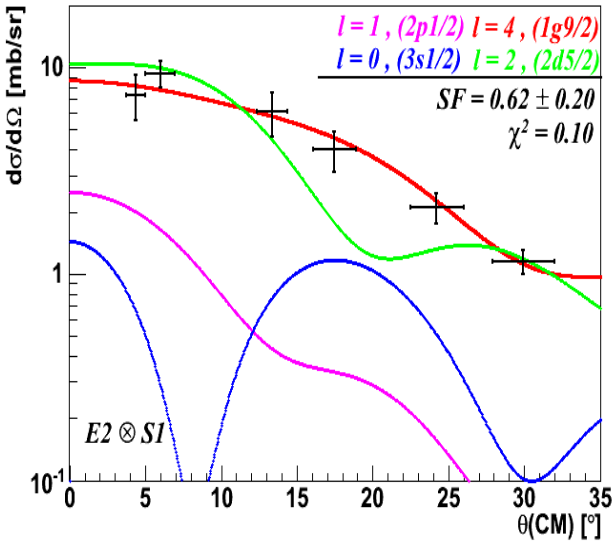

E2 ⊗ S1

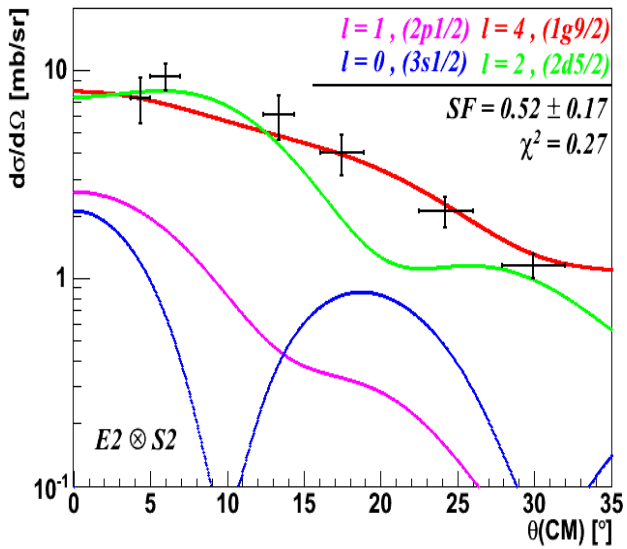

E2 ⊗ S2

- 4 combinations of optical pot.
- G.S. : L = 0, 1, 2 and 4
  - → **L = 4, SF = 0.52 ± 0.17**

- Weak dependency according to the exit pot. parameterization
- Significant dependency according to the entrance pot. parameterization

⇒ Adiabatic potential (E2 ⊗ S2)

Analysed differential cross sections : 1st excited state

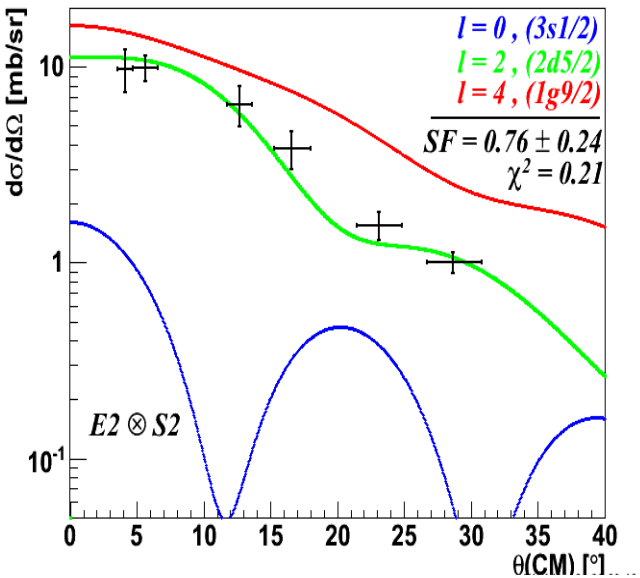

- L = 0, 2 and 4
- E_{exc} = 2.47 MeV
  - → **L = 2, SF = 0.76 ± 0.24**

Analysed differential cross sections : 1st excited state

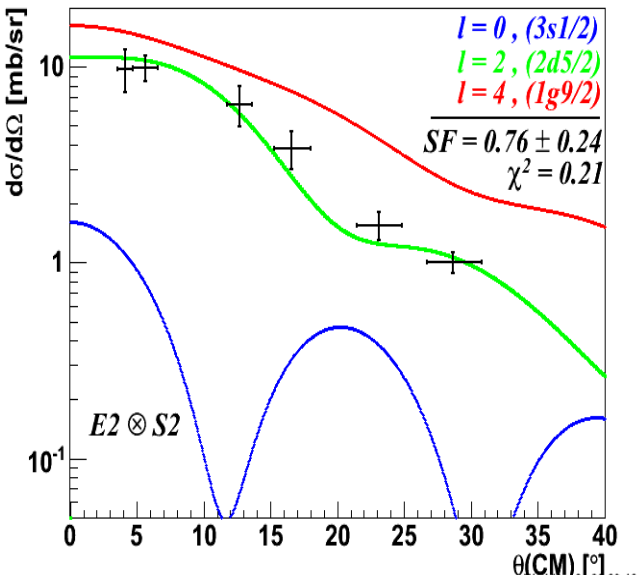

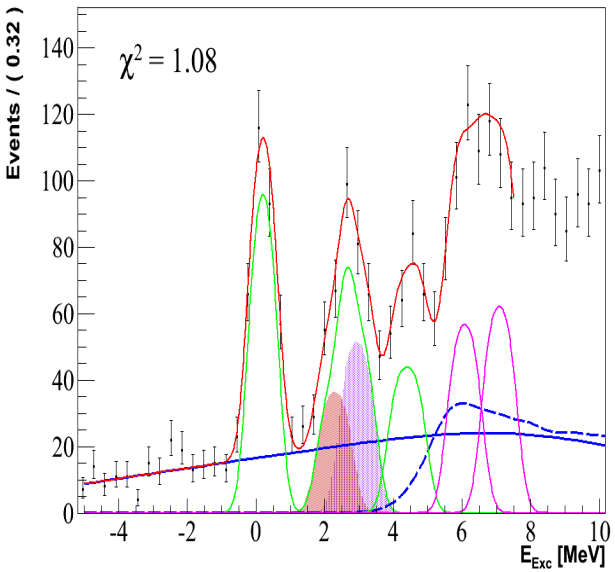

- L = 0, 2 and 4
- E_{exc} = 2.47 MeV
  - → **L = 2, SF = 0.76 ± 0.24**

Analysed differential cross sections : 1st excited state

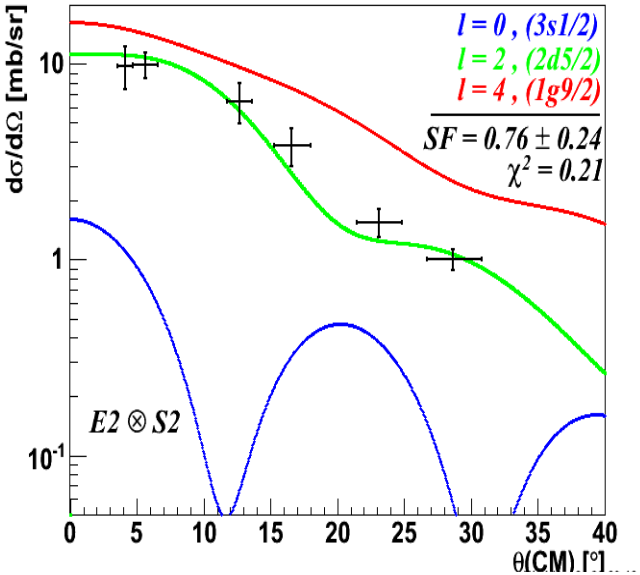

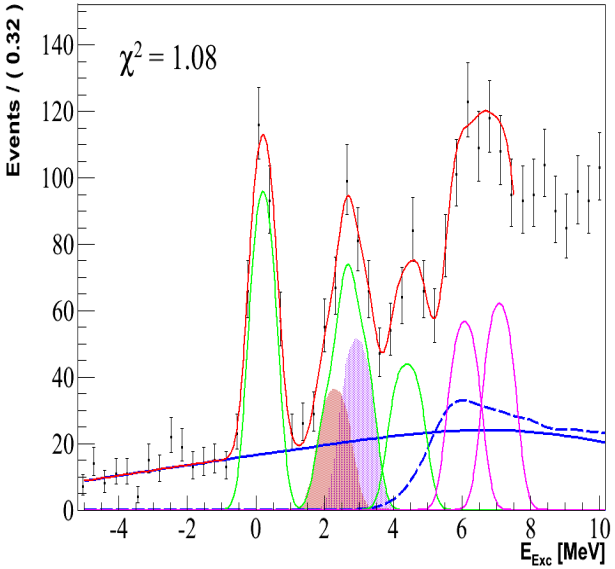

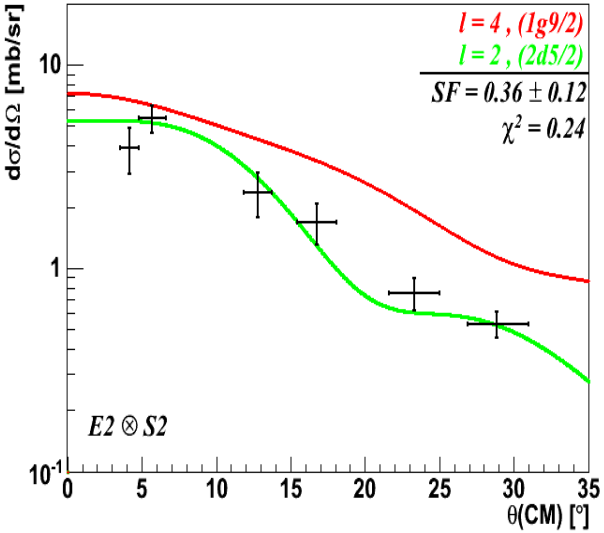

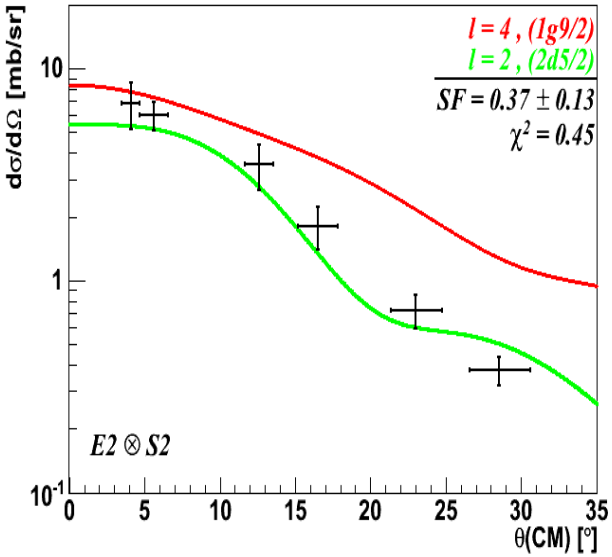

- L = 0, 2 and 4
- E_{exc} = 2.47 MeV
  - → **L = 2, SF = 0.76 ± 0.24**

→ E_{exc} = 2.11 MeV
  - → **L = 2, SF = 0.36 ± 0.12**

→ E_{exc} = 2.76 MeV
  - → **L = 2, SF = 0.37 ± 0.13**

Shell-model calculations

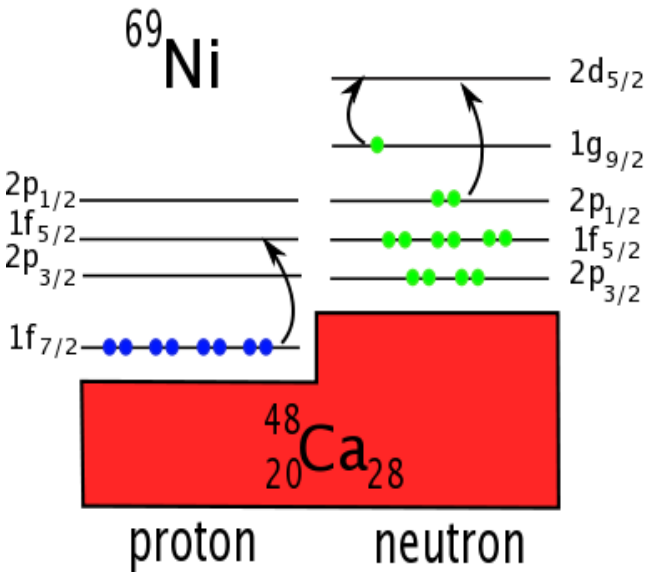

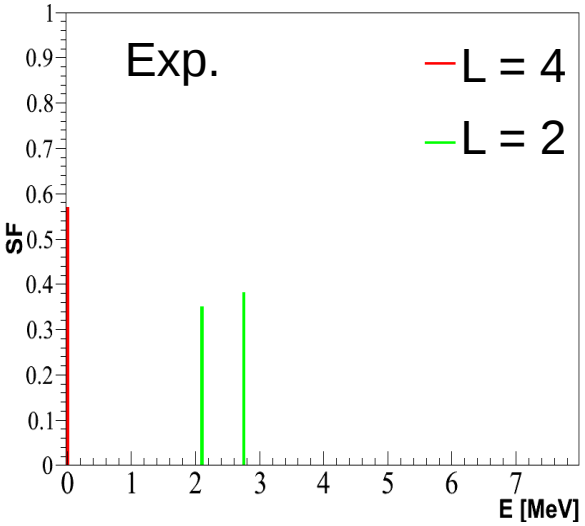

- LNPS Interaction
- fp shell + $1g_{9/2}$ and $2d_{5/2}$

Lenzi et al., PRC 82, 054301, 2010
Sieja and Nowacki, submitted

Shell-model calculations

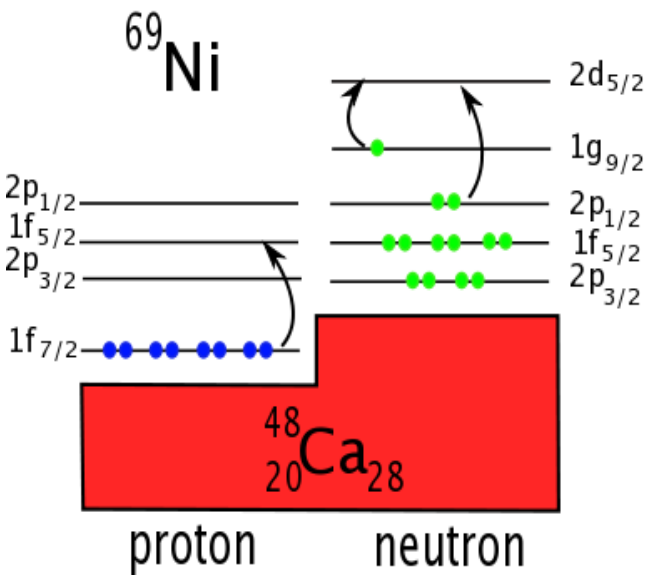

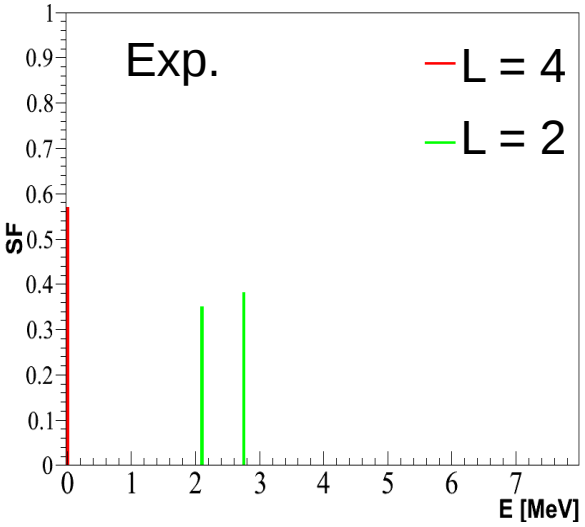

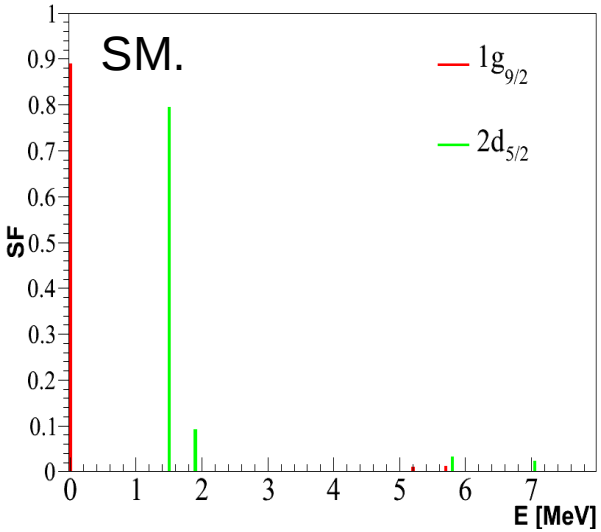

- LNPS Interaction
- fp shell + $1g_{9/2}$ and $2d_{5/2}$

Lenzi et al., PRC 82, 054301, 2010
Sieja and Nowacki, submitted

- Good overall agreement
- $1g_{9/2}$: Large SF at 0 MeV
- $2d_{5/2}$: Doublet of $5/2^+$ states

Shell-model calculations

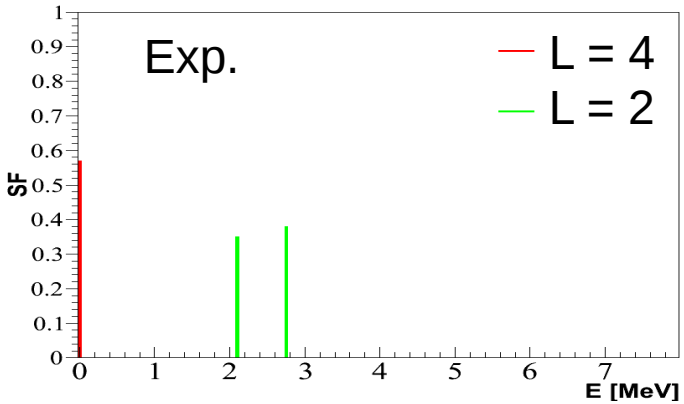

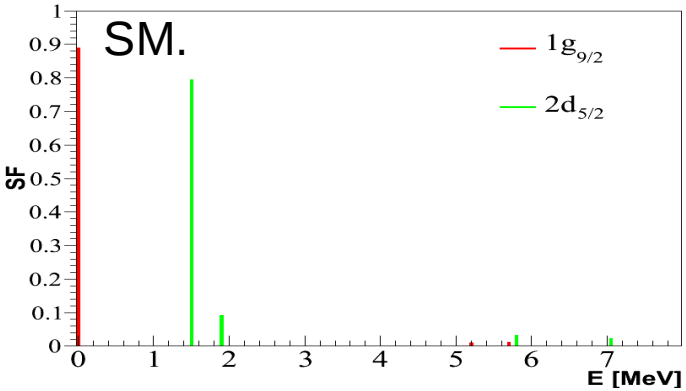

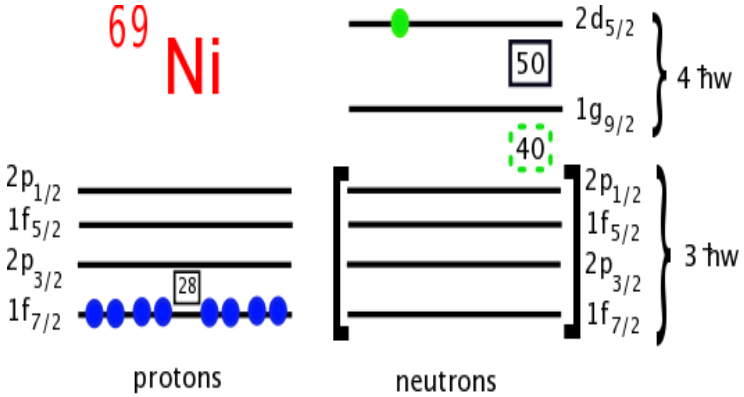

ϕ_1

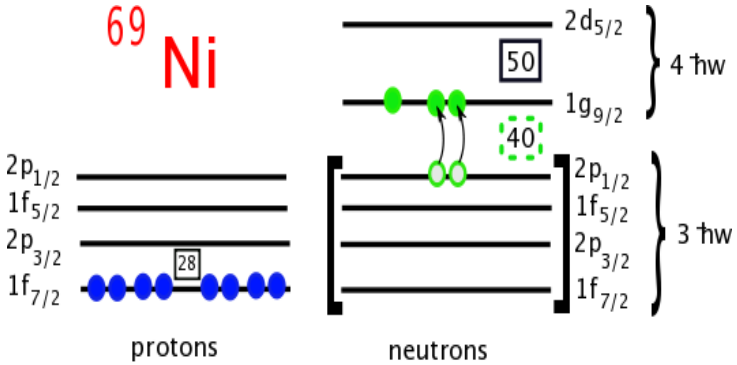

ϕ_2

Shell-model calculations

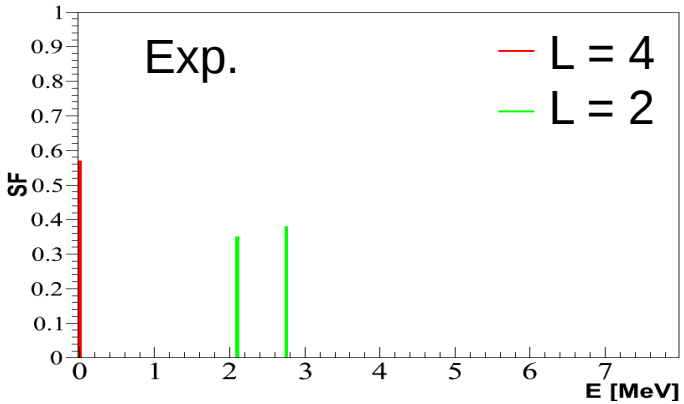

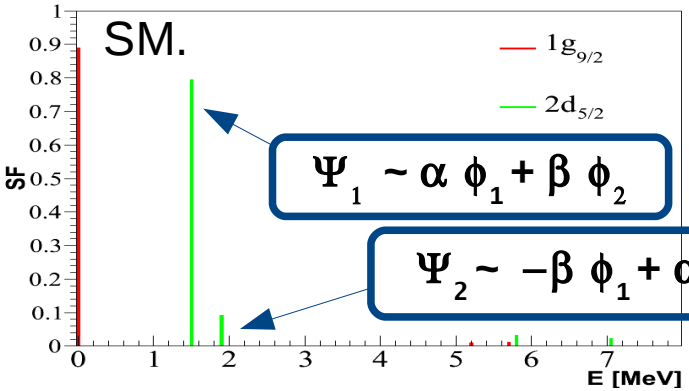

$$\Psi_1 \sim \alpha\, \phi_1 + \beta\, \phi_2$$

$$\Psi_2 \sim -\beta\, \phi_1 + \alpha\, \phi_2$$

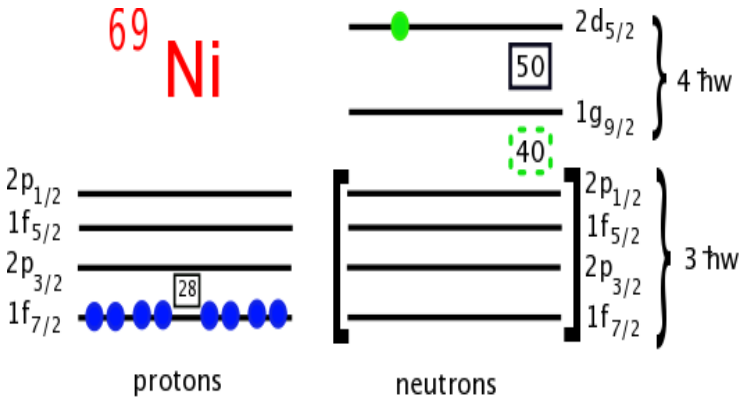

$$\phi_1$$

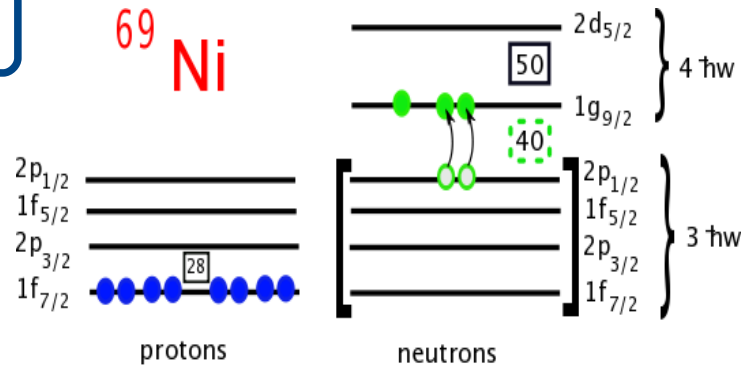

$$\phi_2$$

Shell-model calculations

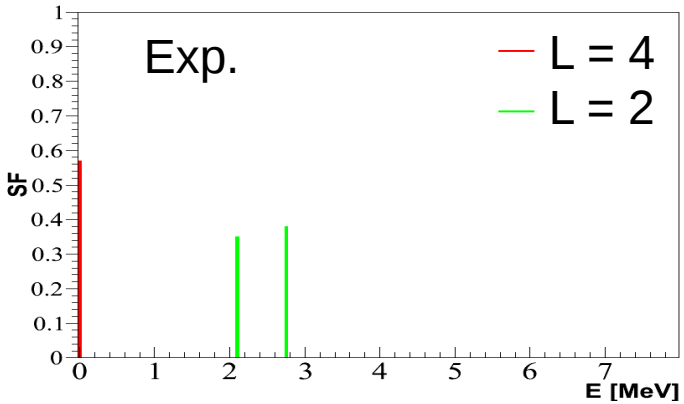

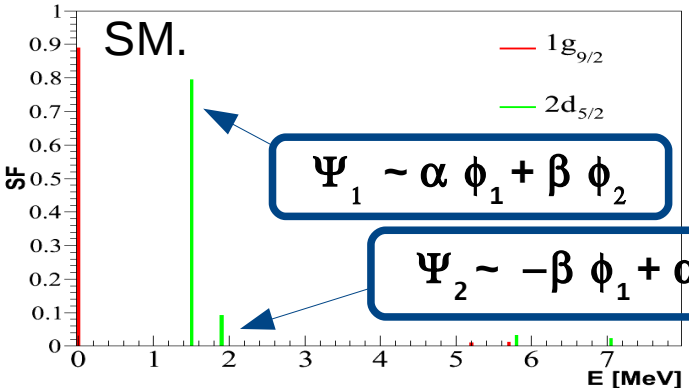

$$\Psi_1 \sim \alpha\, \phi_1 + \beta\, \phi_2$$

$$\Psi_2 \sim -\beta\, \phi_1 + \alpha\, \phi_2$$

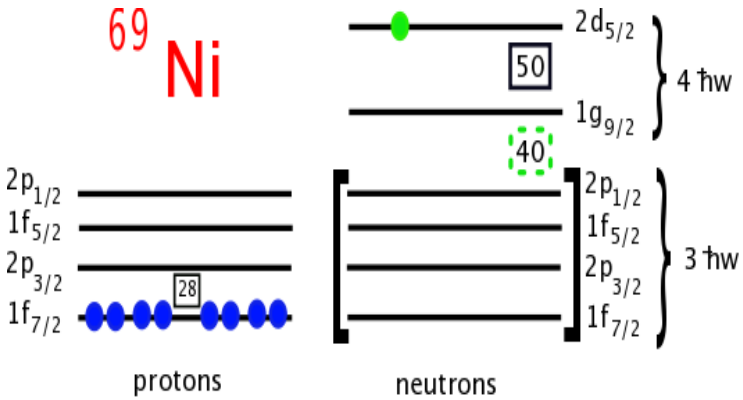

ϕ_1

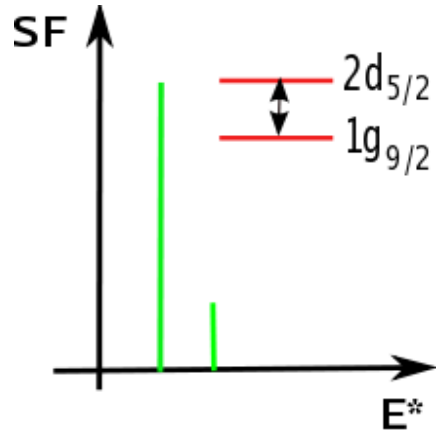

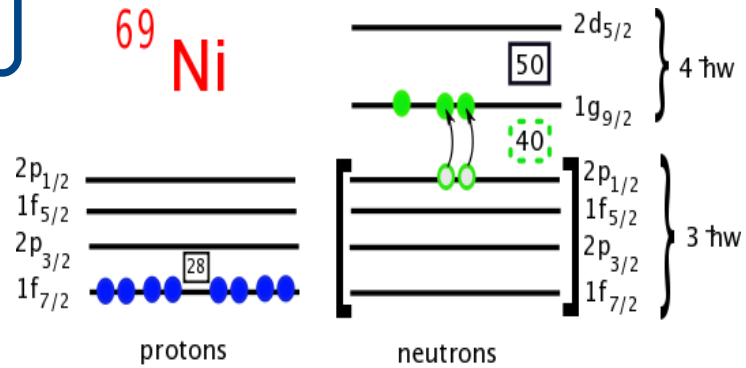

ϕ_2

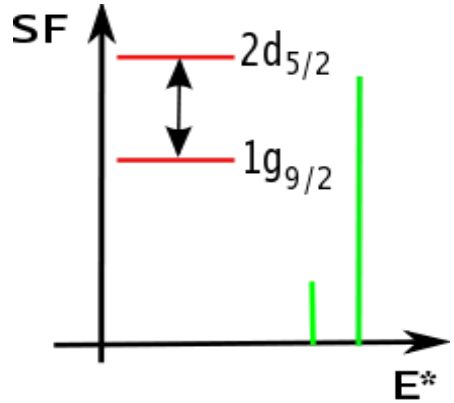

Shell-model calculations

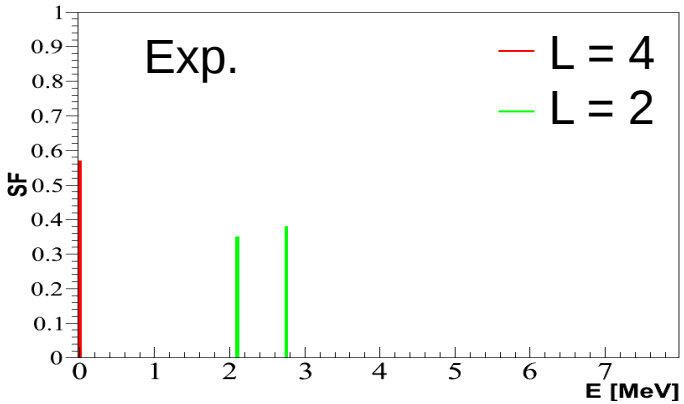

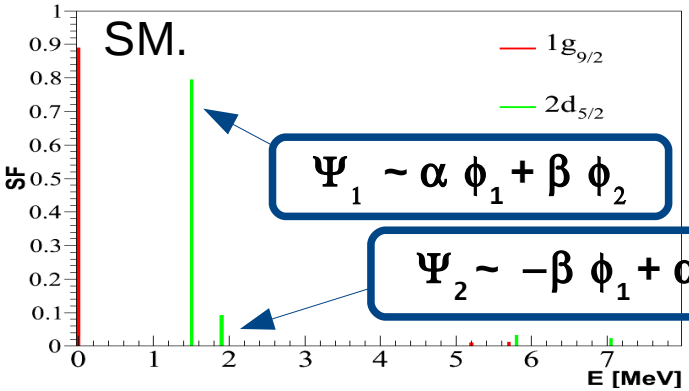

$$\Psi_1 \sim \alpha\, \phi_1 + \beta\, \phi_2$$

$$\Psi_2 \sim -\beta\, \phi_1 + \alpha\, \phi_2$$

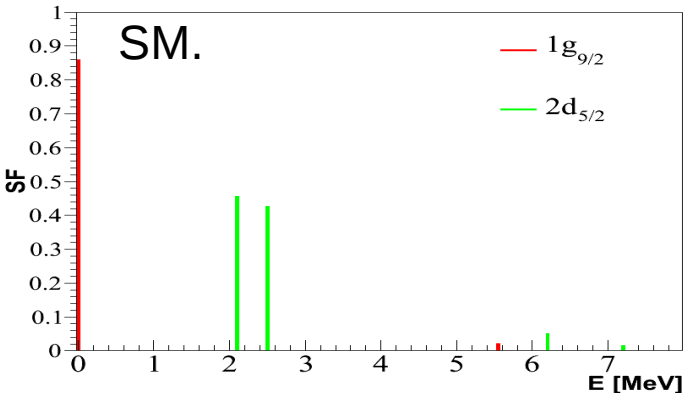

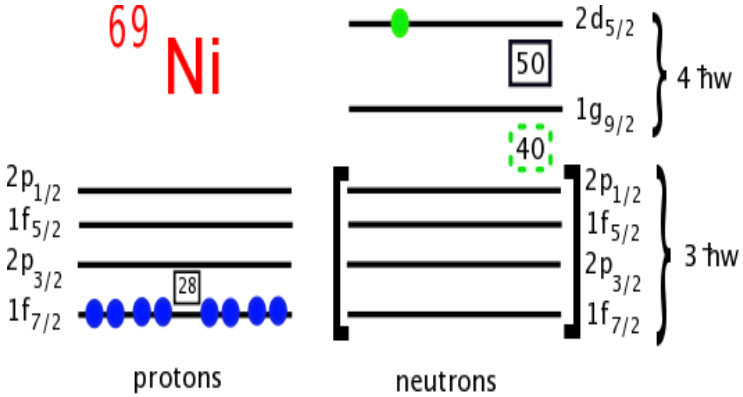

ϕ_1

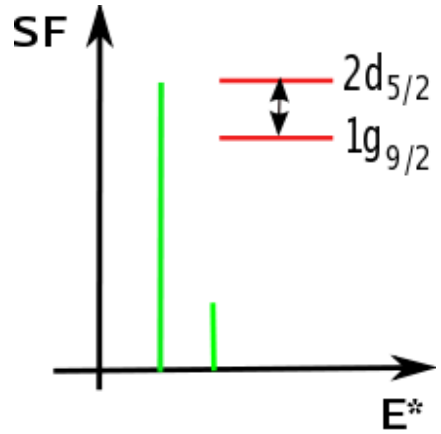

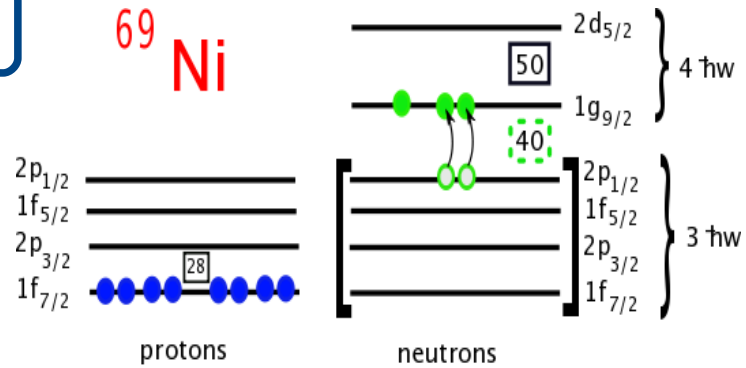

ϕ_2

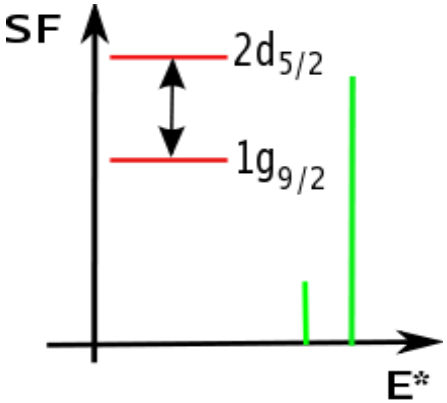

Conclusion and perspective

- Search for the $2d_{5/2}$ neutron orbital in the ^{69}Ni nucleus,
- Study of the d(^{68}Ni,p)^{69}Ni transfer reaction at GANIL,
- Experimental set-up : CATS/MUST2-S1/Plastic,
- Spin and parity assignement $9/2^+$ for the G.S. and $5/2^+$ for the doublet at 2.47 MeV, with an important spectroscopic factor.

Energy [MeV]	L	Jπ	SF (E2⊗S1)	χ2	SF (E2⊗S2)	χ2	SF average
0.00	4	9/2+	0.62±0.20	0,10	0.52±0.17	0,28	0.57±0.19
2.11	2	5/2+	0.37±0.13	0,41	0.36±0.12	0,24	0.36±0.13
2.76	2	5/2+	0.39±0.14	0,58	0.37±0.13	0,45	0.38±0.14

- Good agreement with the shell model calculations,
- Possibility to further constrain of the $2d_{5/2}$ orbital position,
- Validation of the hypothesis postulated by Strasbourg on the small energy difference between the $1g_{9/2}$ and $2d_{5/2}$ orbitals, *(Caurier et al. EPJ, A, 15, 2002, 145)*
- Identification of a neutron state at 4.2 MeV and two resonances at ~5.9 and ~6.9 MeV.

- **Perspective : Data analysis of gamma rays (EXOGAM) for more accurate determination of the excitation energies.**

Collaborators

M. Moukaddam, G. Duchêne, D. Curien, F. Didierjean, Ch. Finck,
F. Haas, F. Nowacki, J. Piot, K. Sieja
(IPHC - Strasbourg, FRANCE)

D. Beaumel, S. Giron, F. Hammache, N. de Séréville, S. Franchoo,
J. Guillot, Y. Matea, A. Matta, L. Perrot, E. Pllumbi, J. A. Scarpaci, I. Stefan
(IPN - Orsay, FRANCE)

G. Burgunder, L. Caceres, E. Clement, B. Fernandez, S. Grevy, J. Pancin, R. Raabe,
O. Sorlin, C. Stoedel, J.C. Thomas
(GANIL - Caen, FRANCE)

F. Flavigny, A. Gillibert, V. Lapoux, L. Nalpas, A. Obertelli
(SPhN - Saclay, FRANCE)

J. Gibelin
(LPC - Caen, FRANCE)

K. Kemper
(Florida State University, USA)

M. Harakeh
(GSI - Darmstadt, Allemagne)

Back up

Island of inversion at N = 40 : Deformation in Fe

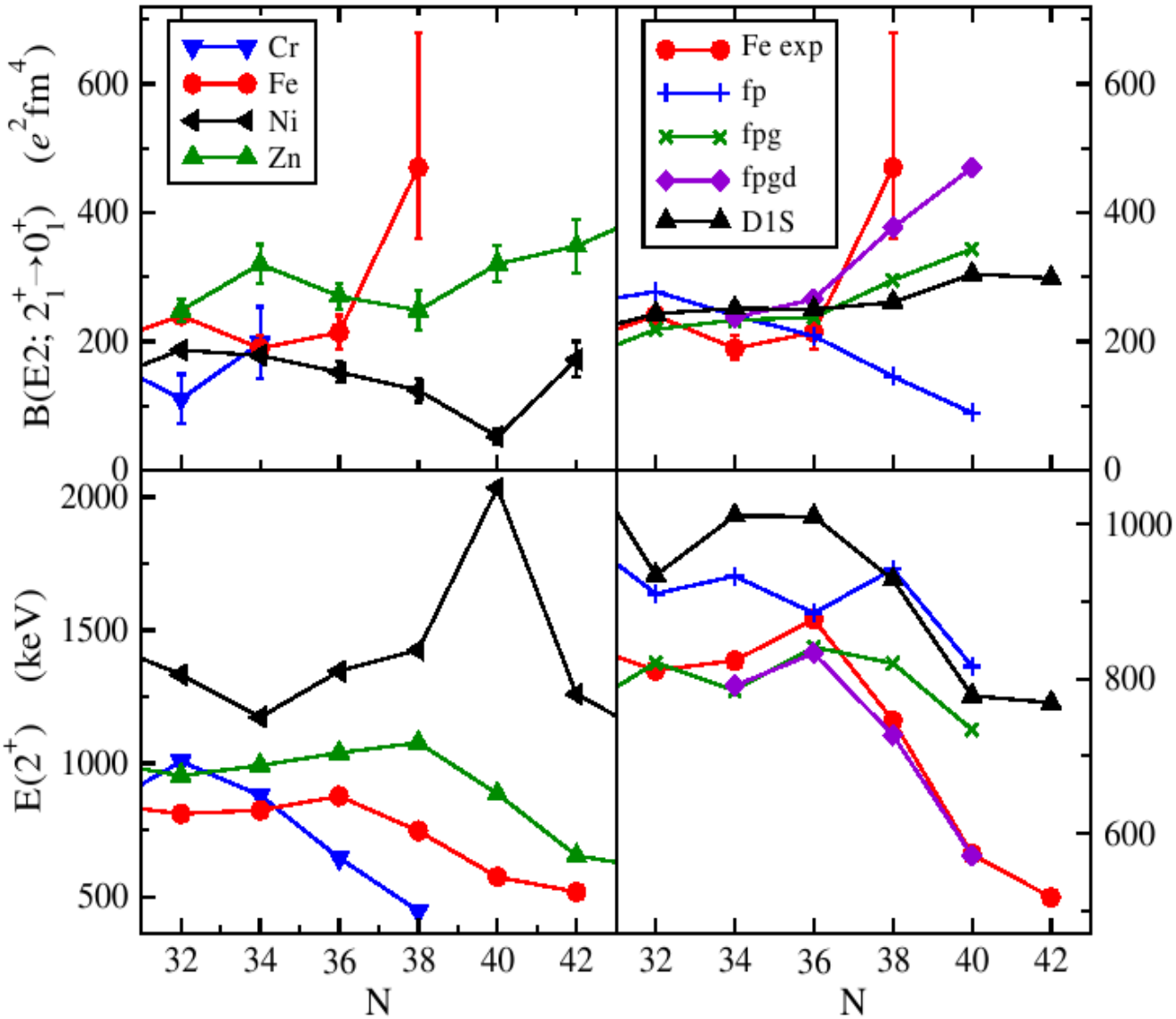

Ljungval et al. Physical Review C 81 (2010) 061301

- **fp**
- **fp + 1g9/2**
- **fp + 1g9/2 + 2d5/2**

Island of inversion - N=20 and N=40

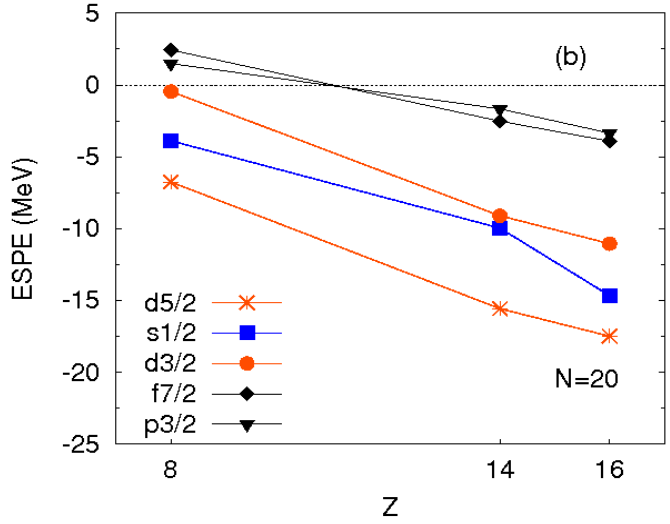

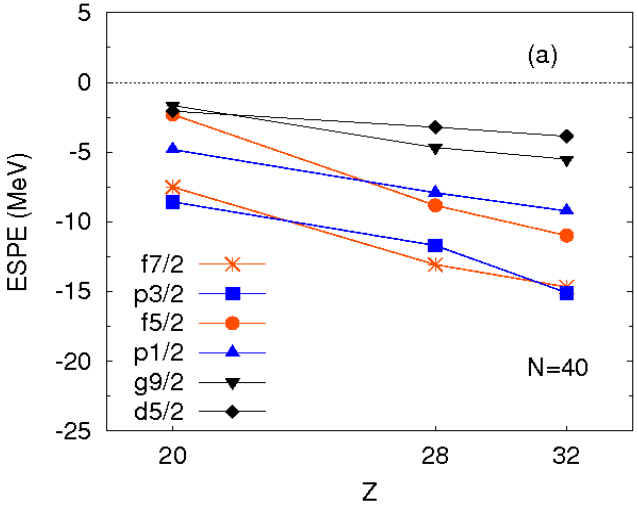

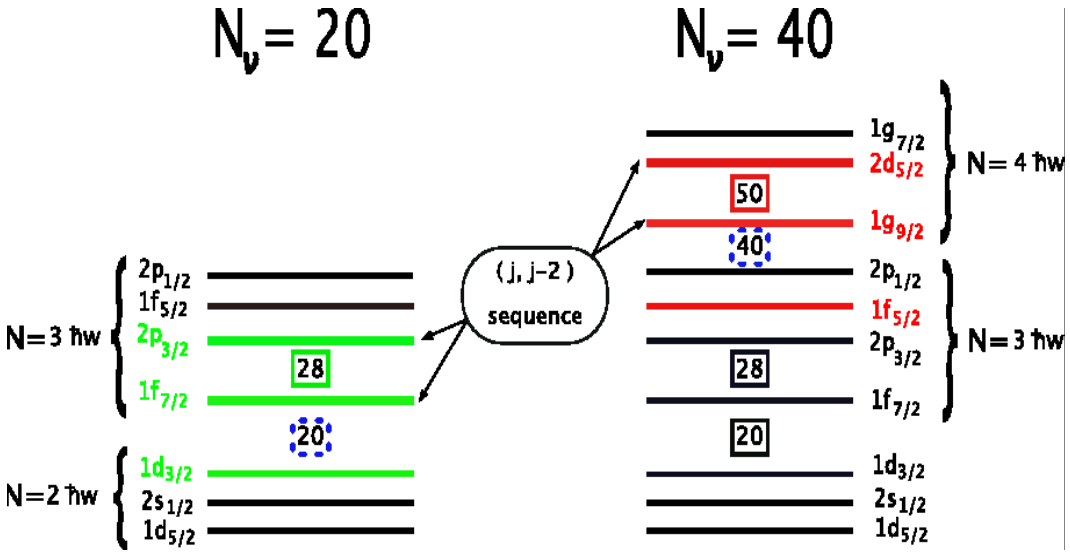

Experimental setup : Inverse kinematics

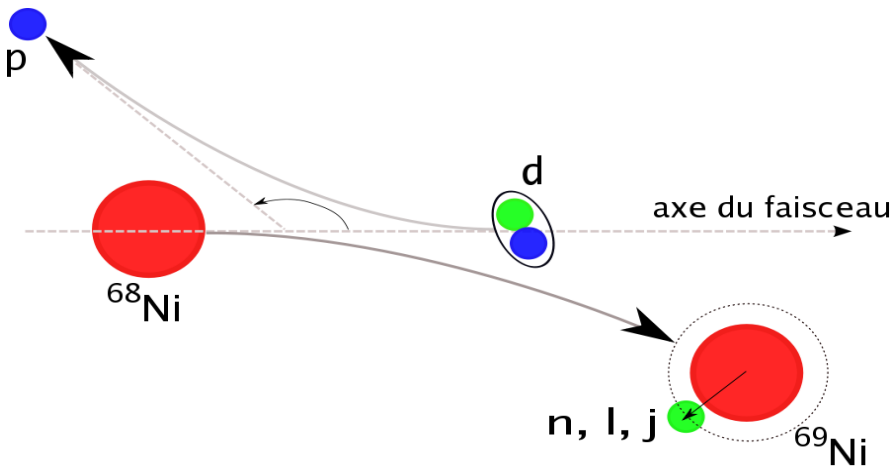

^{68}Ni (T = 29s)

⇒ Inverse kinematics

Forward CM angles

⇔

Backward lab angles

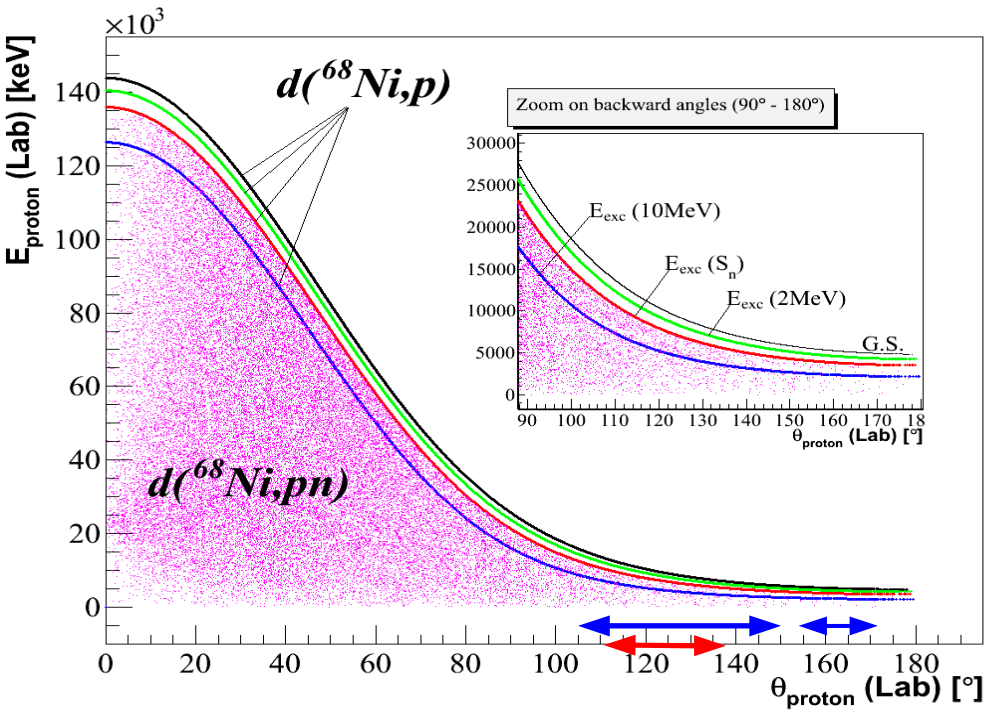

Interesting angular range :

12° - 30° (CM) ⇔ 110° - 140° (Lab.)

Kinematic lines

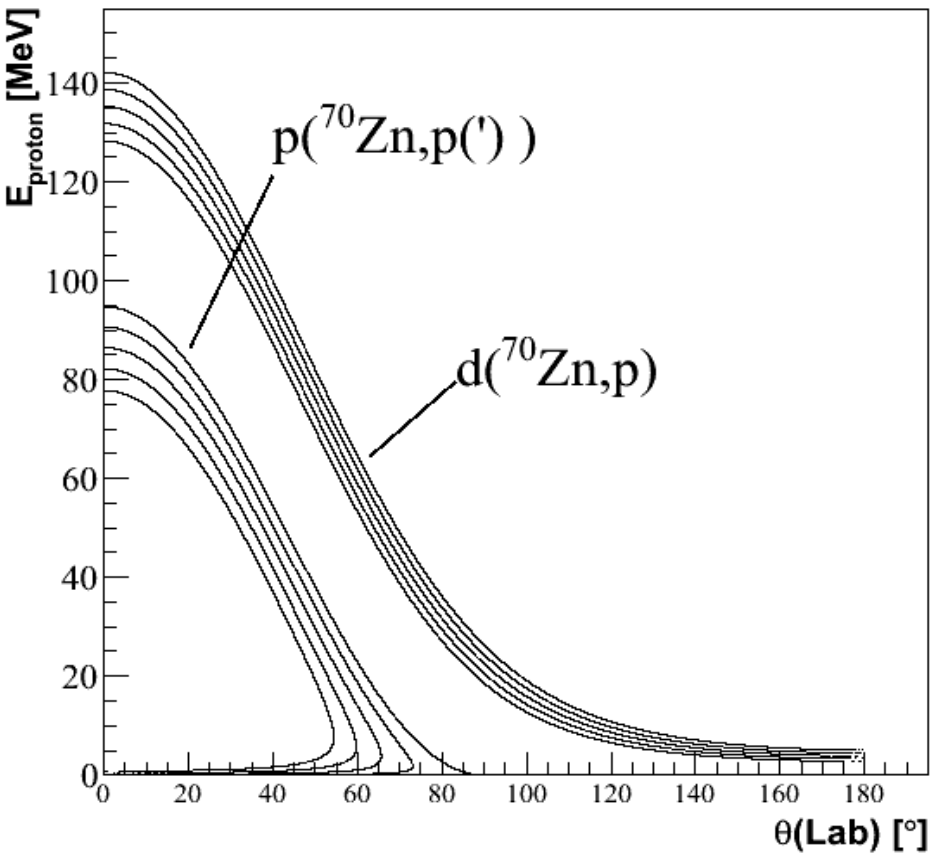

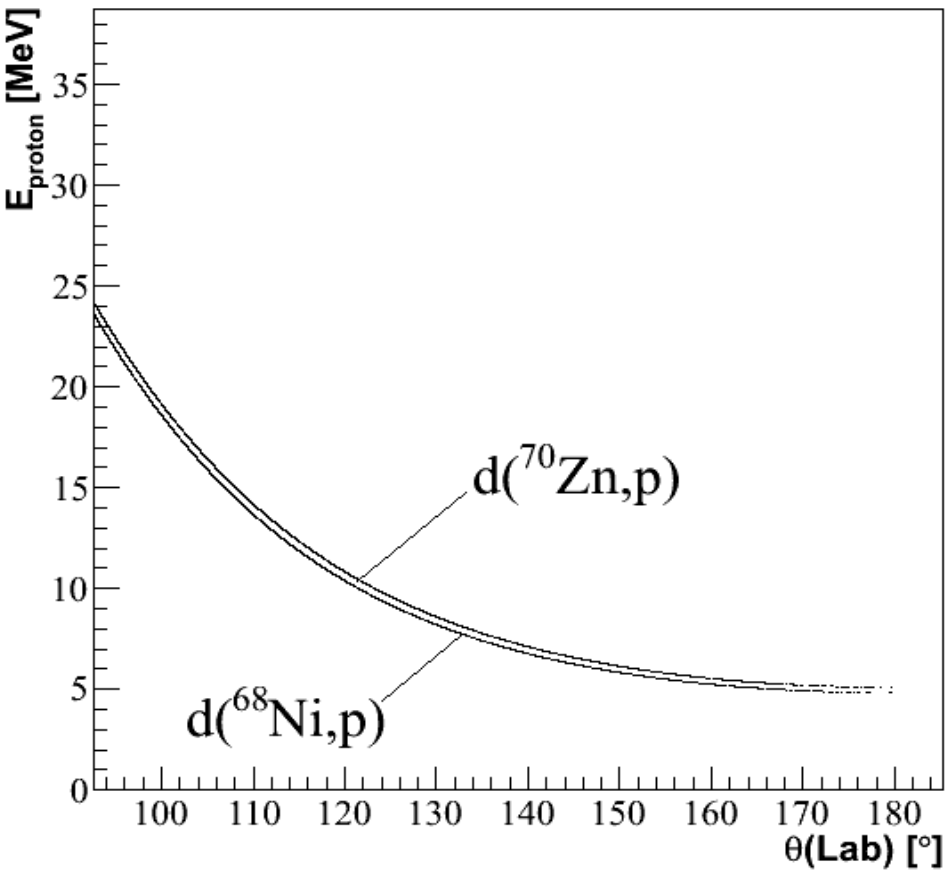

Variation of E_{exc} with respect to proton's energy and angle of emission

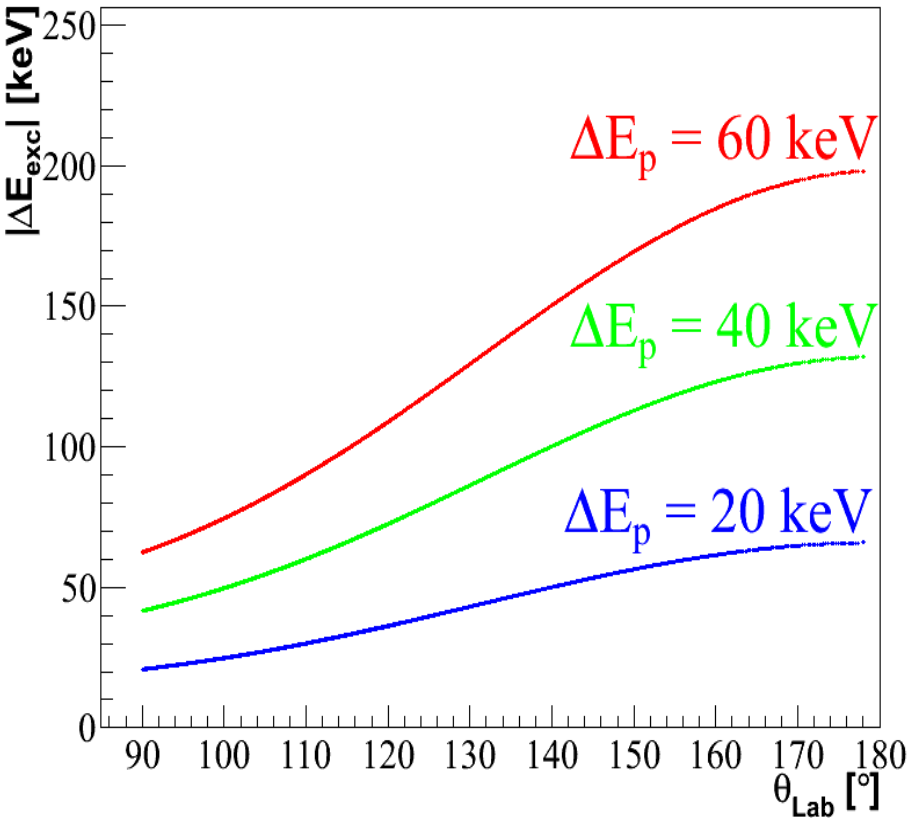

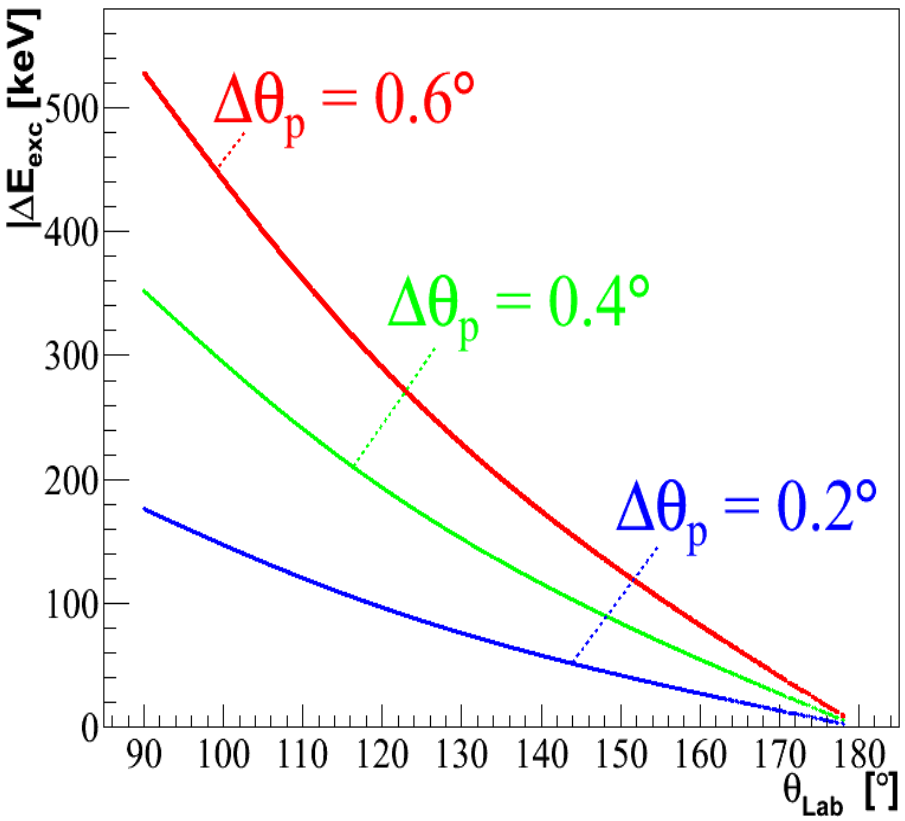

LISE (D4) beam identification

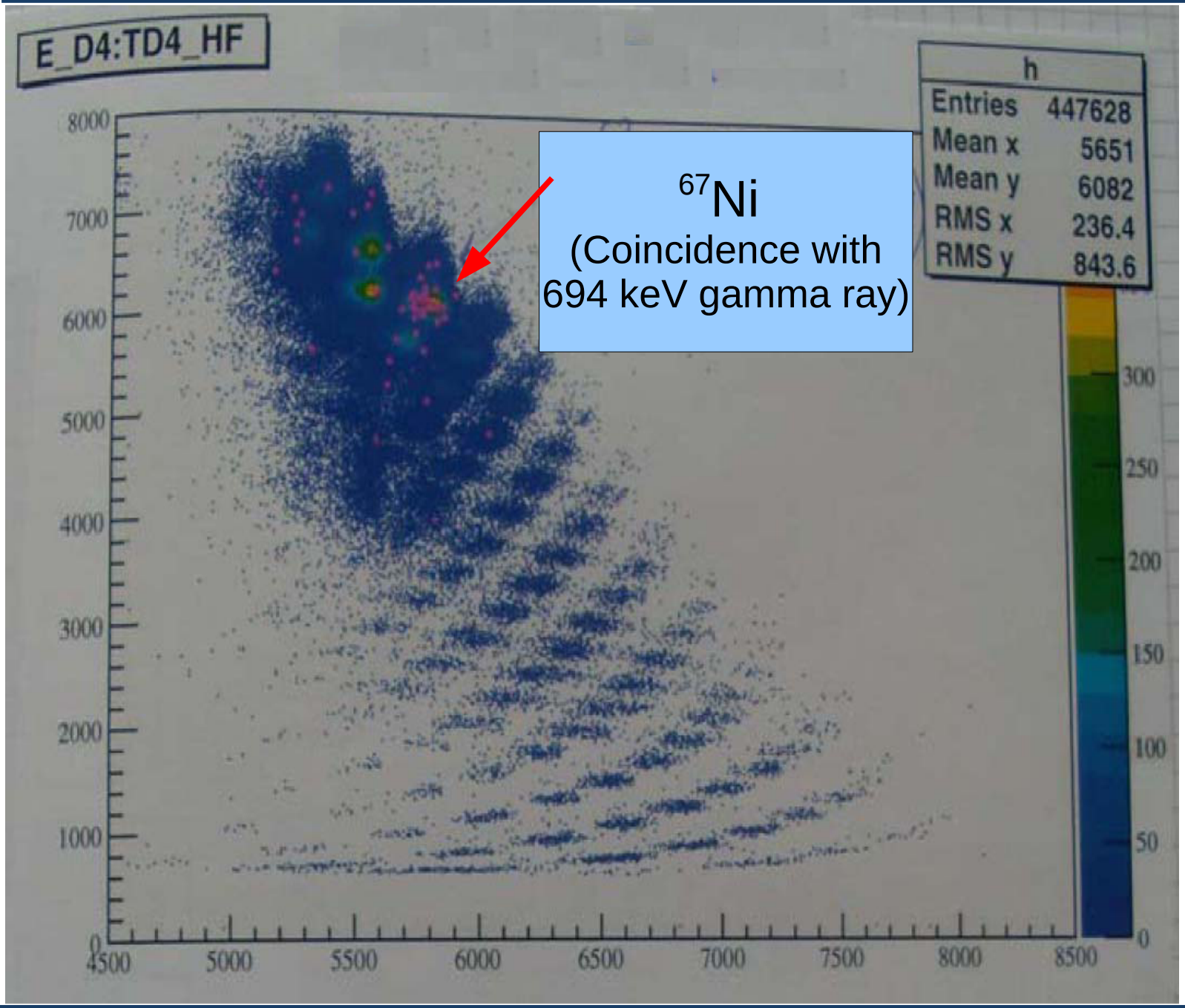

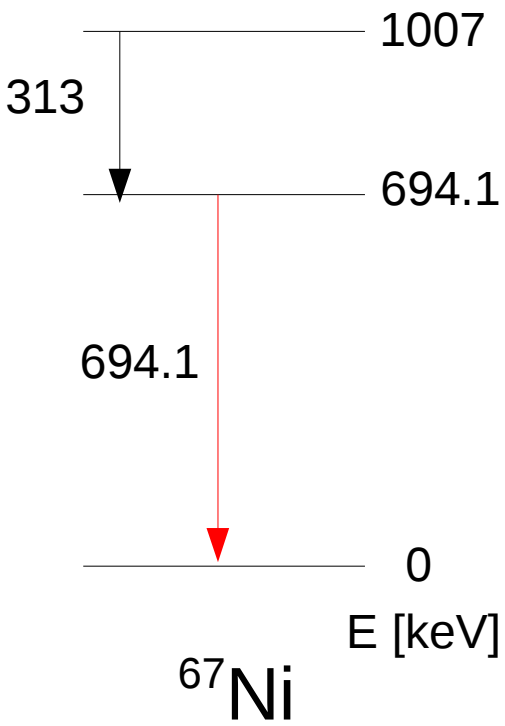

Beam tracker : CATS

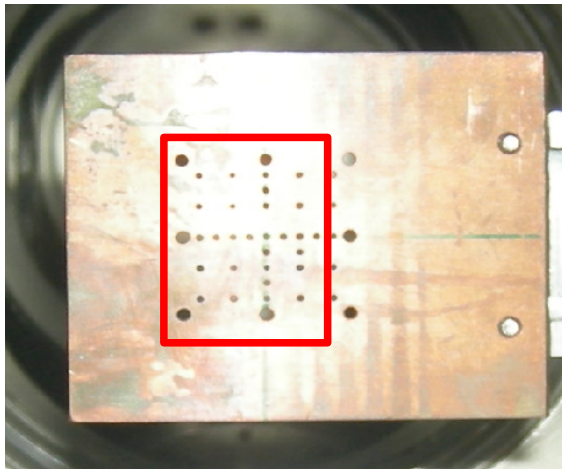

CATS1 mask

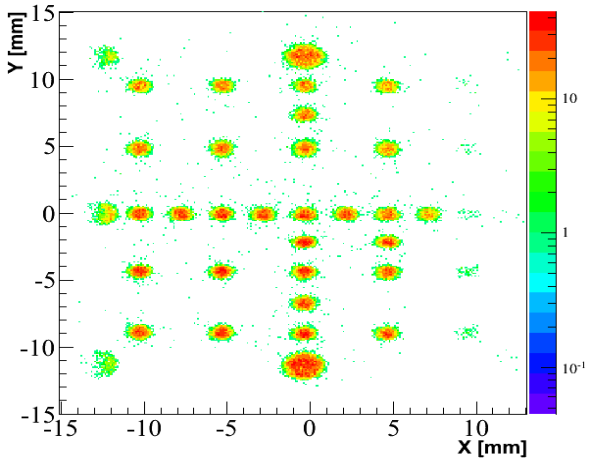

Analytical method :
(Hyperbolic secant squared)

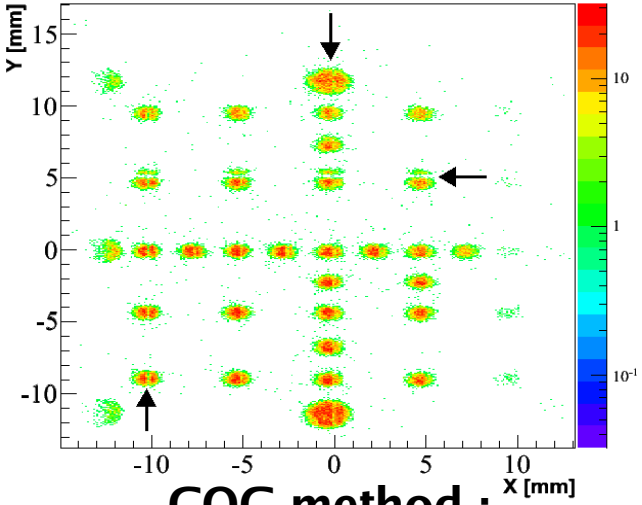

COG method :
(3 strips)

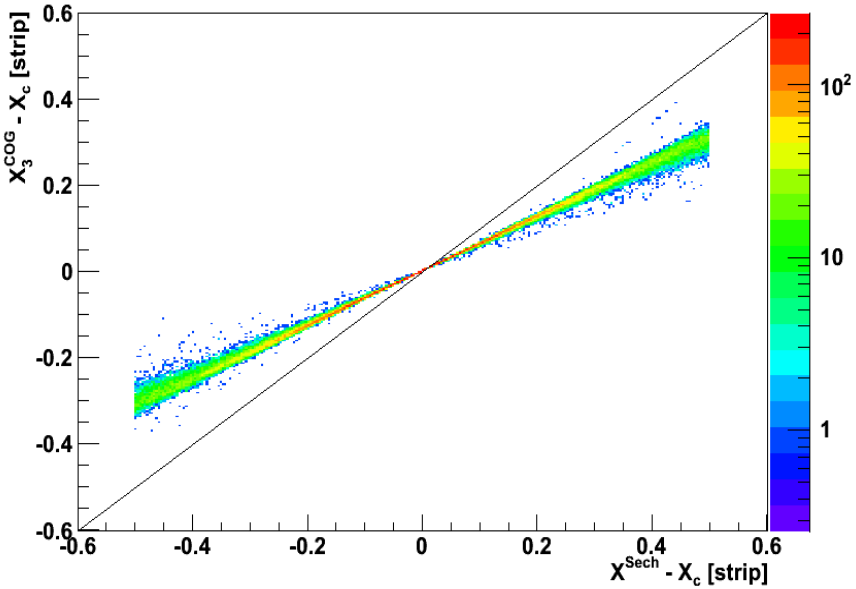

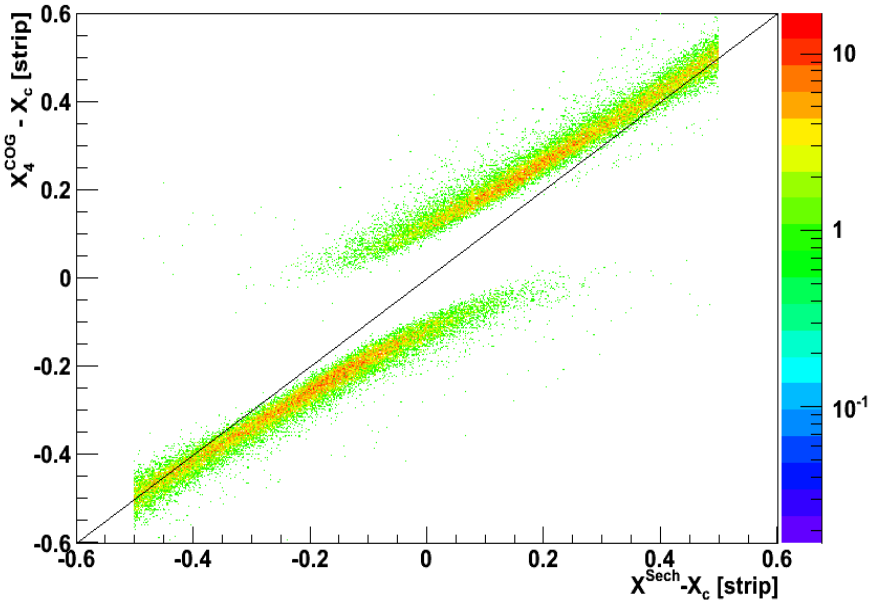

Beam tracker : CATS

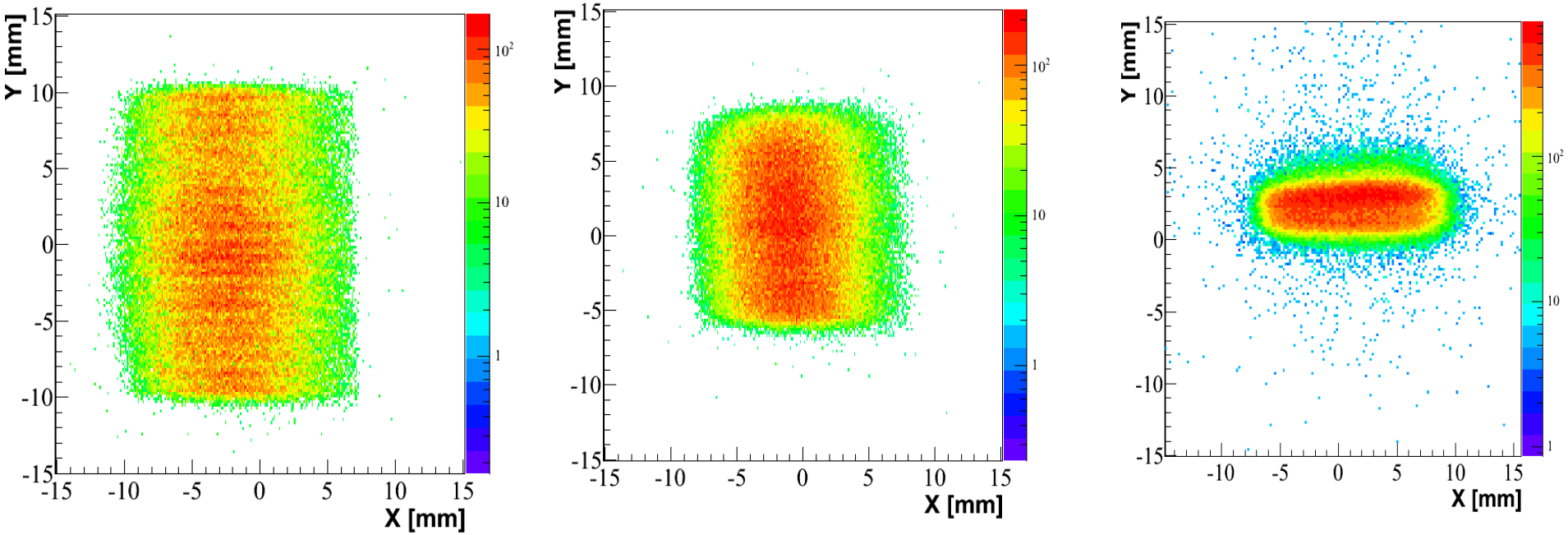

Construction with CATS : systematic errors

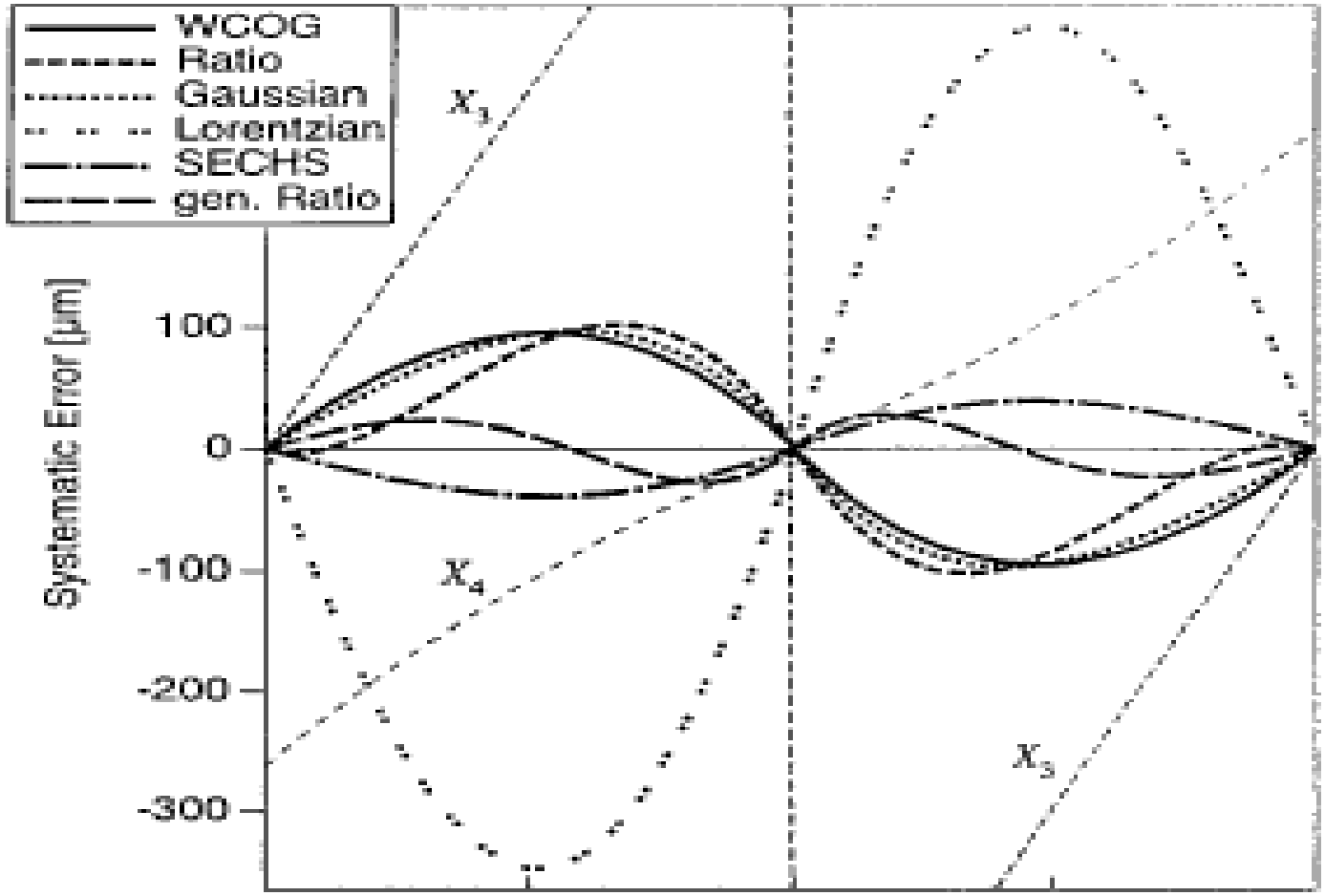

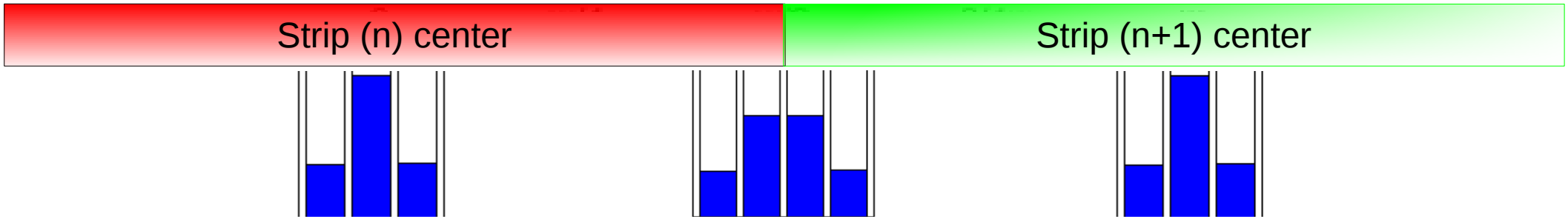

Plastic deterioration

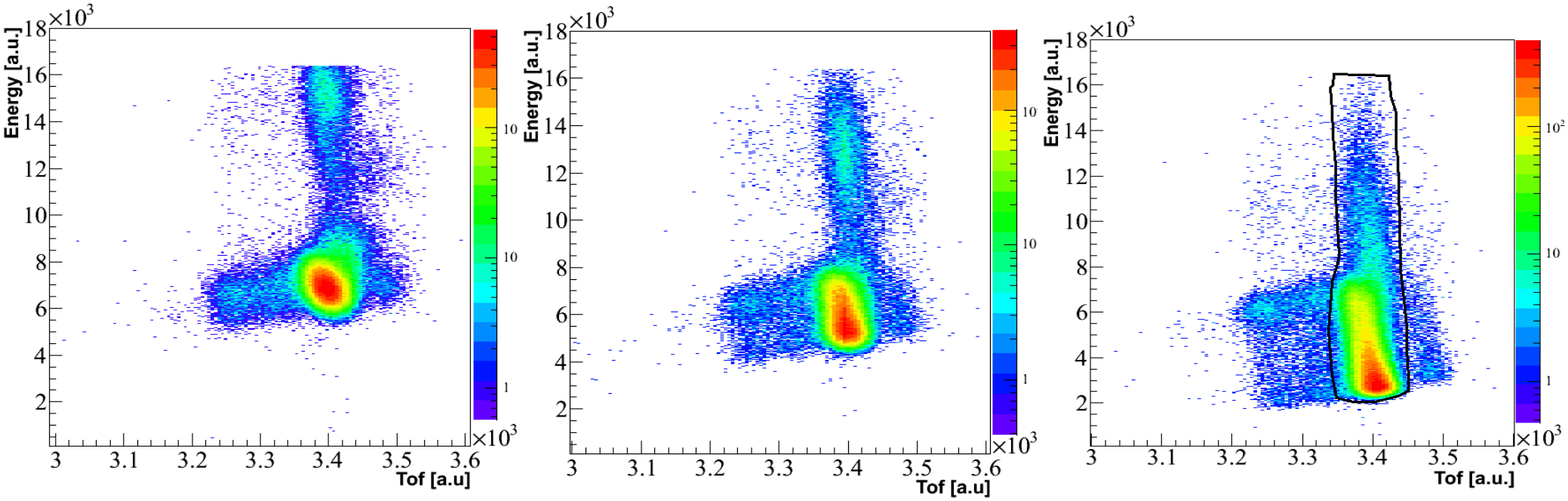

time

Calculated parameters

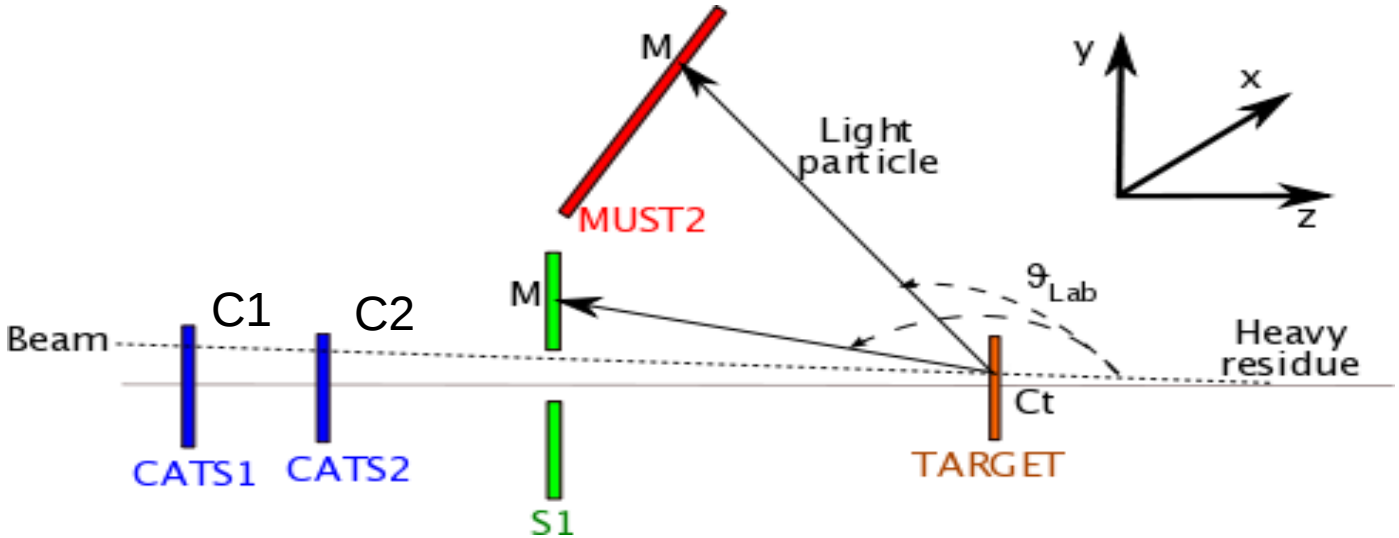

- Reconstruction of angle of emission θ(Lab) (uncert. ~ 0.5°)
- Beam energy correction taking into account the energy losses in the:
  - Beam trackers CATS
  - Target
- Proton energy correction taking into account the energy losses in the :
  - Target
  - Detector dead layers
- Reconstruction of excitation energy using missing mass method

Background reactions : Carbon background

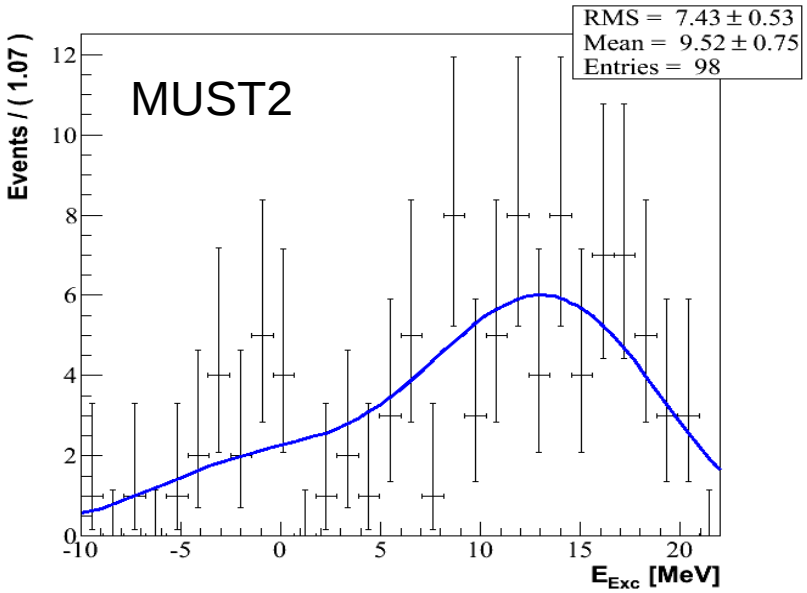

- CD_2 Target ⇒ Carbon background
- Poor statistics
- Estimated with:
  - Linear back-ground
  - **« Kernel estimation»**

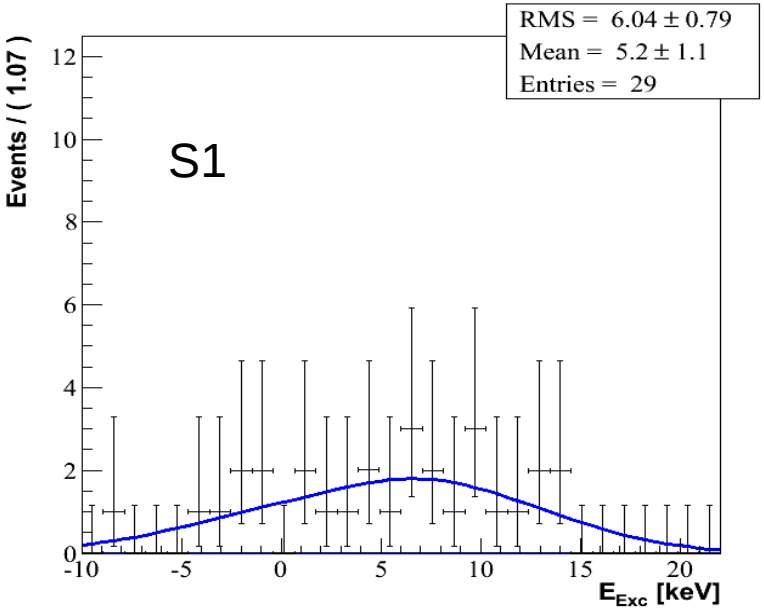

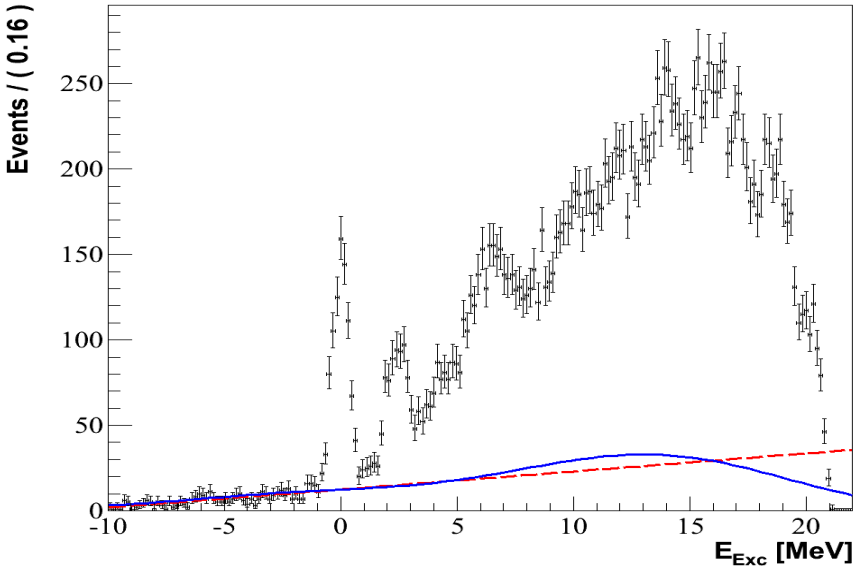

Background reactions : Deuteron break-up

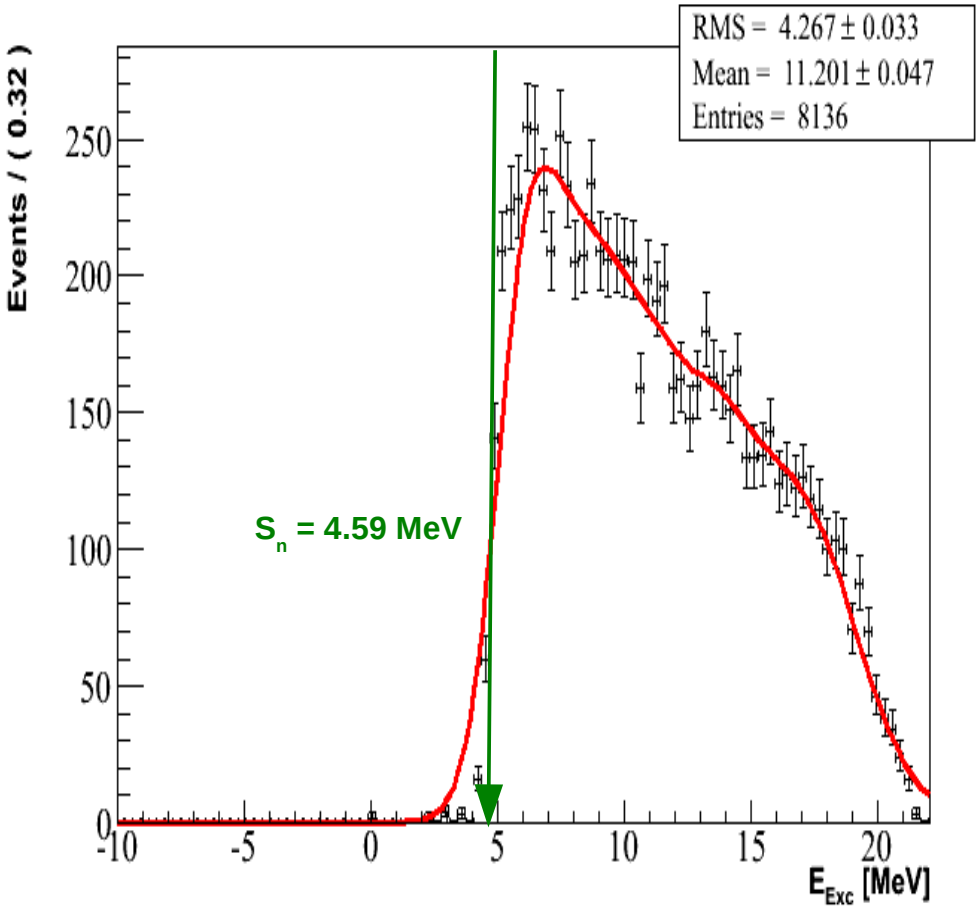

$$^{68}Ni + d \rightarrow {}^{68}Ni + p + n$$

- Deuteron break-up ⇒ 3-body kinematics
- Phase-space calculations
- **« Kernel estimation»**

Excitation energy spectrum : no cuts

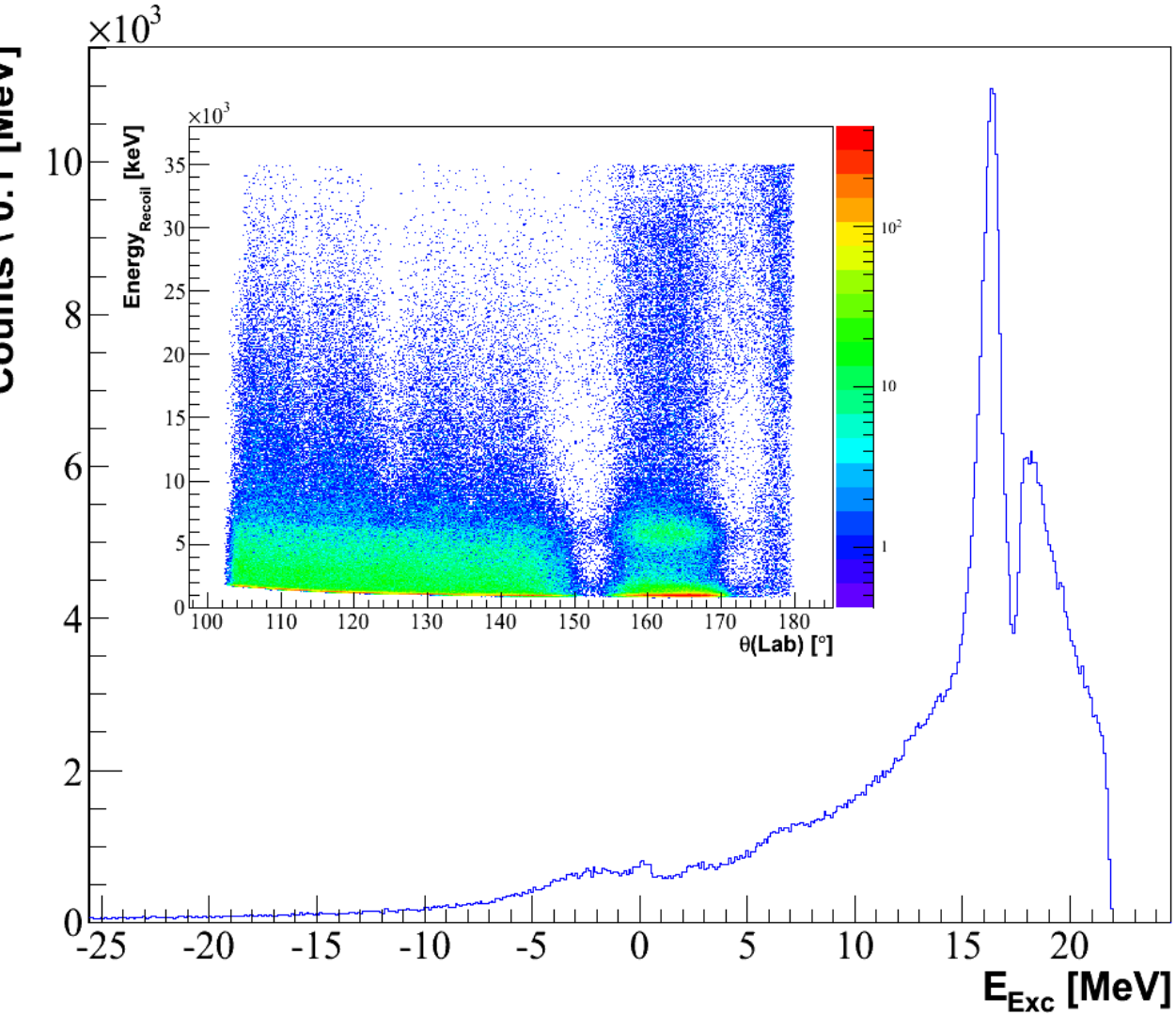

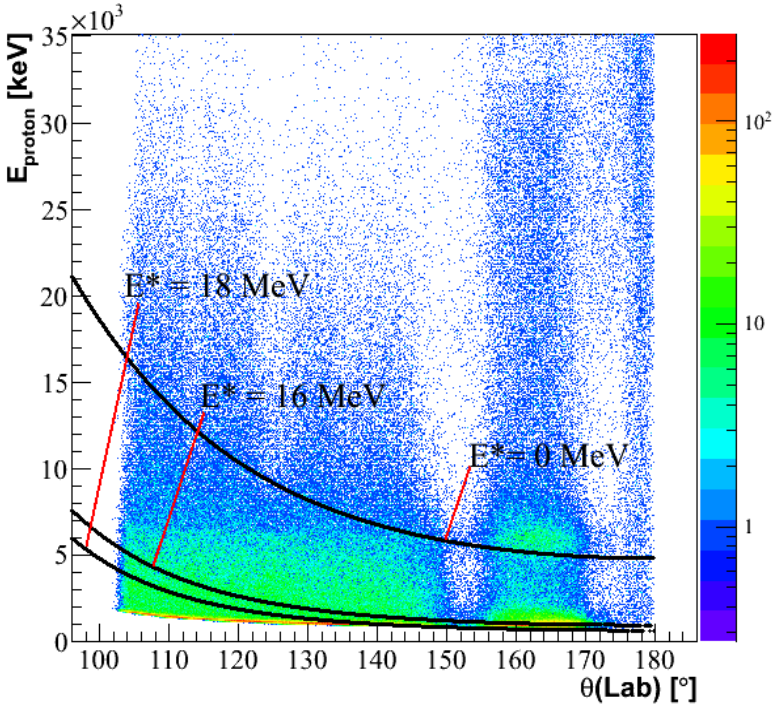

Excitation energy spectrum : gated

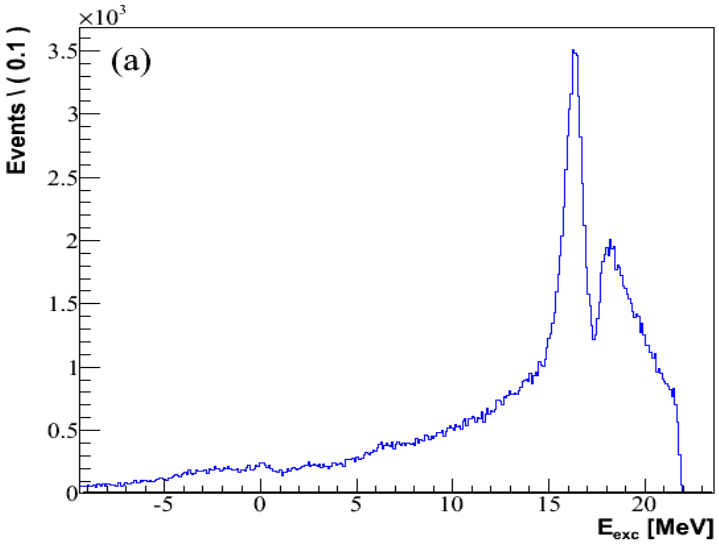

Target gate

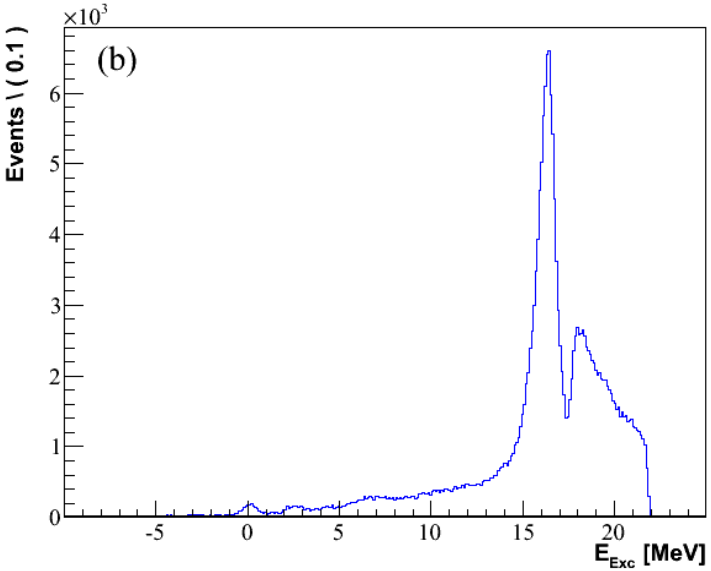

Heavy residue gate

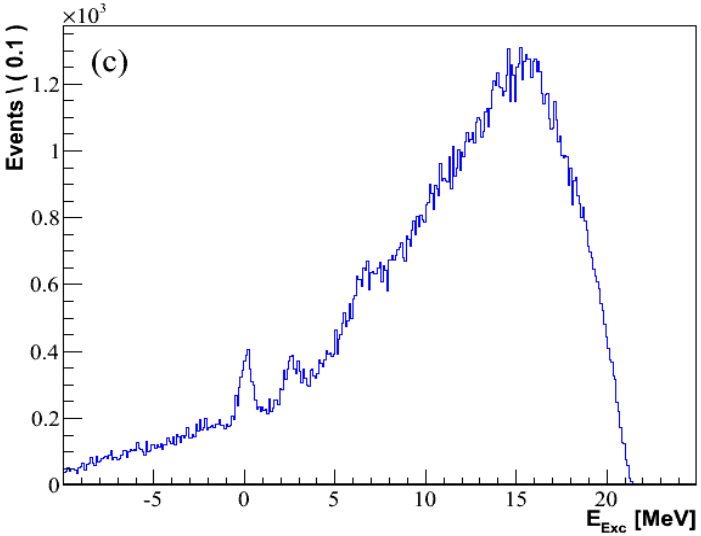

Proton gate

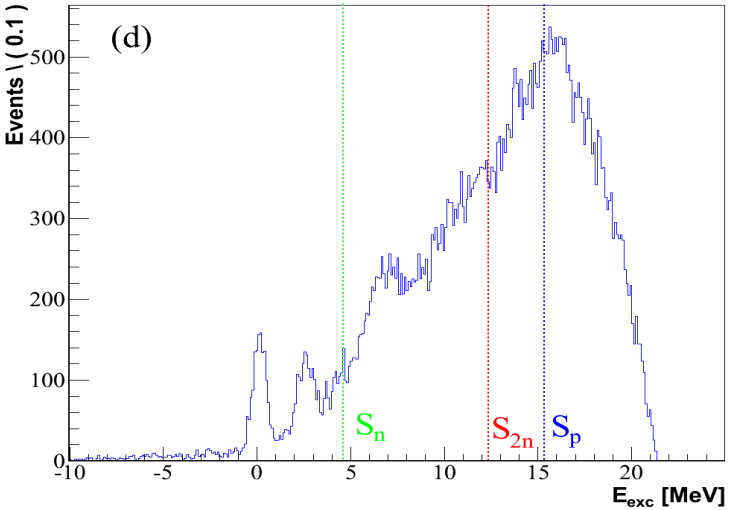

All gates

Angular efficiency

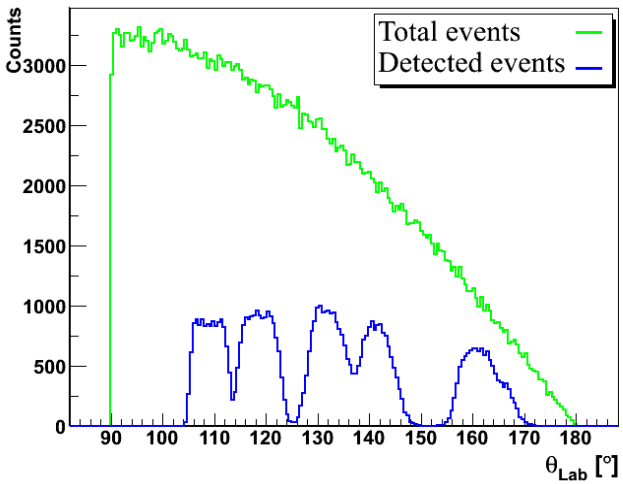

⇒

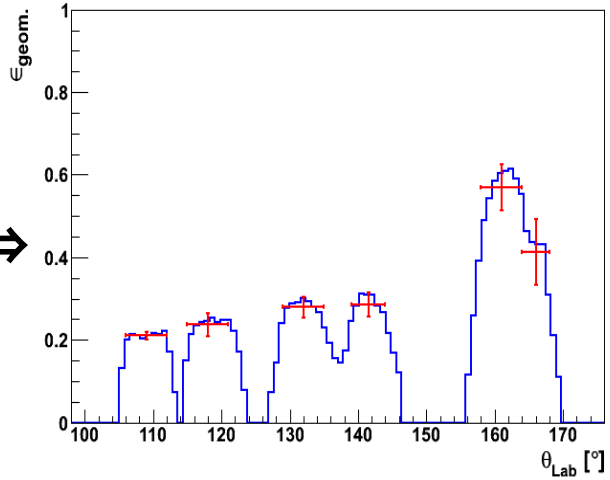

Angular efficiency :

- Detectors geometry
- Position
- Pad/strip state
- Analysis method

  ⇒ Simulation

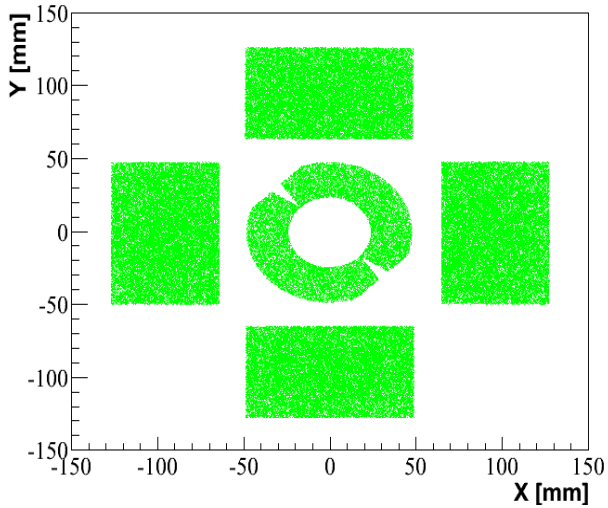

Flawless detector

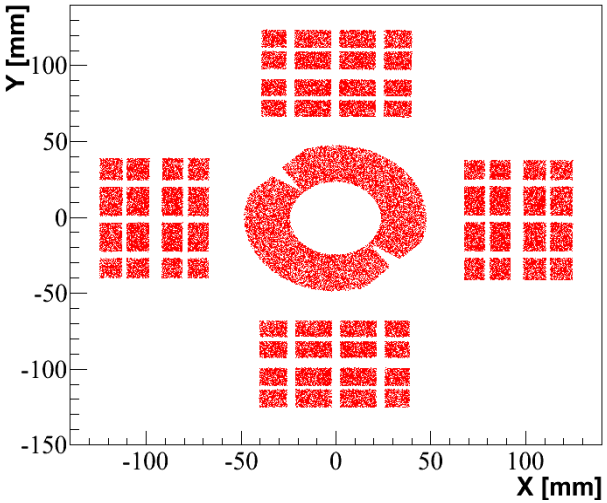

Flawless detector + matching

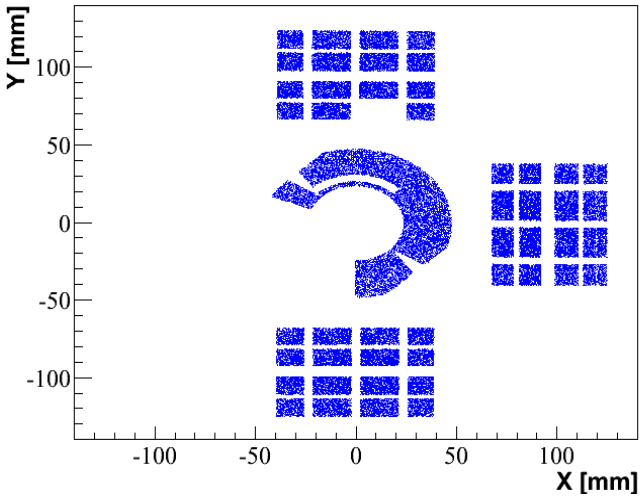

Flawless detector + matching + non-operational strip/pad

Excitation energy spectrum : fit

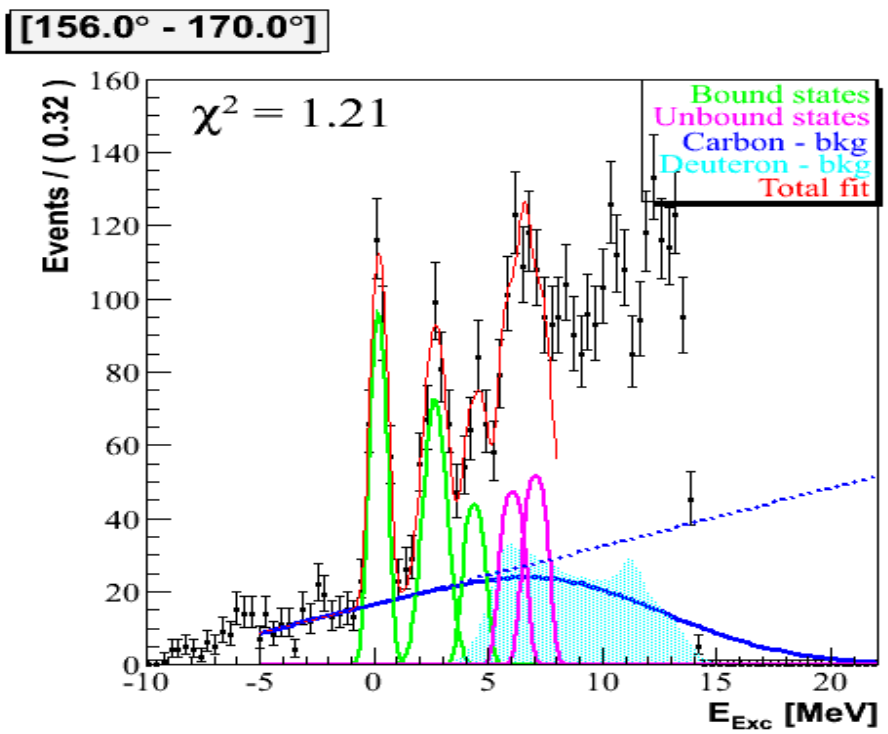

S1 référence en énergie : [156°-170°]

- Less dependant on the constructed angle of proton
- Transfer cross section is maximum

- 3 bound states
- 2 resonances above S_n

États liés

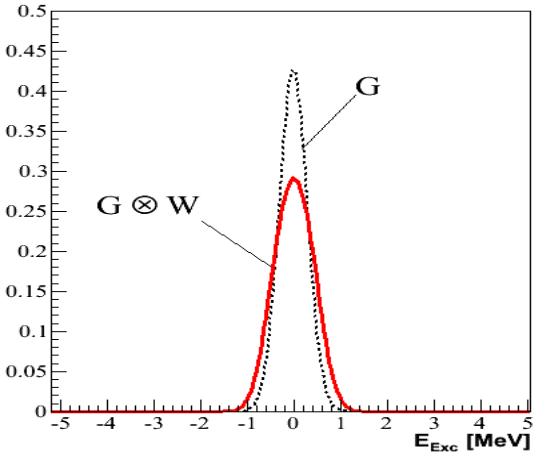

Résonances

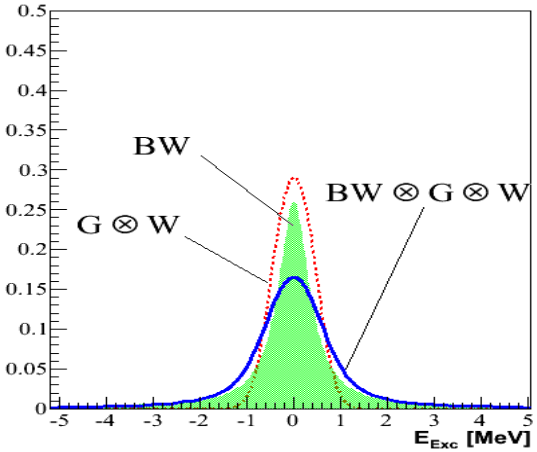

- C back-grd : E_{Exc} <0
- Target thickness ⇒ window function ≡ W
- Bound states : G⊗W
- Resonances : BW⊗G⊗W
- D back-grd : free param.

Excitation energy : spectra analysis

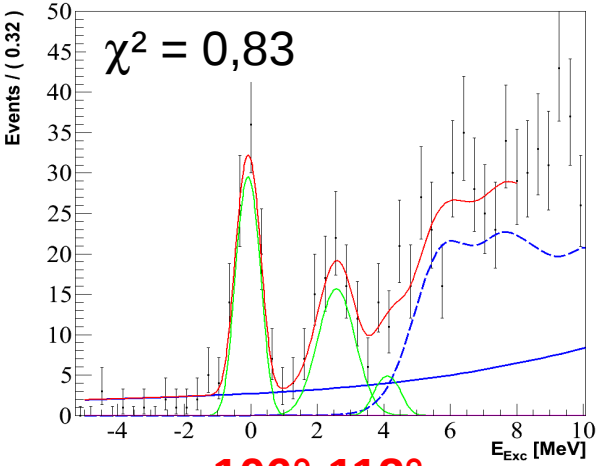

106°-112°

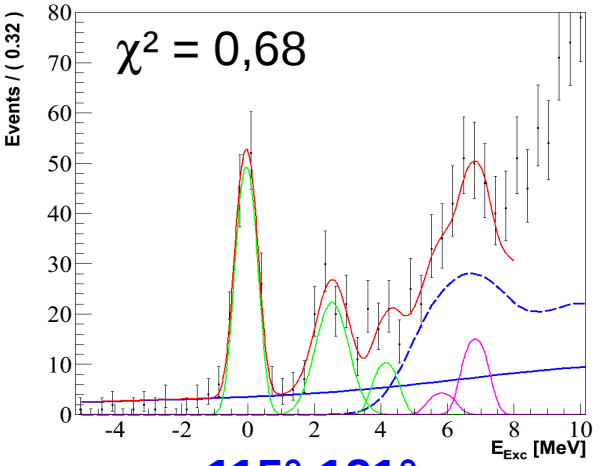

115°-121°

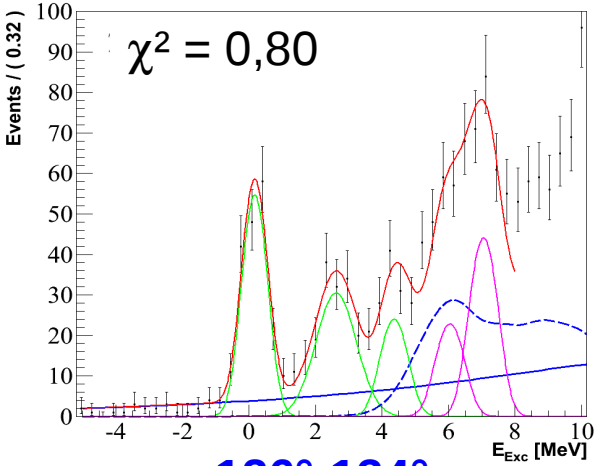

126°-134°

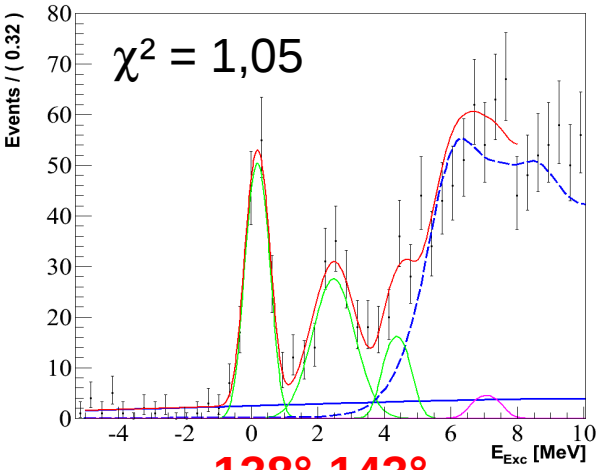

138°-143°

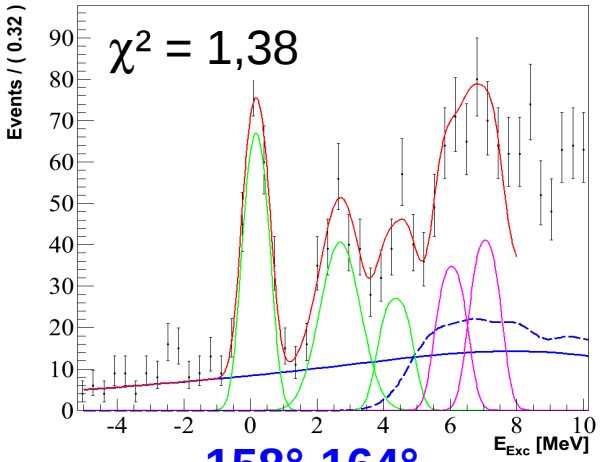

158°-164°

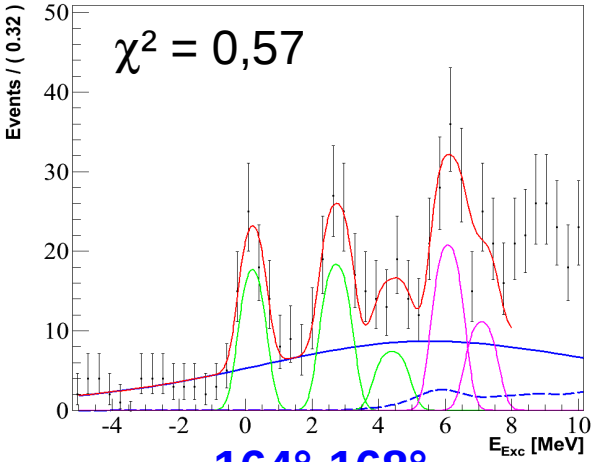

164°-168°

First excited state at 2.47 MeV : doublet structure

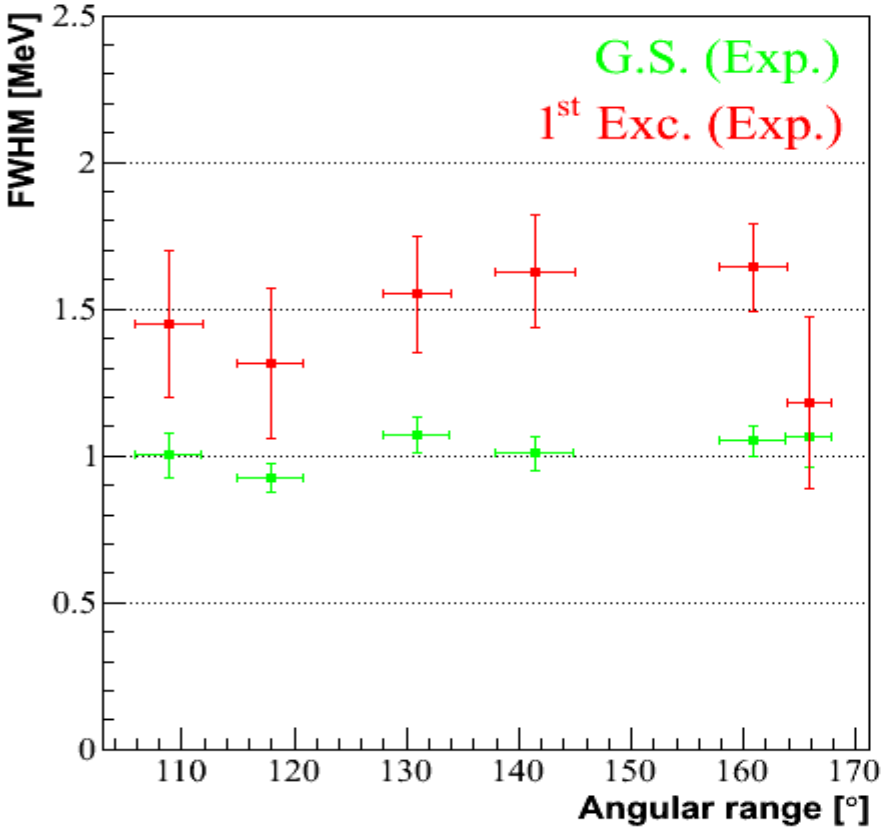

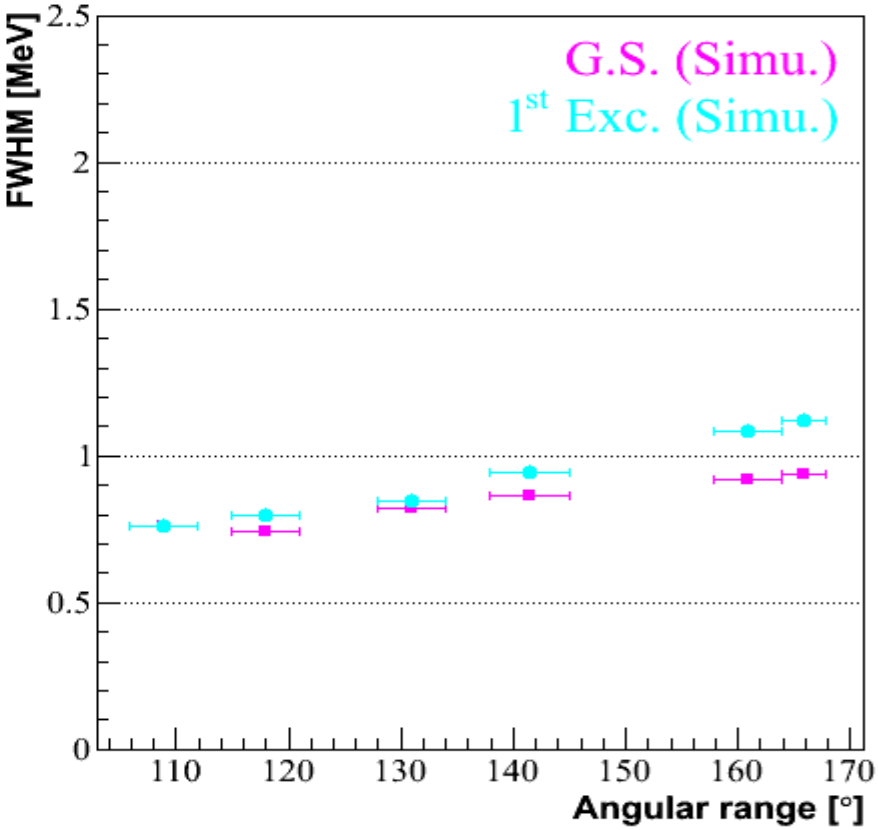

FWHM (1st excited) ~ 1.5 FWHM (G.S.) ⇒ doublet at 2.47 MeV

Differential cross sections

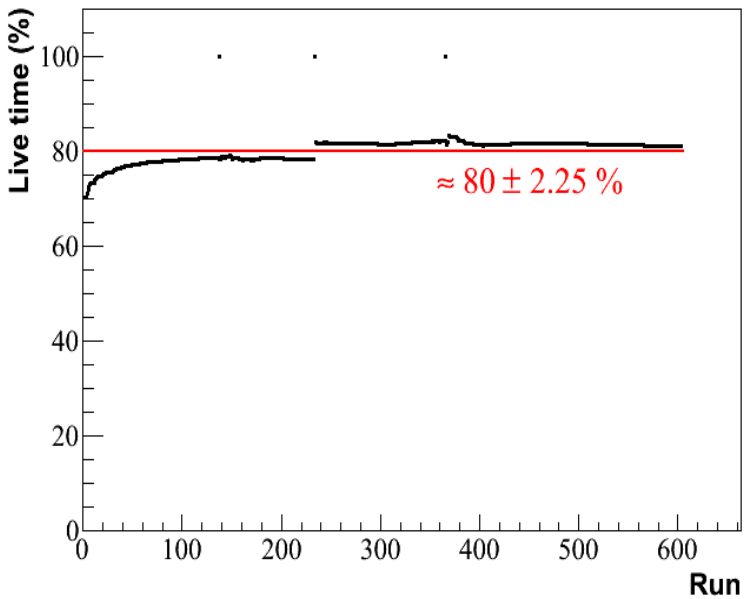

$$\frac{d\sigma}{d\Omega}(\theta_{Lab}) = \frac{N_{det}(\theta_{Lab})\ (1+\epsilon_{temps\,mort})}{N_{faisceau}\ N_{Cible}\ \Delta\Omega(\theta_{Lab})\ \epsilon_{MUST2,S1}}$$

$$\frac{d\sigma}{d\Omega}(\theta_{CM}) = Jacob.(\theta_{Lab})\ \frac{d\sigma}{d\Omega}(\theta_{Lab})$$

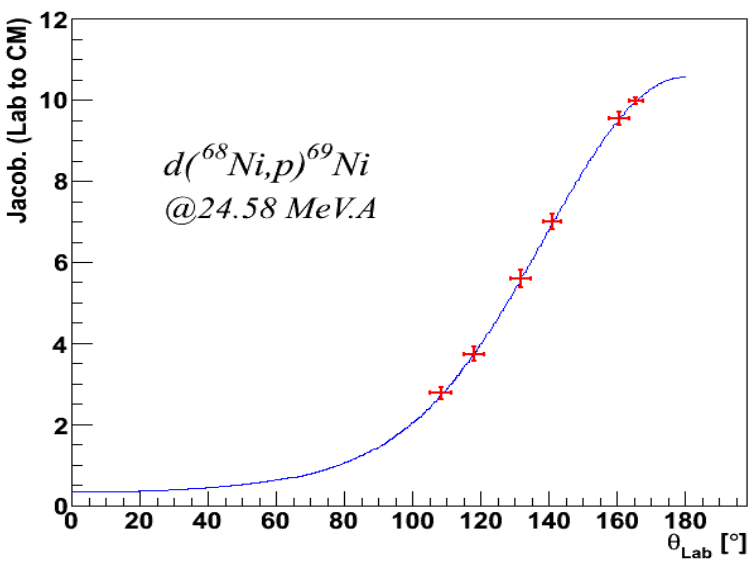

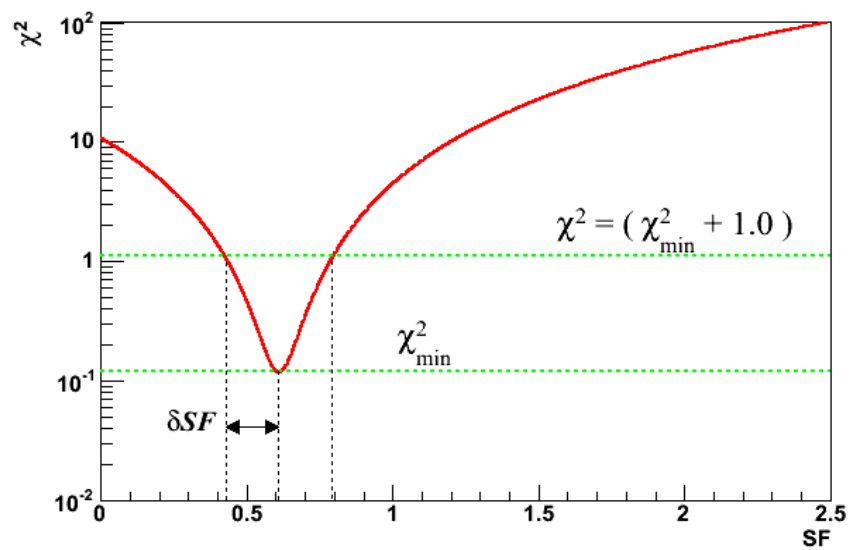

Diff. cross sections analysis : state @ 2.11 MeV

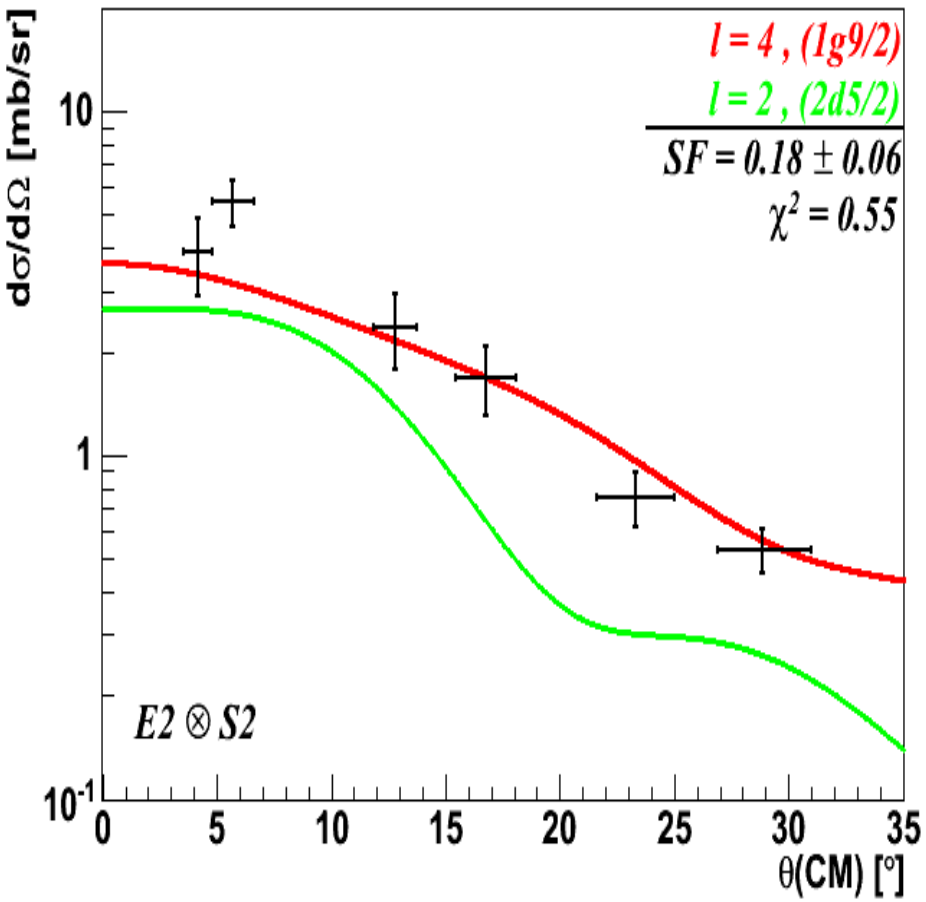

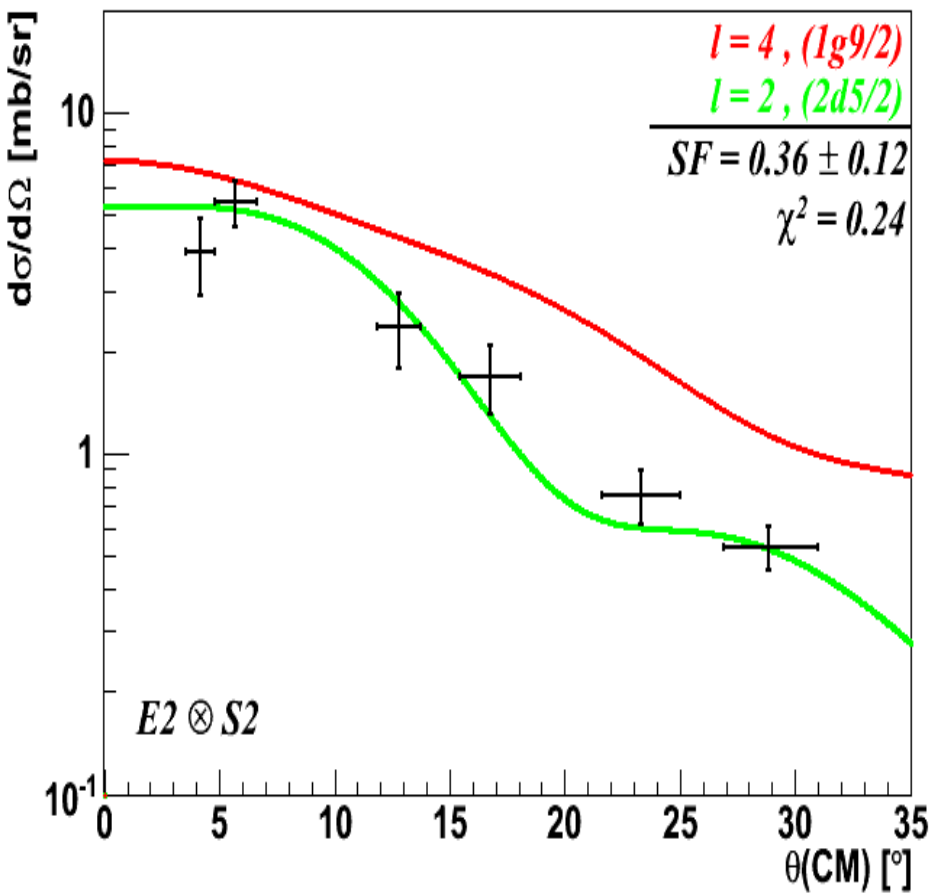

Diff. cross sections analysis : state @ 2.76 MeV

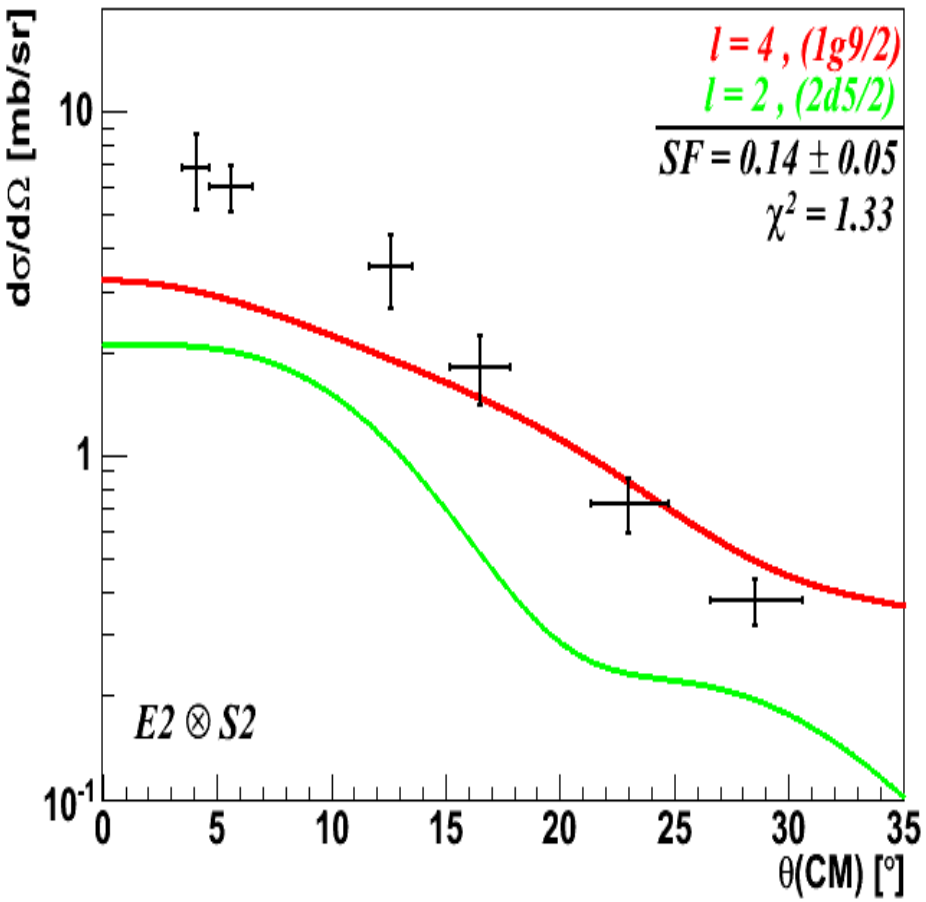

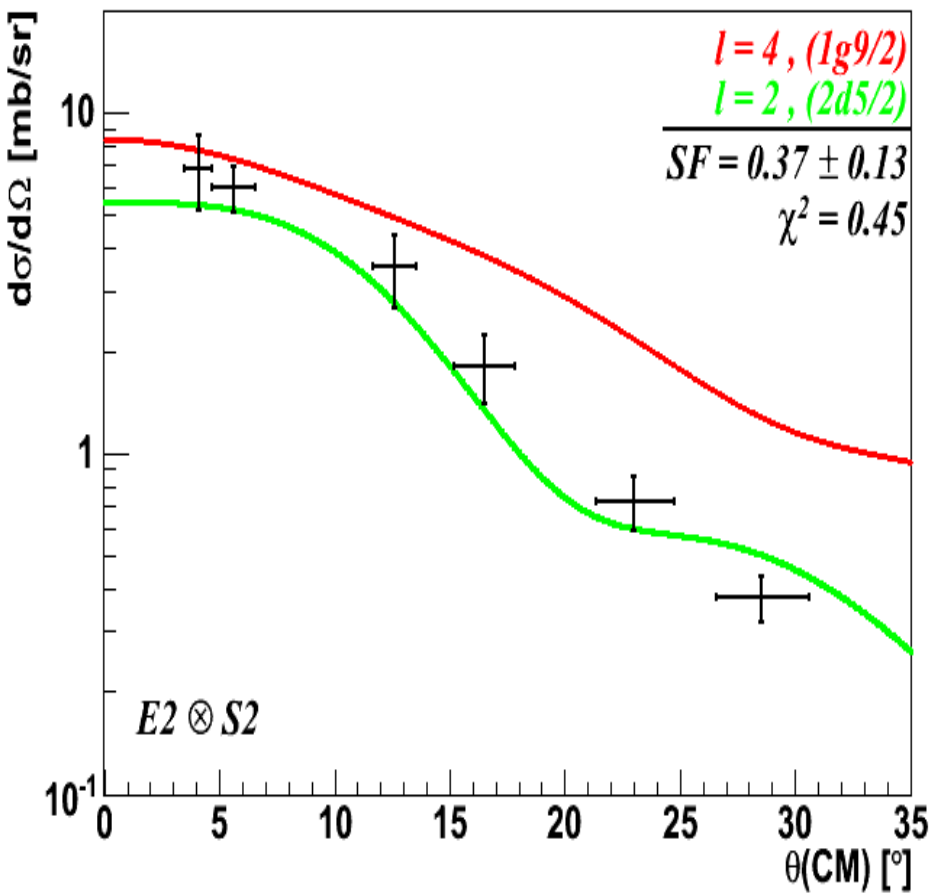

Experiment Vs Shell model calculations

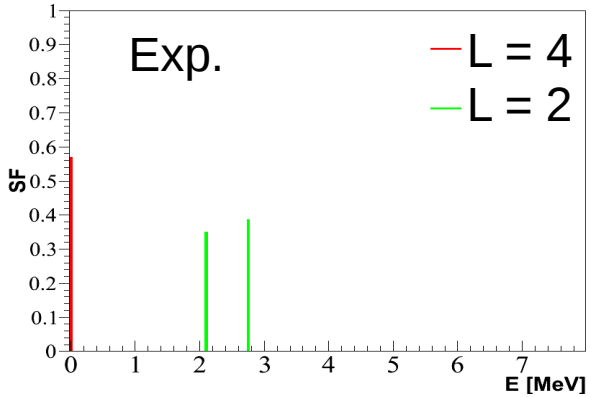

E_{exc}(Exp.) = 2.44 MeV

→ E_{exc} = 2.11 MeV

L = 2, SF = 0.36±0.13

→ E_{exc} = 2.76 MeV

L = 2, SF = 0.38±0.14

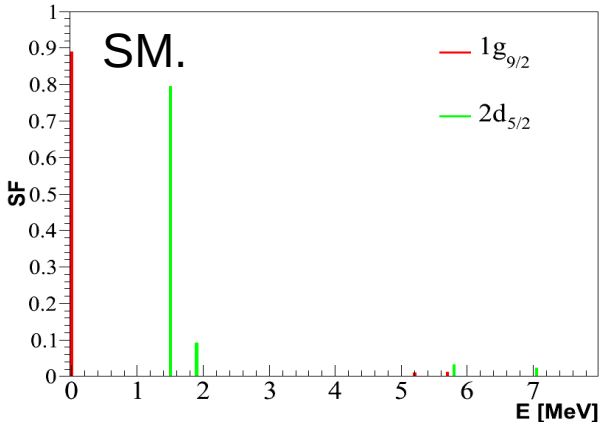

E_{exc}(SM) = 1.53 MeV

→ E_{exc} = 1.49 MeV

L = 2, SF = 0.79

→ E_{exc} = 1.92 MeV

L = 2, SF = 0.09

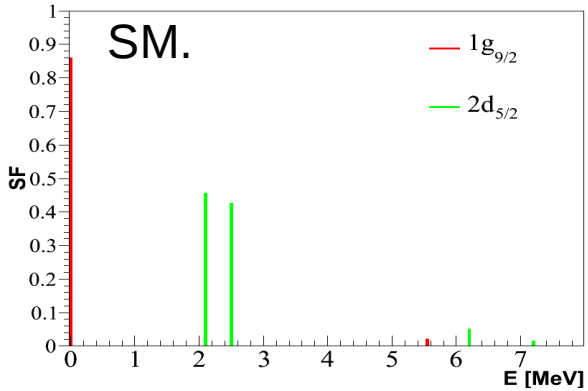

E_{exc}(SM) = 2.30 MeV

→ E_{exc} = 2.12 MeV

L = 2, SF = 0.46

→ E_{exc} = 2.50 MeV

L = 2, SF = 0.43